ELECTRICAL FIELD EFFECTS ON ENDOTHELIAL CELL ADHESION AND GROWTH ON CONDUCTING BIOMATERIALS SURFACES

By

GWEN ELAINE CLARK

A DISSERTATION PRESENTED TO THE GRADUATE SCHOOL
OF THE UNIVERSITY OF FLORIDA IN PARTIAL FULFILLMENT
OF THE REQUIREMENTS FOR THE DEGREE OF
DOCTOR OF PHILOSOPHY

UNIVERSITY OF FLORIDA

1999

Copyright 1999

by

Gwen Elaine Clark

This dissertation is dedicated to my heroes and my supporters: my family and my friends; most especially to the greatest of these - my best friend and the love of my life, Jeff, without whom this work would never have been realized.

ACKNOWLEDGMENTS

I would like to thank Dr. E.P. Goldberg as the advisor and chair of my supervisory committee for his direction, thoughtful insights, and support of my research. I also thank the other members of my committee - Drs. C.D. Batich, A.B. Brennan, R.B. Dickinson, and J.M. Seeger - for their time and commitment to further my education.

I appreciate the support of MKI for partial support of this research and of Milliken, Meadox and Dupont for supplying test materials. Thanks are also due to Dr. J.M. Seeger's, Dr. R.B. Dickinson's and Dr. J.R. Reynold's research groups for their invaluable assistance in my research.

My friends and colleagues were critical to my success by sharing ideas, teaching me laboratory protocols and research techniques, and for challenging me. Thanks to Dr. Christopher Widenhouse for encouraging me to begin my graduate career at the University of Florida, for being a mentor, for assisting me with my research, and for all his input. Thanks to Dr. Drew Amery for always being available for technical assistance and encouragement. Thanks to Mrs. Jackie Hulsey for her support, assistance, and kindness. Thanks to Drs. James Marotta and James Kirk for initiating me to the University and to the lab and for sharing their creative ideas for my research. Thanks to Paul Martin for teaching me cell-culturing techniques and scanning electron microscopy. Thanks to Carlos Beltran, Bob Hadba, and Kaustubh Rau for their insight, friendship, support and technical assistance. Thanks to Jennifer Russo for her insights, her questions, her ability to make me laugh and to let me be myself, her support, and her true friendship.

Finally, I could not have completed this work without the love and support of my family. Thanks to Mom, Jim, Brad, Cindy, Heather, Bill, and Dad for continuing to believe in me even when my own faith in me was faltering. Thanks for your encouragement, your gentle persuasion, your care, and concern. Thanks to Nick and Greg for being so understanding and so patient. Last but definitely not least, thanks to Jeff. My deepest gratitude to you for believing in me and not letting me quit, for your technical assistance and encouragement, for your shoulder to cry on and being there to celebrate with, for your patience and understanding, and for your love and support.

TABLE OF CONTENTS

ACKNOWLEDGEMENTS iv

LIST OF TABLES viii

LIST OF FIGURES x

ABSTRACT xviii

1. INTRODUCTION 1

2. BACKGROUND 4

- The Natural Vascular Vessel 4
- Vascular Prostheses 8
- Electrical Stimulation 11
  - *In Vitro* Electrical Stimulation Studies 11
  - *In Vivo* Electrical Stimulation For Wound Healing 22
    - Bone 35
    - Skin 36
    - Connective Tissue 37
    - Internal Wounds 38
- Vascular Systems and Blood Flow 39
- Substrates Studied in Previous Research 40
  - Indium Tin Oxide 40
  - Carbon 40
  - Gold and Palladium 41
  - Polypyrrole 41
- Objectives of This Research 42

3. MATERIALS 44

- Endothelial Cells 44
- Indium Tin Oxide Glass 44
- Poly(ethylene terephthalate) 44
- Indium Tin Oxide-coated Poly(ethylene terephthalate) 45
- Carbon-coated Mylar® 46
- Gold-Palladium-coated Mylar® 47
- Polypyrrole-coated Dacron® 47
- Growth Medium 48
- Trump's Fixative Solution 49

4. METHODS 50
  Porcine Endothelial Cell Harvesting 50
  Porcine Endothelial Growth Technique 51
  Porcine Endothelial Cell Splitting 52
  Porcine Endothelial Cell Freezing 52
  Porcine Endothelial Cell Thawing 53
  Porcine Endothelial Cell Fixing and Staining 53
  Porcine Endothelial Cell Dehydration 54
  Cell Concentration Experiment 54
  Effect of Trump's Fixative on Morphology 55
  Feeding Rate Experiment 57
  Cytotoxicity Experiments 58
  Chamber Slide Modification 58
  Pilot Experiment for Voltage Effects 58
  Electrostimulated Growth Experiments 59
  Adhesion Experiments 62
  Cell Motility Experiments 67
  Characterization Techniques 68
    Optical Microscopy 68
    Scanning Electron Microscopy 68
    6-keto-Prostaglandin-$F_{1\alpha}$ Assay 69
    Resistivity 70
    Contact Angle 70

5. RESULTS AND DISCUSSION 71

  Cell Concentration Experiment 71
  Effect of Trump's Fixative 72
  Feeding Rate Experiment 77
  Substrate Characterization 82
  Cytotoxicity Experiments 85
  Pilot Experiment for Voltage Effects 88
  Electrostimulated Cell Growth Experiments at 0 to 1 Volt 91
    Summary of Electrostimulated Cell Growth Experiments 116
  Cell Adhesion Experiments 120
    Summary of Cell Adhesion Experiments 131

6. SUMMARY AND CONCLUSIONS 136

7. SUGGESTED FUTURE WORK 138
  Biological Developments 138
  Materials Developments 139

REFERENCES 140

BIOGRAPHICAL SKETCH 157

LIST OF TABLES

Table page

2.1 Tensile Properties of Dacron® and e-PTFE Vascular Grafts 9

5.1 Resistivities of Test Substrates 82

5.2 Contact Angles of Test Substrates 82

5.3 Relative Favorability of Voltages in Growth Experiments 91

5.4 Statistical Significance of Cell Counts when Comparing Substrates with Cell Concentrations of 50,000 cells/mL in Growth Experiments 101

5.5 Statistical Significance of Cell Counts when Comparing Substrates with Cell Concentrations of 100,000 cells/mL in Growth Experiments 101

5.6 Statistical Significance of Cell Counts when Comparing Voltages with Cell Concentrations of 50,000 cells/mL in Growth Experiments 102

5.7 Statistical Significance of Cell Counts when Comparing Voltages with Cell Concentrations of 100,000 cells/mL in Growth Experiments 102

5.8 Currents Through Individual Growth Samples 103

5.9 Statistical Significance of Concentrations of 6-k-PGF$_{1a}$ when Comparing Substrates with Cell Concentrations of 50,000 cells/mL in Growth Experiments 113

5.10 Statistical Significance of Concentrations of 6-k-PGF$_{1a}$ when Comparing Substrates with Cell Concentrations of 100,000 cells/mL in Growth Experiments 114

5.11 Statistical Significance of Concentrations of 6-k-PGF$_{1a}$ when Comparing Voltages with Cell Concentrations of 50,000 cells/mL in Growth Experiments 114

5.12 Statistical Significance of Concentrations of 6-k-PGF$_{1a}$ when Comparing Voltages with Cell Concentrations of 100,000 cells/mL in Growth Experiments 115

5.13 Relative Favorability of Voltages for Release of 6-k-PGF$_{1\alpha}$ in Growth Experiments 115

5.14 Statistical Significance of Cell Counts when Comparing Substrates with Cell Concentrations of 50,000 cells/mL in Adhesion Experiments 126

5.15 Statistical Significance of Cell Counts when Comparing Substrates with Cell Concentrations of 100,000 cells/mL in Adhesion Experiments 127

5.16 Statistical Significance of Cell Counts when Comparing Voltages with Cell Concentrations of 50,000 cells/mL in Adhesion Experiments 127

5.17 Statistical Significance of Cell Counts when Comparing Voltages with Cell Concentrations of 100,000 cells/mL in Adhesion Experiments 128

5.18 Currents Through Individual Adhesion Samples 128

5.19 Statistical Significance of Concentrations of 6-k-PGF$_{1a}$ when Comparing Substrates with Cell Concentrations of 50,000 cells/mL in Adhesion Experiments .135

5.20 Statistical Significance of Concentrations of 6-k-PGF$_{1a}$ when Comparing Substrates with Cell Concentrations of 100,000 cells/mL in Adhesion Experiments135

LIST OF FIGURES

Figure page

1.1 Cumulative Patency vs. Time for Vascular Graft Materials 2

2.1 Schematic Diagram of the Cross-section of a Vessel Wall 5

2.2 Endothelial Cells: Spread Morphology 7

2.3 Endothelial Cells: Ball and Stick Morphology 7

2.4 Endothelial Cells: Rounded Morphology 7

2.5 Qualitative comparisons of factors showing 75% or more cell viability in *in vitro* studies. Areas in black show that (1) surface roughness had the highest cell viability of all the sources of charge, and (2) DC can increase cell viability 13

2.6 Qualitative comparisons of factors showing 75% or more cell viability in *in vitro* studies. Areas in black show that (1) no particular voltage had a significant affect on cell viability, and (2) a capacitance of 0.94 had the highest cell viability. 14

2.7 Qualitative comparisons of factors showing increased cell proliferation in *in vitro* studies. Areas in black show that (1) voltage, surface charge, and magnetic fields were the primary sources of charge to promote cell proliferation, and (2) DC had a limited effect on cell proliferation. 15

2.8 Qualitative comparisons of factors showing increased cell proliferation in *in vitro* studies. Areas in black show that (1) a wide range of voltages had a positive impact on cell proliferation, and (2) field strength had a limited impact on cell proliferation, although cell proliferation appears to increase more at low field strengths. 16

2.9 Qualitative comparisons of factors showing increased cell proliferation in *in vitro* studies. Areas in black show that (1) some studies reported low currents increased cell proliferation, and (2) sinusoidal and triangular sinusoidal waveforms were effective at increasing cell proliferation. 17

2.10 Qualitative comparisons of factors showing increased cell proliferation in *in vitro* studies. Areas in black show that (1) increased cell proliferation was not influenced by polarity, and (2) constant stimulation was somewhat more effective at increasing cell proliferation than is pulsed or approximately constant. 18

2.11 Qualitative comparisons of factors showing increased cell adherence in *in vitro* studies. Areas in black show that (1) surface charge and surface roughness had the most affect on increased cell adherence, and (2) lower frequencies increased cell adhesion more than higher frequencies. 19

2.12 Qualitative comparisons of factors showing increased cell adherence in *in vitro* studies. Areas in black show that (1) positive, polyionic and neutral surfaces increased cell adherence more than alternating or negatively charged surfaces, and (2) constant stimulation was somewhat more effective at increasing cell adhesion than was pulsed or approximately constant stimulation. 20

2.13 Qualitative comparisons of factors showing increased wound healing in *in vivo* studies. Areas in black show that (1) studies on both humans and animals showed successful wound healing, and (2) skin was the most common tissue, treated most successfully. 23

2.14 Qualitative comparisons of factors showing increased wound healing in *in vivo* studies. Areas in black show that (1) successful wound healing studies were performed on various animal species, and (2) stainless steel and silver nylon were the most effective electrodes for wound healing, although several showed positive results. 24

2.15 Qualitative comparisons of factors showing increased wound healing in *in vivo* studies. Areas in black show that (1) the size of electrodes was not a critical parameter for wound healing, although most successful studies used electrodes smaller than 100 cm^2, and (2) placement of electrodes anywhere except outside the wound area was effective for wound healing. 25

2.16 Qualitative comparisons of factors showing increased wound healing in *in vivo* studies. Areas in black show that (1) current was the most effective source of charge for increased wound healing, and (2) there was not a significant difference between AC and DC when comparing successful wound healing. 26

2.17 Qualitative comparisons of factors showing increased wound healing in *in vivo* studies. Areas in black show that (1) a broad range of voltages were effective for increased wound healing, and (2) currents below 100 mA increased wound healing in some cases. 27

2.18 Qualitative comparisons of factors showing increased wound healing in *in vivo* studies. Areas in black show that (1) current densities of 0.0049 or 0.51 mA/cm^2 were the most effective for wound healing, and (2) lower resistance showed increased wound healing. 28

2.19 Qualitative comparisons of factors showing increased wound healing in *in vivo* studies. Areas in black show that (1) several waveforms were effective for wound healing, and (2) frequencies less than 5000 Hz were the most effective for wound healing. 29

2.20 Qualitative comparisons of factors showing increased wound healing in *in vivo* studies. Areas in black show that pulse widths below 10 msec were most effective for wound healing. 30

2.21 Qualitative comparisons of factors showing increased wound healing in *in vivo* studies. Areas in black show that either positive or negative polarity, or alternating polarity, had a positive effect on wound healing. 31

2.22 Qualitative comparisons of factors showing increased wound healing in *in vivo* studies. Areas in black show that (1) a wide range of magnetic fields were effective in increasing wound healing, and (2) there was little difference in wound healing between pulsed and constant stimulation. 32

2.23 Qualitative comparisons of factors showing increased wound healing in *in vivo* studies. Areas in black show that (1) the length of treatment had little effect on wound healing, and (2) length of stimulation was also not a critical parameter for wound healing. 33

2.24 Qualitative comparisons of factors showing increased wound healing in *in vivo* studies. Areas in black show that (1) although increased wound healing was observed with up to three treatments per day, the most successful studies used one treatment per day, and (2) up to seven treatments per week were found to increase wound healing. 34

3.1 Structure of Poly(ethylene terephthalate)....45

3.2 Diagram of SC-Mylar Coatings....47

3.3: Structure of Polypyrrole....48

4.1 Configuration of Cell Concentration Experiment Culture Plate....55

4.2 Alternating Row Configuration of Trump's Experiment....56

4.3 Alternating Column Configuration of Trump's Experiment....56

4.4 Adjacent Column Configuration of Trump's Experiment....57

4.5 4-well plate Configuration of Trump's Experiment....57

4.6 Growth plate schematic....60

4.7 Photograph of Growth Plate....61

4.8 Incubation/Stimulation Chamber....63

4.9 Adhesion Flow Chamber....64

4.10 Typical flow Waveform of the Adhesion Flow Chamber....................................67

5.1 Cell Counts as a Function of Time at Various Cell Concentrations..........................72

5.2 Alternating Row Configuration of Trump's Experiment...73

5.3 Alternating Column Configuration of Trump's Experiment......................................74

5.4 Adjacent Column Configuration of Trump's Experiment..75

5.5 4-well plate Configuration of Trump's Experiment..76

5.6 Feeding Rate Study: 50,000 cells/mL at 18 hours..78

5.7 Feeding Rate Study: 100,000 cells/mL at 18 hours..79

5.8 Feeding Rate Study: 50,000 cells/mL at 48 hours..80

5.9 Feeding Rate Study: 100,000 cells/mL at 48 hours..81

5.10 SEM of Glass..83

5.11 SEM of Mylar 83

5.12 SEM of ITO-Glass..83

5.13 SEM of ITO-Mylar 84

5.14 SEM of C-Mylar...84

5.15 SEM of AuPd-Mylar...84

5.16 SEM of PPy-Dacron...85

5.17 Cytotoxicity Test with Glass 85

5.18 Cytotoxicity Test with Mylar 85

5.19 Cytotoxicity Test with ITO-Glass...86

5.20 Cytotoxicity Test with ITO-Mylar..86

5.21 Cytotoxicity Test with C-Mylar..86

5.22 Cytotoxicity Test with AuPd-Mylar 87

5.23 Cytotoxicity Test with PPy-Dacron 87

5.24 Endothelial Cells at 0 volts, 24 hours...88

5.25 Endothelial Cells at 0.5 volts, 24 hours....89

5.26 Endothelial Cells at 1 volt, 24 hours....89

5.27 Endothelial Cells at 2 volts, 24 hours....90

5.28 Endothelial Cells at 5 volts, 24 hours....90

5.29 Proliferation of Endothelial Cells on Glass....92

5.30 Proliferation of Endothelial Cells on Mylar....92

5.31 Proliferation of Endothelial Cells on ITO-Glass (50,000 cells/mL) at 0 volts, 0.5 volt, and 1 volt....93

5.32 Proliferation of Endothelial Cells on ITO-Glass (100,000 cells/mL) at 0 volts, 0.5 volt, and 1 volt....93

5.33 Proliferation of Endothelial Cells on ITO-Mylar (50,000 cells/mL) at 0 volts, 0.5 volt, and 1 volt....94

5.34 Proliferation of Endothelial Cells on ITO-Mylar (100,000 cells/mL) at 0 volts, 0.5 volt, and 1 volt....94

5.35 Proliferation of Endothelial Cells on C-Mylar (50,000 cells/mL) at 0 volts, 0.5 volt, and 1 volt....95

5.36 Proliferation of Endothelial Cells on C-Mylar (100,000 cells/mL) at 0 volts, 0.5 volt, and 1 volt....95

5.37 Proliferation of Endothelial Cells on SC-Mylar (50,000 cells/mL) at 0 volts, 0.5 volt, and 1 volt....96

5.38 Proliferation of Endothelial Cells on SC-Mylar (100,000 cells/mL) at 0 volts, 0.5 volt, and 1 volt....96

5.39 Proliferation of Endothelial Cells on AuPd-Mylar (50,000 cells/mL) at 0 volts, 0.5 volt, and 1 volt....97

5.40 Proliferation of Endothelial Cells on AuPd-Mylar (100,000 cells/mL) at 0 volts, 0.5 volt, and 1 volt....97

5.41 Growth Rate versus Conductivity for 50,000 cells/mL Growth Samples....98

5.42 Growth Rate versus Conductivity for 100,000 cells/mL Growth Samples....98

5.43 Growth Rate versus Contact Angle for 50,000 cells/mL Growth Samples....99

5.44 Growth Rate versus Contact Angle for 100,000 cells/mL growth samples....99

5.45 Statistical Significance Rankings of Cell Counts from Substrates used in Growth Experiments........100

5.46 Growth Rate versus Individual Sample Current for 50,000 cells/mL Growth Samples........103

5.47 Growth Rate versus Individual Sample Current for 100,000 cells/mL Growth Samples........104

5.48 Release of 6-k-PGF-1α from Endothelial Cells on Glass at 50,000 cells/mL and at 100,000 cells/mL........106

5.49 Release of 6-k-PGF-1α from Endothelial Cells on Mylar at 50,000 cells/mL and at 100,000 cells/mL........106

5.50 Release of 6-k-$PGF_{1\alpha}$ from Endothelial Cells on ITO-Glass (50,000 cells/mL) at 0 volts, 0.5 volt, and 1 volt........107

5.51 Release of 6-k-$PGF_{1\alpha}$ from Endothelial Cells on ITO-Glass (100,000 cells/mL) at 0 volts, 0.5 volt, and 1 volt........107

5.52 Release of 6-k-$PGF_{1\alpha}$ from Endothelial Cells on ITO-Mylar (50,000 cells/mL) at 0 volts, 0.5 volt, and 1 volt........108

5.53 Release of 6-k-$PGF_{1\alpha}$ from Endothelial Cells on ITO-Mylar (100,000 cells/mL) at 0 volts, 0.5 volt, and 1 volt........108

5.54 Release of 6-k-$PGF_{1\alpha}$ from Endothelial Cells on C-Mylar (50,000 cells/mL) at 0 volts, 0.5 volt, and 1 volt........109

5.55 Release of 6-k-$PGF_{1\alpha}$ from Endothelial Cells on C-Mylar (100,000 cells/mL) at 0 volts, 0.5 volt, and 1 volt........109

5.56 Release of 6-k-$PGF_{1\alpha}$ from Endothelial Cells on SC-Mylar (50,000 cells/mL) at 0 volts, 0.5 volt, and 1 volt........110

5.57 Release of 6-k-$PGF_{1\alpha}$ from Endothelial Cells on SC-Mylar (100,000 cells/mL) at 0 volts, 0.5 volt, and 1 volt........110

5.58 Release of 6-k-$PGF_{1\alpha}$ from Endothelial Cells on AuPd-Mylar (50,000 cells/mL) at 0 volts, 0.5 volt, and 1 volt........111

5.59 Release of 6-k-$PGF_{1\alpha}$ from Endothelial Cells on AuPd-Mylar (100,000 cells/mL) at 0 volts, 0.5 volt, and 1 volt........111

5.60 Release of 6-k-$PGF_{1\alpha}$ from Endothelial Cells on PPy-Dacron (50,000 cells/mL) at 0 volts, 0.5 volt, and 1 volt........112

5.61 Release of 6-k-PGF$_{1\alpha}$ from Endothelial Cells on PPy-Dacron (100,000 cells/mL) at 0 volts, 0.5 volt, and 1 volt 112

5.62 Statistical Significance Rankings of 6-k-PGF$_{1\alpha}$ Release from Endothelial Cells on Substrates used in Growth Experiments 113

5.63 Release Rate of 6-k-PGF$_{1\alpha}$ versus Conductivity for 50,000 cells/mL Growth Samples 117

5.64 Release Rate of 6-k-PGF$_{1\alpha}$ versus Conductivity for 100,000 cells/mL Growth Samples 117

5.65 Release Rate of 6-k-PGF$_{1\alpha}$ versus Contact Angle for 50,000 cells/mL Growth Samples 118

5.66 Release Rate of 6-k-PGF$_{1\alpha}$ versus Contact Angle for 100,000 cells/mL Growth Samples 118

5.67 Release Rate of 6-k-PGF$_{1\alpha}$ versus Individual Sample Current for 50,000 cells/mL Growth Samples 119

5.68 Release Rate of 6-k-PGF$_{1\alpha}$ versus Individual Sample Current for 100,000 cells/mL Growth Samples 119

5.69 Adhesion of Endothelial Cells on Glass 121

5.70 Adhesion of Endothelial Cells on Mylar 121

5.71 Adhesion of Endothelial Cells on ITO-Glass (50,000 cells/mL) at 0 volts, 0.5 volt, and 1 volt 122

5.72 Adhesion of Endothelial Cells on ITO-Glass (100,000 cells/mL) at 0 volts, 0.5 volt, and 1 volt 122

5.73 Adhesion of Endothelial Cells on ITO-Mylar (50,000 cells/mL) at 0 volts, 0.5 volt, and 1 volt 123

5.74 Adhesion of Endothelial Cells on ITO-Mylar (100,000 cells/mL) at 0 volts, 0.5 volt, and 1 volt 123

5.75 Adhesion of Endothelial Cells on C-Mylar (50,000 cells/mL) at 0 volts, 0.5 volt, and 1 volt 124

5.76 Adhesion of Endothelial Cells on C-Mylar (100,000 cells/mL) at 0 volts, 0.5 volt, and 1 volt 124

5.77 Adhesion of Endothelial Cells on AuPd-Mylar (50,000 cells/mL) at 0 volts, 0.5 volt, and 1 volt 125

5.78 Adhesion of Endothelial Cells on AuPd-Mylar (100,000 cells/mL) at 0 volts, 0.5 volt, and 1 volt 125

5.79 Statistical Significance Rankings of Cell Counts from Substrates used in Adhesion Experiments 126

5.80 Cell adhesion versus Conductivity for 50,000 cells/mL adhesion samples 129

5.81 Cell adhesion versus Conductivity for 100,000 cells/mL adhesion samples 129

5.82 Cell adhesion versus Contact Angle for 50,000 cells/mL adhesion samples 130

5.83 Cell adhesion versus Contact Angle for 100,000 cells/mL adhesion samples 130

5.84 Release of 6-k-PGF$_{1\alpha}$ from Endothelial Cells on Glass at 50,000 cells/mL and at 100,000 cells/mL 132

5.85 Release of 6-k-PGF$_{1\alpha}$ from Endothelial Cells on Mylar at 50,000 cells/mL and at 100,000 cells/mL 132

5.86 Release of 6-k-PGF$_{1\alpha}$ from Endothelial Cells on ITO-Glass at 50,000 cells/mL and at 100,000 cells/mL 133

5.87 Release of 6-k-PGF$_{1\alpha}$ from Endothelial Cells on ITO-Mylar at 50,000 cells/mL and at 100,000 cells/mL 133

5.88 Release of 6-k-PGF$_{1\alpha}$ from Endothelial Cells on C-Mylar at 50,000 cells/mL and at 100,000 cells/mL 134

5.89 Release of 6-k-PGF$_{1\alpha}$ from Endothelial Cells on AuPd-Mylar at 50,000 cells/mL and at 100,000 cells/mL 134

Abstract of Dissertation Presented to the Graduate School
of the University of Florida in Partial Fulfillment of the
Requirements for the Degree of Doctor of Philosophy

ELECTRICAL FIELD EFFECTS ON ENDOTHELIAL CELL ADHESION AND GROWTH ON CONDUCTING BIOMATERIALS SURFACES

By

Gwen Elaine Clark

May 1999

Chairman: Eugene P. Goldberg
Major Department: Materials Science and Engineering

A major problem for vascular graft implants is poor long-term patency for small-diameter (<6 mm) prostheses. Small-diameter woven Dacron® or expanded polytetrafluoroethylene (e-PTFE) grafts often occlude in a short time due to thrombus or intimal hyperplasia. It has generally been considered that an endothelial cell lining of such grafts might reduce thrombogenicity and thereby produce a more biomimetic prosthesis.

Electrical stimulation has been studied for effects on *in vitro* cell growth, motility, and adhesion characteristics, as well as for *in vivo* wound healing. A comprehensive literature review was conducted which suggested the need for further research concerning the effects of electrical fields on endothelial cell adhesion and growth properties.

The focus of these studies was therefore to determine the effect of electrical fields on the proliferation and adhesion characteristics of endothelial cells cultured on various substrates using low-voltage direct current. Voltages of 0, 0.5, and 1 volt were used for *in vitro* endothelial cell cultures plated at 50,000 and 100,000 cells/mL. Growth experiments were performed on glass, Mylar®, Indium Tin Oxide (ITO)-glass, on ITO-, carbon-, and gold-palladium-coated Mylar®, and on polypyrrole-coated Dacron®. Proliferation of endothelial cells was determined at 12, 24, and 36 hours. Adhesion characteristics were measured using a novel flow adhesion system. Characterization was via cell staining in conjunction with optical microscopy and a 6-keto-prostaglandin-F$_{1\alpha}$ assay to measure cell viability.

Results of these cell growth studies in electric fields indicate that low voltage stimulation moderately increased endothelial cell growth on most substrates. The release of 6-keto-prostaglandin-F$_{1\alpha}$ decreased over time at most cell concentrations and voltage levels. Cell adhesion experiments provided contrary results to the growth studies and suggested that low-voltage electric fields may be detrimental to cell adhesion. These findings imply that current density may be more important than voltage drop across a surface.

Based on this research, further studies of low-voltage electric field effects on endothelial cell growth characteristics appear warranted, with emphasis on cell adhesion; with the ultimate goal of increasing endothelialization and patency for small-diameter vascular grafts and other vascular prostheses.

CHAPTER 1
INTRODUCTION

One of the most common complications in vascular procedures today is damage to the endothelial lining of the blood vessels. This typically is seen after surgical procedures (e.g., balloon angioplasty), mechanical manipulation, exposure to cardioplegic solutions, or after placement of a synthetic vascular graft where the endothelial cell lining is non-existent (e.g., Dacron® vascular graft) (Pop 90, Zil 93).

The vascular graft market has sales of over $200 million worldwide. Dacron® grafts are implanted in 350,000 cardiovascular surgeries per year, and the other approximately 20 percent of the total market is e-PTFE grafts (Bro 95a, Gol 96). Most vascular grafts are implanted because of atherosclerosis, both occlusional and aneuryismal (Gre 91).

There are many requirements for vascular grafts. To provide long-term patency, they must be bioacceptable, nontoxic, durable yet compliant, non-irritating to tissue, non-thrombogenic, non-degradable, and infection resistant, and they must release no foreign bodies into the bloodstream (Bro 95a, Gre 91). There are currently no materials available that provide all these requirements for long-term patency of small diameter grafts. However, Dacron® and e-PTFE grafts offer biocompatibility, resiliency, flexibility, durability, and resistance to sterilization and biodegradation (Bro 95a).

Large-diameter vessels (greater than 6 mm inner diameter) made from these two materials, when placed in vessels that have higher flow rates, generally do not occlude even though the surfaces are thrombogenic and do not encourage endothelial cell growth. In fact, they have been reported to exhibit greater than 95 percent patency at five years (Gre 91). In contrast, small-diameter vascular grafts occlude within a much shorter period of time as shown in Figure 1.1 (Abb 80). The causes of occlusion are typically thrombosis, which is often seen in the first six months, or intimal hyperplasia, which is generally seen within 6 months to 2 years after implantation (Gre 91). Occlusion leads to ischemia and usually the need for additional surgery.

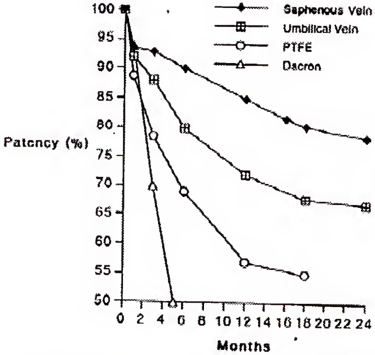

Figure 1.1: Cumulative Patency vs. Time for Vascular Graft Materials (taken from Abb 80)

The endothelial lining of blood vessels limits thrombosis through a complex and dynamic process. When minor damage occurs to the endothelium (e.g., denuded area 1 to 2 cells in width), endothelial cells are replaced within 6 to 8 hours. Denuded areas 2 to 20 cells wide do not increase smooth muscle cell proliferation, and smooth muscle cell lesions form only in areas of the denuded endothelium that take more than 7 days to heal. These data indicate that a critical amount of endothelium must be damaged before endothelialization is seriously compromised (Sta 91). If a vascular graft could be formed with an endothelial cell lining, it is anticipated to be non-thrombogenic and function more like a natural vessel (Tsu 93).

A primary area of research to increase patency in vascular prostheses has been to seed with endothelial cells before implanting. This technique has been successful in *in vivo* animal studies, including canine, sheep, and baboon models (Gol 90, Jam 90, Pas 96). Unfortunately, the same level of success has not been observed in human subjects (Smy 95, Pas 90, Wel 92).

In wound-healing research, electrical stimulation has been used to increase bone, dermal, and soft tissue healing rates, experimentally and clinically. Research has also shown that cell motility, adhesion, and growth are affected by electrical stimulation. Repair or growth of endothelial cells may be viewed as a wound-healing process. Wong, et al. have shown that endothelial cells can be grown on polypyrrole, an electrically conducting polymer, when it is electrically charged (Won 94).

The general goal of this research is to obtain a confluent endothelial cell lining in vascular grafts to increase the patency of small-diameter grafts by reducing the thrombogenicity and realizing a more biomimetic prosthesis. It is thought that this might be achieved by electrical stimulation of endothelial cell growth and adhesion on Dacron® or e-PTFE vascular grafts. This particular study therefore was designed to explore the effect of electrical stimulation on endothelial cell growth rates and adhesion characteristics on various substrates.

CHAPTER 2
BACKGROUND

The Natural Vascular Vessel

Natural vessels are made up of three distinct layers- the tunica adventitia, the tunica media, and the tunica intima (otherwise known as the endothelium). The tunica adventitia, composed of extracellular matrix, elastic, and collagenous fibers, provides the mechanical integrity of the vessel. The tunica media provides contraction of the vessel, with smooth muscle cells arranged in spiraling layers and circular elastic fibers. The endothelium (tunica intima) is a layer of endothelial cells, which are sheet-like in nature, with a sublayer of connective tissue and circular elastin fibers. Elastic layers, known as the internal and external elastic membranes, store energy and provide an consistent, pulsatile flow of blood through the vessel. Figure 2.1 shows a schematic of the cross-section of an artery. (And 94, Bro 95a).

The endothelial cells which form the lining of blood vessels exhibit several key properties in the functionality of the blood vessel. They allow for blood compatibility via anti-coagulants present in surface components and through cellular metabolism. They form a permeability layer through which only certain chemicals are transported and form a barrier to others such as lipids, circulating cytokines and growth factors. Endothelial cells also control interactions with other cells such as macrophages. They control myogenic tone through excretion of vasodilators (e.g. prostacyclin) and vasoconstrictors (e.g. thromboxane). Endothelial cells regulate the pathological consequences of vascular injury, disorders such as atherosclerosis, and wound healing by regulating smooth muscle cell proliferation and modulating extracellular protein production and degradation (Dav 95).

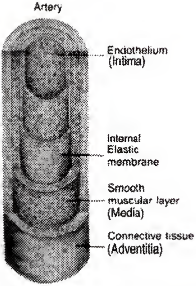
Artery
Endothelium (Intima)
Internal Elastic membrane
Smooth muscular layer (Media)
Connective tissue (Adventitia)

Figure 2.1 Schematic Diagram of the Cross-section of a Vessel Wall (And 94)

Endothelial cells generally extend 50-100 μm in length (Sar 95). Hemodynamic factors influence endothelial cell biology (Dav 95). It has been shown that in laminar flow, cells align in the direction of the shear stress, and there is little cell turnover (Dav 84). If a vessel is denuded of its endothelium, reendothelialization usually occurs within 7-10 days. However, the function of the endothelium remains abnormal for 4-12 weeks, and prostacyclin (PGI_2) release may be permanently reduced (Zil 93).

Endothelial cells vary from species to species. The ultimate application of this research is to test electrical stimulation on human endothelial cells. However, porcine endothelial cells harvested from the pulmonary vein were used because they are more robust. The research was therefore focused on growth and adhesion characteristics of porcine endothelial cells rather than on the methods to grow and maintain viability of human endothelial cells.

The morphology of endothelial cells *in vitro* is an indication of cell health. If the cells are well spread as shown in Figure 2.2, they are considered to be healthy and well adjusted to their growth environment. Figure 2.3 shows the ball and stick morphology of endothelial cells which indicates that growth conditions are not ideal, but the cells are still alive and growing. When the cells are rounded, as shown in Figure 2.4, they are very unhealthy, denoting poor growth conditions.

PGI_2 is a vasodilator and an inhibitor of platelet aggregation that is excreted from endothelial cells even after numerous subcultures *in vitro* (Mon 82). It has been shown that arteries produce more PGI_2 than veins and that its half-life is 3 minutes in 37°C blood. PGI_2 inhibits white cell adherence to vessel walls lined with endothelial cells and also changes the deformability of red blood cells (Mon 82). PGI_2 protects platelets against deterioration, cardiac myocytes against hypoxic damage, glial cells and neurons against anoxic injury, and hepatocytes against chemical damage *in vitro* (Bot 89).

While PGI_2 does inhibit platelet aggregation, it does not affect platelet adhesion (Zil 93). Uninjured endothelial cells in the vicinity of an injured area will increase PGI_2 production to counterbalance the thrombogenicity of that area. This is the cellular response to the secretion of clotting factors and platelet secretions (Zil 93). However, there is a delicate physiological balance between PGI_2 and thromboxane (TXA_2) activities between beneficial reparation and detrimental thrombogenisis (Sta 91). This balance also regulates vascular tone and a "background" vasodilating tone which constantly prevents vasospasm (Zil 93).

Johnson et al. showed that cultures of endothelial cells from pulmonary and umbilical vessels formed PGI_2 in response to mechanical stimulation (Joh 80). Further research was published indicating that confluent subcultures of endothelial cells produced less PGI_2 than shortly after they were split or fed (Age 82). Levels of PGI_2 production per cell are inversely related to cell density, and they increase with rapid cell proliferation or exposure to traumatic stimuli (Age 82). Gillis et al. reported that stimulated cells seeded on expanded polytetrafluoroethylene (e-PTFE) grafts precoated with Collagen Type-1 and on porcine aorta showed high production levels of PGI_2 (Gil 96).

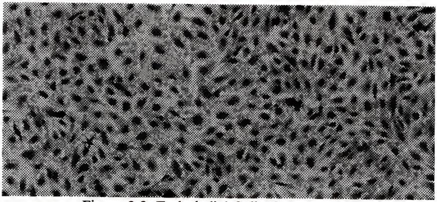

Figure 2.2 Endothelial Cells: Spread Morphology

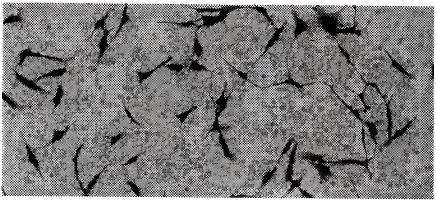

Figure 2.3 Endothelial Cells: Ball and Stick Morphology

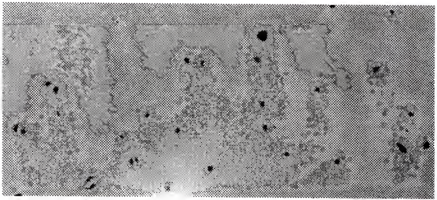

Figure 2.4 Endothelial Cells: Rounded Morphology

Reports indicate that *in vivo* PGI_2 promotes healing of ischemic skin ulcers via intravenous infusion, and it protects against post-ischemic reperfusion damage to animal brains and hearts. Additionally, continuous infusions for up to 2 years allowed patients with severe pulmonary hypertension to live independent lives while awaiting heart-lung transplants (Bot 89).

Since the half-life of PGI_2 is so short, the stable breakdown product, 6-keto-prostaglandin-$F_{1\alpha}$ (6-k-$PGF_{1\alpha}$), is typically used as an indication of PGI_2 levels. The 6-k-$PGF_{1\alpha}$ is typically measured via radioimmunoassay or Enzyme-Linked Immunosorbent Assay (ELISA) where 6-k-$PGF_{1\alpha}$ and enzyme conjugate compete for a limited number of binding sites on an antibody-coated plate (Neo 98).

Vascular Prostheses

Woven Dacron® vascular grafts, when implanted without coatings or seeded endothelial cells, are thrombogenic and are not conducive to endothelial cell growth. In fact, endothelium only regenerates 1-2 cm from both anastomoses. This is a result of some cell migration and proliferation from the adjacent artery. The endothelial cell proliferation is high near the anastomoses but further endothelialization does not occur (Gre 91). Because an endothelial lining does not form on Dacron® or e-PTFE grafts, thrombogenicity continues to be an issue. Smooth muscle cell growth involved in intimal hyperplasia is not controlled, resulting in graft failure (Zil 93).

Vascular grafts are commonly made of Dacron® tubes, either knitted or woven with various crimping patterns employed, or expanded polytetrafluoroethylene (e-PTFE). Typical tensile properties of woven Dacron® and e-PTFE vascular grafts are shown in Table 2.1 (All 90, Bro 95a, Dav 84, Wid 96).

Table 2.1: Tensile Properties of Dacron® and e-PTFE Vascular Grafts

Property	Dacron®	e-PTFE
Tensile Strength	700 MPa	14 MPa
Elongation	30 to 300%	200 to 400%
Tensile Modulus	2.8 GPa - 4.2 GPa	0.5 GPa
Hydrophobicity	hydrophobic	hydrophobic

Although there are many problems associated with both Dacron and e-PTFE grafts, they continue to be used because in large-diameter vessels (> 6 mm) they work reasonably well and extend the lives of many patients. Surgeons use Dacron® grafts because of their good handling characteristics, due in part to knitting techniques and crimping techniques for woven fabrics (Bro 95a, Gre 91, Sta 91).

Grafts made of e-PTFE are preferred for small diameter vascular grafts because they have a lower platelet activating potential than Dacron®, and they elicit an angiogenic healing response (Zil 93). e-PTFE also offers the following benefits: impermeability to blood (negates the need for preclotting), resistance to aneuryismal formation, ease of declotting, low thrombogenicity, and superior handling qualities (Gre 91, Sta 91).

Zacharias et al. published a comparison of 4 mm Dacron® and e-PTFE grafts in baboons. Grafts were assessed for percent endothelial coverage, endothelial cell proliferation, intimal area, and smooth muscle cell proliferation at 2, 4, and 12 weeks. e-PTFE grafts were completely covered with endothelial cells at all three time periods and only 5 of 22 total Dacron® grafts were covered. The intima of the e-PTFE grafts consisted of only endothelial cells and smooth muscle cells. Dacron® had both cell types as well but also had thrombus. All other responses were similar between the two types of grafts (Zac 87).

Another study by Zacharias et al. showed that e-PTFE graft healing in baboons is related to the porosity size of the graft. Results indicated that grafts of 60µm porosity heal most quickly in baboons after 1 and 3 months. Graft healing was markedly worse with larger or smaller pore sizes (Gol 90). The 60µm porous e-PTFE grafts develop a complete endothelial layer 2 weeks after implantation in baboons. The intima of these grafts thicken, contrary to uninjured arteries, due to the proliferation of smooth muscle cells that have an overlying endothelial layer present. This research suggests that the growth of smooth muscle cells is regulated by factors produced by vascular wall cells (Zac 88).

Different methods of obtaining endothelial linings for prosthetic materials have been developed, including facilitated endothelial cell migration and endothelial cell seeding with venous or microvascular endothelial cells (Zil 93). Much work has been done to refine these techniques. Positive results have frequently been seen in animal models, but that success has not been observed in human studies.

Single-staged seeding using venous cells entails removing venous cells and directly seeding them onto the vascular graft to be implanted. The problem with this approach is that most people do not have a sufficient number of cells to reach a minimum seeding level, and cells wash away when implanted. Microvascular cells have also been used to seed arterial prostheses, but results were inconclusive, since contamination of other cell types was found.

In two-staged seeding, the patient donates endothelial cells which are then cultured for several weeks to obtain the quantities of cells necessary for successful implantation. Results have been promising with this technique. The *in vitro*-lined endothelium has persisted and shown low thrombogenicity. However, the procedures must be carried out in the vicinity of cell culturing facilities and the waiting period for the cell culturing is often longer than patients can wait (Zil 93).

Electrical Stimulation

Many wounded tissues exhibit changes in the electrical potentials normally associated with them, including the peritoneal cavity, the epithelial surface of the cornea, and the skin (Can 31, Soo 90, She 96, Igl 96, Chi 92, Dav 93, Bar 45). These electrical potential changes have been credited with attracting electrostatically charged particles, stimulating cell migration (galvanotaxis), and increasing the rate of wound healing. It is less clear at the present time whether the electrical potential gradients are a specific result of injury or whether they are always present.

In Vitro Electrical Stimulation Studies

A comprehensive literature review was performed in order to determine appropriate electrical stimulation parameters to be used in this research (Nae 91, Tam 93, Rap 95b, Mak 93, Ish 94, Ito 95, Sho 92, Gho 93, Val 93, Rap 95a, Eri 84, Bro 94, She 96, Soo 90, Spa 95, Nuc 83, Soo 90b, Moh 94, Rob 85, Ros 90, Koj 91, Lyt 91, Kat 95, Guz 94, Fit 92, Tao 90, Val 92, Bad 93, Lib 93, Mar 91, Nor 93, Par 93, Liv 91, Kin 89, Lam 97, Sch 97, Kot 96, Lee 94, Tam 94, Pig 97, Nuc 88).

Comparing the *in vitro* experiments cited in the literature quantitatively was perplexing since there were no common parameters between studies by different authors. Figures 2.5-2.8 show a qualitative analysis of the information given in the literature. Indicated is the effect of several parameters on cell viability, proliferation, and adhesion. The black regions denote studies with successful results using that specific parameter. From these graphs, it is evident that low voltages (between 0 and 20,000 mV, generally best between 0 and 1000 mV) increase the viability and proliferation of cells. Direct current (DC) was more effective than alternating current (AC). Constant stimulation was more effective than pulsed. The most effective current level according to these graphs is between 0.1 and 5 μA. These values were used in determining the electrical parameters used in the research presented in this dissertation.

Electrical currents have been shown to both stimulate and retard cell growth. More normal cell growth has been observed in some cases with reduction in tumor growth, and the growth of some other cell types has been enhanced. One example of this phenomenon, described by Vodovnik et al. is that the transmembrane potential (TMP) of cells is changed so that the TMP of mature cells is reduced from its typically high value and the TMP of cancerous cells is increased from its normally low value (Vod 92b). The conclusion is that growth of healthy cells may be increased and proliferation of cancerous cells reduced. Other research has shown that the effect on cells is simply due to the electrical parameters used. If the frequency, amplitude, or voltage are in one specific range, cell growth is stimulated. If they are outside that range, no increase in cell proliferation is observed (Ros 90, Koj 91, Lyt 91, Yao 90).

Britland et al.; Kato et al.; and Guzelsu et al. have shown that electrical stimulation can indeed promote cell growth and increase the rate of wound healing (Bri 96, Kat 95, Guz 94). Fitzsimmons et al. published research on bone cell proliferation that indicates the cell growth is mediated by increased release of growth factors due to low-amplitude, low-frequency electrical field stimulation (Fit 92). Sakai et al. reported that pulsed electromagnetic fields increased rabbit and human cartilage cell proliferation via a cellular membrane dependent mechanism (Sak 91).

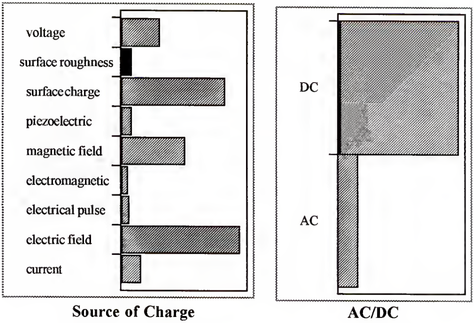

Source of Charge

Level	Count
current	17
electric field	93
electrical pulse	8
electromagnetic	7
magnetic field	51
piezoelectric	10
surface charge	82
surface roughness	10
voltage	32
Total	310

AC/DC

Level	Count
AC	15
DC	89
Total	104

Figure 2.5 Qualitative comparisons of factors showing 75% or more cell viability in *in vitro* studies. Areas in black show that (1) surface roughness had the highest cell viability of all the sources of charge, and (2) DC can increase cell viability.

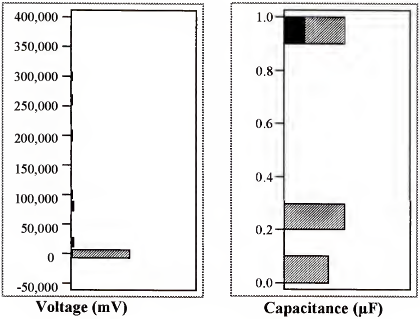

Level	**Count**
<0	1
0-10,000	50
10,000-50,000	4
50,001-100,000	7
100,001-150,000	2
150,001-200,000	2
200,001-250,000	3
250,001-300,000	3
300,001-400,000	1
Total	73

Level	**Count**
0.01	6
0.2	8
0.94	8
Total	22

Figure 2.6 Qualitative comparisons of factors showing 75% or more cell viability in *in vitro* studies. Areas in black show that (1) no particular voltage had a significant affect on cell viability, and (2) a capacitance of 0.94 had the highest cell viability.

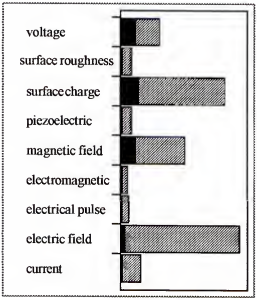

Source of Charge

Level	Count
current	17
electric field	93
electrical pulse	8
electromagnetic	7
magnetic field	51
piezoelectric	10
surface charge	82
surface roughness	10
voltage	32
Total	310

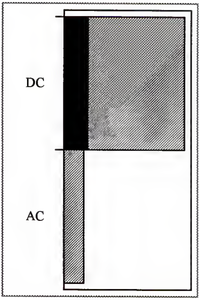

AC/DC

Level	Count
AC	15
DC	89
Total	104

Figure 2.7 Qualitative comparisons of factors showing increased cell proliferation in *in vitro* studies. Areas in black show that (1) voltage, surface charge, and magnetic fields were the primary sources of charge to promote cell proliferation, and (2) DC had a limited effect on cell proliferation.

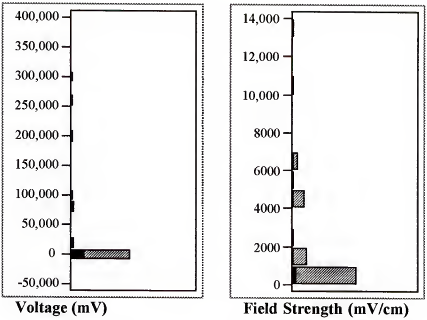

Level	Count
<0	1
0-10,000	50
10,000-50,000	4
50,001-100,000	7
100,001-150,000	2
150,001-200,000	2
200,001-250,000	3
250,001-300,000	3
300,001-400,000	1
Total	73

Level	Count
0-1000	49
1001-2000	7
2001-3000	1
3001-4000	9
4001-5000	2
5001-6000	5
10,000	2
13,000	2
Total	77

Figure 2.8 Qualitative comparisons of factors showing increased cell proliferation in *in vitro* studies. Areas in black show that (1) a wide range of voltages had a positive impact on cell proliferation, and (2) field strength had a limited impact on cell proliferation, although cell proliferation appears to increase more at low field strengths.

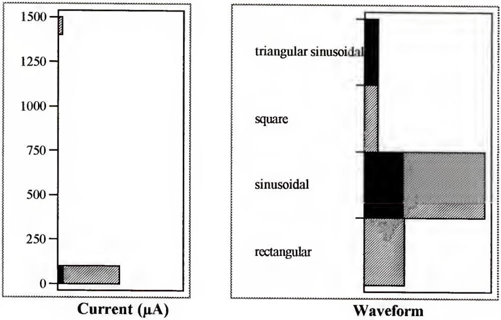

Level	**Count**
0-100	26
1500	2
Total	28

Level	**Count**
rectangular	3
sinusoidal	9
square	1
triangular sinusoidal	1
Total	14

Figure 2.9 Qualitative comparisons of factors showing increased cell proliferation in *in vitro* studies. Areas in black show that (1) some studies reported low currents increased cell proliferation, and (2) sinusoidal and triangular sinusoidal waveforms were effective at increasing cell proliferation.

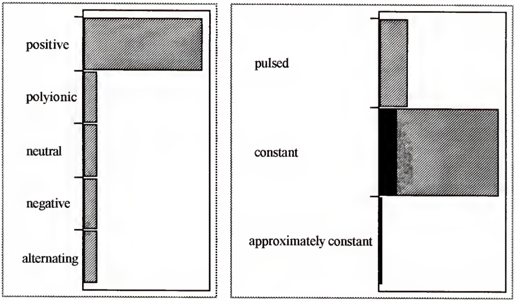

Polarity

Pulsed/Constant

Level	Count
alternating	1
negative	1
neutral	1
polyionic	1
positive	8
Total	12

Level	Count
approximately constant	5
constant	114
pulsed	28
Total	147

Figure 2.10 Qualitative comparisons of factors showing increased cell proliferation in *in vitro* studies. Areas in black show that (1) increased cell proliferation was not influenced by polarity, and (2) constant stimulation was somewhat more effective at increasing cell proliferation than is pulsed or approximately constant.

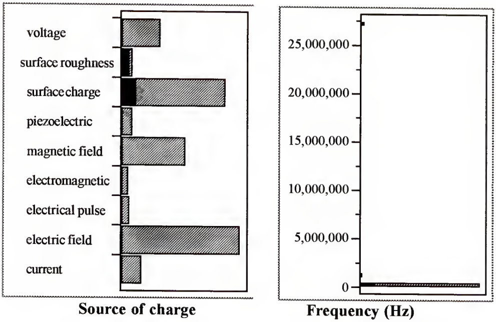

Level	Count
current	17
electric field	93
electrical pulse	8
electromagnetic	7
magnetic field	51
piezoelectric	10
surface charge	82
surface roughness	10
voltage	32
Total	310

Level	Count
0-1	9
10-100	35
1000-5000	31
1,000,000	2
27,120,000	3
Total	80

Figure 2.11 Qualitative comparisons of factors showing increased cell adherence in *in vitro* studies. Areas in black show that (1) surface charge and surface roughness had the most affect on increased cell adherence, and (2) lower frequencies increased cell adhesion more than higher frequencies.

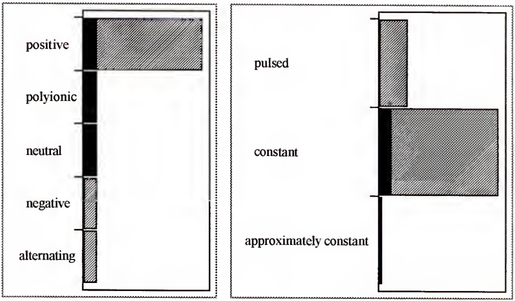

Polarity

Level	Count
alternating	1
negative	1
neutral	1
polyionic	1
positive	8
Total	12

Pulsed/Constant

Level	Count
approximately constant	5
constant	114
pulsed	28
Total	147

Figure 2.12 Qualitative comparisons of factors showing increased cell adherence in *in vitro* studies. Areas in black show that (1) positive, polyionic and neutral surfaces increased cell adherence more than alternating or negatively charged surfaces, and (2) constant stimulation was somewhat more effective at increasing cell adhesion than was pulsed or approximately constant stimulation.

Galvanotaxis, the directional locomotion of cells due to electrical fields, is apparent in a wide variety of cells and occurs at field strengths similar to those found physiologically. These electrical cues may be the reason cells migrate during embryogenesis and wound healing. Some of the observed motility is believed to be ionically regulated (Eri 84). Other research by Brown et al. show that some of these electrically stimulated motions are independent of calcium regulation and are solely dependent on the applied field (Bro 94). Sheridan et al., on the other hand, show that cell motility may be a combination of both electrical and physiological ionic currents (She 96). While these studies indicate that there may be different mechanisms by which the electric fields are produced, they generally agree that cells are sensitive to electric currents which is shown by their migration and alignment patterns (Soo 90, Rob 85).

The electromotility of guinea pig outer hair cells has been studied to better understand the mechanisms by which these cells move. This research is important in understanding the sensitivity of the cochlea at low stimulus intensities. It has been found that elementary motors are distributed along the length of the cells and are responsible for generating cell length change in response to a local command voltage. As these motors work together, the length of the cell changes in different areas resulting in motion (Hal 93).

Valentini et al. used piezoelectric polymers such as polyvinylidene fluoride (PVDF) to provide electrical charges to investigate effects on cell growth. Neurons showed more process outgrowth and greater neurite lengths when placed on positively- or negatively-charged PVDF versus uncharged samples (Val 92). This research has important implications in the nerve regeneration field.

The response of endothelial cell motility to electrical stimulation has been researched using a variety of techniques. Some researchers have studied the effects of growth factors with electric fields to promote motility (Fle 96, Bus 92, Tar 90). Techniques to encourage angiogenesis for wound healing with electrical stimulation have been the subject of other studies. Several researchers have also examined approaches to inhibit endothelial cell motility to reduce angiogenesis related to tumor growth (Nic 95, Nic 94, Ngu 93).

Adherence of cells is typically used as a measure of growth although few investigators have evaluated the effect of electrical stimulation on cell attachment itself. Kim et al. found that pulsed electromagnetic fields stimulated production of a cell spreading factor which in turn enhanced the adhesion of human periodontal ligament fibroblasts (Kim 90). A second study by Naegele et al. indicates that electrical stimulation increased the adherence of human osteosarcoma-derived cells (Nae 91).

In Vivo Electrical Stimulation for Wound Healing

The literature reviewed for an understanding of the effects of electrical stimulation on wound healing included: Lee 93, Lun 92, Rei 91, Chu 90, Cas 95, Kam 93, Ste 93, Gog 92, Woo 93, Gau 76, Chu 96, Ågr 94, Fee 85, Sal 95, Ito 91, Chu 91, Chu 95, Bro 95b, Ier 90, Klo 88, Pre 95, Mui 91, Fit 93, Gri 91, Byl 94, Lef 94, Fee 91, Mam 93, Cha 91, Sha 90, Moo 90, Kah 94, Muh 91, Bor 93, Kah 90, Lit 94, Lin 92, Lip 90, Sak 91, Gre 92, Sha 95, Bla 92, Per 87, Din 93.

Quantitative comparisons were difficult due to the many differences between studies even though there were some overlapping electrical parameters. Figures 2.9 - 2.15 qualitatively show the factors reported in the literature that increase wound healing. Most of the studies which showed an increase in wound healing used electromagnetic or current stimulation. Voltages up to 200 V and very low currents were most effective in improving healing rates. Additionally, lower current density, charge density, resistance, frequency, and repetition frequency showed increased healing. Pulse widths of less than 20 msec were associated with increased wound healing rates. There was no clear indication of success at a specific strength of magnetic field, length of time of treatment, length of time of stimulation or polarity. Best wound healing results were seen within 3 weeks of the start of the experiments.

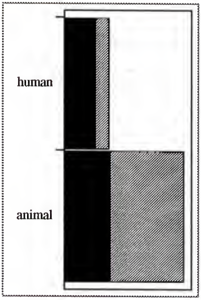

Human/Animal

Level	Count
animal	161
human	62
Total	223

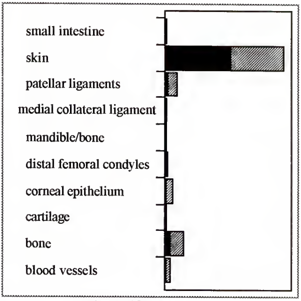

Tissue/Organ

Level	Count
blood vessels	9
bone	25
cartilage	3
corneal epithelium	12
distal femoral condyles	5
mandible/bone	2
medial collateral ligament	4
patellar ligaments	16
skin	143
small intestine	4
Total	223

Figure 2.13 Qualitative comparisons of factors showing increased wound healing in *in vivo* studies. Areas in black show that (1) studies on both humans and animals showed successful wound healing, and (2) skin was the most common tissue, treated most successfully.

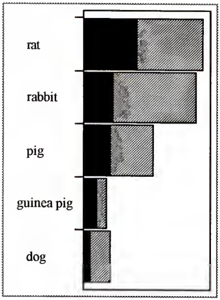

Animal Model

Level	Count
dog	13
guinea pig	11
pig	32
rabbit	51
rat	54
Total	161

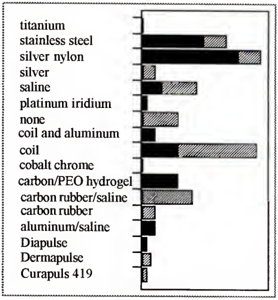

Type of Electrodes

Level	Count
Curapuls 419	2
Dermapulse	3
Diapulse	2
aluminum/saline	4
carbon rubber	4
carbon rubber/saline	14
carbon/PEO hydrogel	10
cobalt chrome	1
coil	31
coil and aluminum	4
none	10
platinum iridium	2
saline	15
silver	4
silver nylon	32
stainless steel	23
titanium	1
Total	162

Figure 2.14 Qualitative comparisons of factors showing increased wound healing in *in vivo* studies. Areas in black show that (1) successful wound healing studies were performed on various animal species, and (2) stainless steel and silver nylon were the most effective electrodes for wound healing, although several showed positive results.

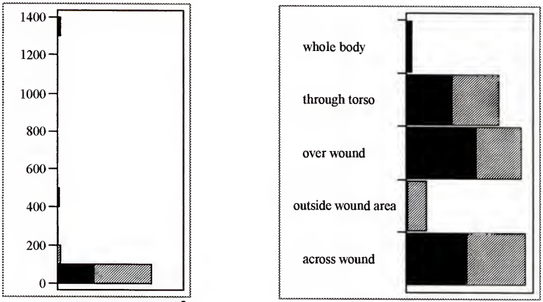

Size of Electrodes (cm^2)

Placement of Electrodes

Level	**Count**
0-100	96
100-200	3
220	1
410	2
1400	4
Total	106

Level	**Count**
across wound	66
outside wound area	12
over wound	64
through torso	52
whole body	4
Total	198

Figure 2.15 Qualitative comparisons of factors showing increased wound healing in *in vivo* studies. Areas in black show that (1) the size of electrodes was not a critical parameter for wound healing, although most successful studies used electrodes smaller than 100 cm^2, and (2) placement of electrodes anywhere except outside the wound area was effective for wound healing.

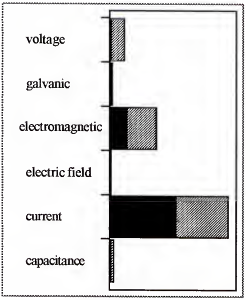

Source of Charge

Level	Count
capacitance	6
current	134
electric field	2
electromagnetic	55
galvanic	5
voltage	19
Total	221

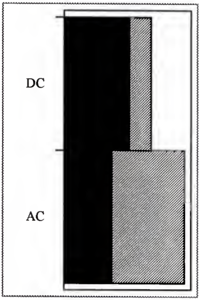

AC/DC

Level	Count
AC	93
DC	68
Total	161

Figure 2.16 Qualitative comparisons of factors showing increased wound healing in *in vivo* studies. Areas in black show that (1) current was the most effective source of charge for increased wound healing, and (2) there was not a significant difference between AC and DC when comparing successful wound healing.

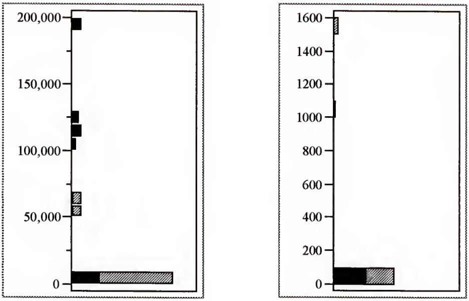

Voltage (mV)

Level	**Count**
0-50,000	38
50,001-100,000	10
100,001-150,000	7
150,001-200,000	4
Total	59

Current (mA)

Level	**Count**
0-100	118
1000	4
1500	9
Total	131

Figure 2.17 Qualitative comparisons of factors showing increased wound healing in *in vivo* studies. Areas in black show that (1) a broad range of voltages were effective for increased wound healing, and (2) currents below 100 mA increased wound healing in some cases.

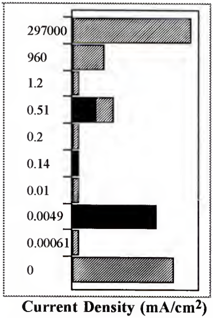

Level	Count
0	12
0.00061	1
0.0049	10
0.01	1
0.14	1
0.2	1
0.51	5
1.2	1
960	4
297000	14
Total	50

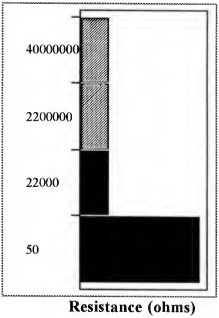

Level	Count
50	4
22000	1
2200000	1
40000000	1
Total	7

Figure 2.18 Qualitative comparisons of factors showing increased wound healing in *in vivo* studies. Areas in black show that (1) current densities of 0.0049 or 0.51 mA/cm^2 were the most effective for wound healing, and (2) lower resistance showed increased wound healing.

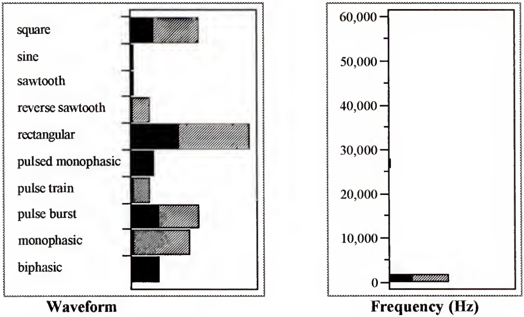

Level	Count
biphasic	6
monophasic	12
pulse burst	14
pulse train	4
pulsed monophasic	5
rectangular	24
reverse sawtooth	4
sawtooth	1
sine	1
square	14
Total	85

Level	Count
0-5000	152
10000	2
27120	4
60000	1
Total	159

Figure 2.19 Qualitative comparisons of factors showing increased wound healing in *in vivo* studies. Areas in black show that (1) several waveforms were effective for wound healing, and (2) frequencies less than 5000 Hz were the most effective for wound healing.

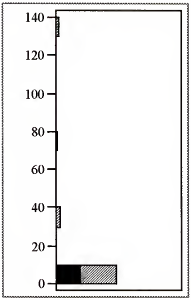

Pulse Width (msec)

Level	Count
0-20	90
30	6
76	3
140	5
Total	104

Figure 2.20 Qualitative comparisons of factors showing increased wound healing in *in vivo* studies. Areas in black show that pulse widths below 10 msec were most effective for wound healing.

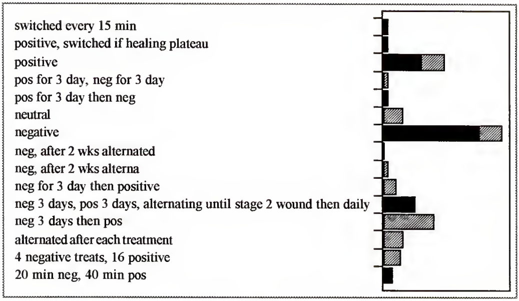

Polarity

Level	Count
20 min neg., 40 min pos.	3
4 negative treats, 16 positive	5
alternated after each treatment	6
neg. 3 days then pos.	14
neg. 3 days, pos. 3 days, alternating	9
neg. for 3 day then positive	4
neg., after 2 weeks alternating	2
neg., after 2 weeks alternated	1
negative	32
neutral	6
pos. for 3 day then neg.	2
pos. for 3 day, neg. for 3 day	2
positive	17
positive, switched if healing	2
switched every 15 min	2
Total	107

Figure 2.21 Qualitative comparisons of factors showing increased wound healing in *in vivo* studies. Areas in black show that either positive or negative polarity, or alternating polarity, had a positive effect on wound healing.

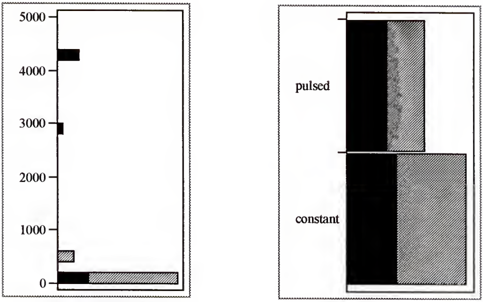

Magnetic Field (µT)

Level	Count
0-1000	25
2800	1
4320	4
Total	30

Pulsed/Constant

Level	Count
constant	128
pulsed	84
Total	212

Figure 2.22 Qualitative comparisons of factors showing increased wound healing in *in vivo* studies. Areas in black show that (1) a wide range of magnetic fields were effective in increasing wound healing, and (2) there was little difference in wound healing between pulsed and constant stimulation.

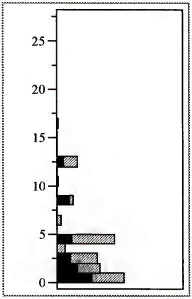

Length of Treatment (weeks)

Level	Count
0	15
≤ 1	50
1-2	49
2-3	14
3-4	44
4-5	4
6-8	5
8-9	13
9-11	3
12	16
16	2
25.7	1
Total	216

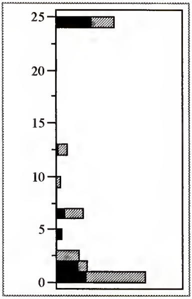

Length of Stimulation (hours)

Level	Count
0	37
0-1	63
2	19
4	6
6	23
7	1
8	1
9	4
12	9
20	1
24	48
Total	212

Figure 2.23 Qualitative comparisons of factors showing increased wound healing in *in vivo* studies. Areas in black show that (1) the length of treatment had little effect on wound healing, and (2) length of stimulation was also not a critical parameter for wound healing.

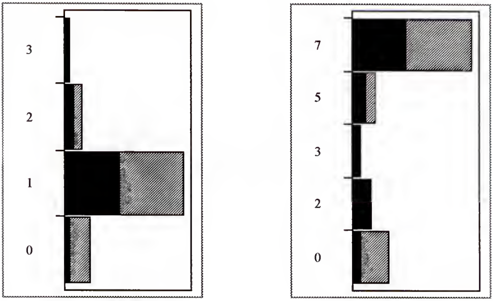

Treatments per day

Treatments per week

Level	**Count**
0	34
1	147
2	24
3	9
Total	214

Level	**Count**
0	33
2	18
3	9
5	22
7	106
Total	188

Figure 2.24 Qualitative comparisons of factors showing increased wound healing in *in vivo* studies. Areas in black show that (1) although increased wound healing was observed with up to three treatments per day, the most successful studies used one treatment per day, and (2) up to seven treatments per week were found to increase wound healing.

The *in vivo* literature analysis yielded different results from the *in vitro* literature analysis in a number of ways. No successful *in vitro* experiments identified polarity as an important parameter in the studies, yet in the *in vivo* studies, polarity was clearly identified as an important parameter. In the *in vitro* studies, only constant stimulation was successful, but in the *in vivo* studies both pulsed and constant stimulation showed positive results. Electromagnetic fields and current were used much more frequently *in vivo* versus the *in vitro* experiments. Results were similar in that low currents or low voltages promoted the best healing characteristics, and DC was better than AC. *In vivo* versus *in vitro* data were also generally similar in showing overall positive results, i.e. increased cell proliferation, growth, adhesion, motility, wound healing, using electrical stimulation.

Several different approaches have been taken to understand the effect of electrical stimulation in wound healing. Increased wound healing has been indicated for treatments of bone, dermal wounds, connective tissue, and internal wounds. Electrical stimulation has been shown to increase capillary growth using a rabbit model (Gre 92) and increase the healing rate of corneal epithelial injury (Per 87). Numerous experimental conditions have been used in a wide range of studies with various levels of success. Bone and dermal wound healing have seemed most responsive to electrical stimulation. Connective tissues and internal wound healing, on the other hand, have shown mixed results.

Bone

Bone has been shown to have piezoelectric properties and thus has been the subject of multiple studies using electrical stimulation to join delayed unions and nonunions (Alb 91, Sne 90). Osteoporosis, rheumatoid arthritis, cancer-related skeletal defects are also areas in which electrical stimulation has been shown to provide positive results (Moh 94, Nae 91). Models have been developed to understand the most effective treatment therapies (Gup 91, Gup 91). Even though the treatments vary from study to study, success has been seen in most research.

Research with electrical stimulation has been conducted for several applications in the dental area (Ste 90). Pulsed electromagnetic fields have been shown to deter residual ridge resorption which is common after extraction of teeth (Ort 92). Low amperage direct current has also been shown to promote osseointegration of titanium dental implants (Sha 95).

Tibial fractures in humans and dogs were both shown to have increased rates of healing with electrical stimulation (Sha 90, Ceb 91). A double blind study by Mammi et al. involving tibial osteotomies performed in humans indicated a significant increase in healing rate (Mam 93). Research on rabbit fibulae, using histological examination, suggested that pulsed capacitively-coupled electric field stimulation increased the bone healing rate (Cha 91). Direct current stimulation enhanced the bending rigidity, tissue, mineral and matrix densities, and the mineral-to-matrix ratio of canine radius fracture healing (Cha 90).

Skin

Data from numerous human and animal studies indicate that electrical stimulation can be beneficial to patients with dermal wounds, which include pressure sores, burns, and venous ulcers. Using various electrical parameters, several processes of wound healing have been observed, such as decreased edema, debrided necrotic tissue, neutrophil and macrophage attraction, growth factor receptor site stimulation, increased blood flow, neurite growth stimulation, bacterial inhibition, and mast cell reduction (Gen 91, Vod 92a, Rei 91). Some research suggests that electrical stimulation may even be effective as a preventative measure for pressure sores (Yar 94).

Both direct current stimulation and pulsed electromagnetic therapies have been used in burn wound treatments. Studies using direct current stimulation in rats and guinea pigs reported increased reepithelialization rate, decreased contraction, improved hair survival, and reduced burn edema (Chu 90, Chu 96). Pulsed electrical stimulation in other *in vivo* animal studies showed increased collagenase levels (an indication of the process of epithelialization) in pigs and an organized healing process resulting in skin with similar appearance to unharmed control skin in rats (Ågr 94, Cas 95).

Pressure ulcer healing is another area of active electrical stimulation therapy research. Patients that are confined to a bed or a wheelchair, such as the elderly or those having suffered spinal cord injuries, are often subject to painful pressure sores. Research has been performed on both humans and animals in this area with positive results for both. Kambie et al. published a study of alternating and direct electrical current performed on pigs which showed a reduced healing time and new collagen formation oriented in a pattern similar to normal skin (Kam 93). Human studies have focused on determining the ideal pulsed electric field parameters for pressure sore treatment, the use of low intensity direct current (LIDC), and pulsed LIDC. The healing rate of the ulcers was reported to increase up to 50% for all three studies mentioned (Ste 93, Gau 76, Woo 93).

Venous leg ulcers commonly found in diabetic patients are yet another type of chronic, recurrent problem that have been improved by electrical stimulation. However, results do not clearly demonstrate that ulcer area is reduced after treatment. A study published by Lundeberg et al. indicates that electrical nerve stimulation increased the blood flow to ischemic skin flaps thereby decreasing the area of the wounds after twelve weeks of treatment (Lun 92). Mixed results of the effect of electrical stimulation on venous ulcers are reported in a literature review by D.J. Margolis and J.H. Cohen published in 1994 (Mar 94). A third study determined that high voltage galvanic stimulation had no effect on the area or depth of the wounds (Gog 92).

Connective Tissue

Electrical stimulation has been reported to be therapeutic in connective tissue repair. In many studies, experimental and clinical, accelerated synthesis of the extracellular matrix and healing of tissue has been observed (Aar 93).

Research has been performed on ligaments using both rat and rabbit models. Direct electrical current was used in the rat studies. The medial collateral ligaments receiving stimulation showed statistically significant improvement in four properties indicative of ligament healing: maximum rupture force, energy absorbed, stiffness, and laxity (Lit 94). The patellar ligaments of rabbits were shown to have an increased healing rate when pulsed electromagnetic fields were utilized. Tensile strength and histology were the characterization methods used in this study (Lin 92).

Tendon healing and cartilage repair may also be affected by electrical stimulation. Fujita et al. performed an *in vitro* study on rabbit flexor tendons indicating that low-amperage, direct electrical currents promoted collagen synthesis and suppressed adhesions (Fuj 92). Pulsed-direct current enhanced the quality of repair of osteochondral defects in the distal femoral condyles of rabbits. This improved healing rate of the articular cartilage was observed via histological and histochemical analysis (Lip 90).

Internal Wounds

Little research has been done on the healing of internal wounds by electrical stimulation. However, two studies reported here indicated statistically significant effects on wound healing time. The first study investigated the differences in the effects of electromagnetic field (EMF) stimulation on intestinal wound healing in rats treated and not treated with corticosteriods. The results suggest that EMF stimulation increased the healing rate in rats not treated with corticosteroids and significantly reduced the inhibitory effect of corticosteriods on the healing of the small intestine anastomoses in treated animals (Din 93). The second study determined histologically that abdominal hernias in rats, when subjected to a pulsed current, healed more quickly. This was indicated by the early formation of fibroblasts, the deposition of collagen, and the rapid maturation and longitudinal alignment of the collagen fibers (Fra 90).

Vascular Systems and Blood Flow

The flow of blood in the vascular system is very complex and only partially understood. There are two principal vectors in the force of blood flow. One is perpendicular to the vessel wall and is representative of blood pressure, which can be in the range of 10 - 130 mmHg depending on type and function of vessel. The other is a parallel force which translates to the shear stress of blood along the vessel wall. Typical arterial wall shear stresses are 20 - 40 dyn/cm^2 for regions of vessels that have uniform geometry (Dav 95).

Understanding blood flow in the vascular system is important for several reasons. Some research has demonstrated a correlation of blood flow rate with intimal thickening. Minimal intimal thickening was observed at high flow rates in baboon PTFE grafts, and at lower flow rates there was a marked increase in the intima thickness (Gea 93). Reduction of neointima is also observed at higher blood flow rates (Mat 97). Stresses on the vessel wall are important to understand when using seeded vascular grafts, since it would be counterproductive if the cells did not adhere well and were therefore quickly dispersed in the blood stream. In *in vitro* studies, cells respond to flow and cyclic stretch with changes in shape and/or orientation, proliferation, mechanical stiffness, and synthesis and secretions of proteins (Zie 94).

Several devices have been developed to test cellular responses to physiological conditions found in the vascular system. The "vascular simulating device" is a compliant tubular system that reproduces vascular mechanical and hemodynamic forces. Endothelial cells are grown directly on silicone tubing and a mechanical pump supplied known levels of pressure and flow (Ben 94). A rotating disc apparatus has been developed by Pratt et al. to examine the kinetics of endothelial cell attachment at controlled shear stresses. Cells are plated at 25,000 cells/cm^2 and incubated for thirty minutes. The 60 mm plate is then inverted and rotated at 700 rpm for 30 minutes in culture medium. Cells are then examined by light microscopy (Pra 88). A third system entails a microcantilever which applies a lateral load to a cell attached to a test substrate. It directly measures the shear force needed to detach a single cell from a material (Yam 98). Scientists at Cornell University have experimented with channels etched in mirror image patterns on microscope slides. This experimental device is designed to mimic vessel geometry and flow conditions to scale (Sar 95).

Substrates Studied in Previous Research

Indium Tin Oxide

Qiu et al. cultured rat marrow stromal cells on ITO surfaces with positive, neutral, and negative surface charges. Cell attachment, morphology, and protein release were measured at 0.7, 0.8, 0.9, and 1.0 v. They found that surfaces with a positive charge increased attachment and decreased spreading and differentiation (Qiu 98).

Carbon

Carbon has been shown to be bioacceptable in many applications. Carbon fibers have been used in composite materials for biomedical applications such as total knee replacements. The fibers are incorporated in high-density polyethylene (HDPE) or ultra-high-molecular weight polyethylene (UHMWPE) to add strength to the polymer material used. Carbon has also been used in joint lubrication.

Of particular interest to this research, pyrolytic carbon has been studied extensively for heart valves and blood vessel prostheses (Bro 95). In a study by Bernex et al. pyrolytic carbon was vapor-deposited on Dacron® vascular grafts to study the adherence and growth of porcine aortic endothelial cells. Cells were seeded onto experimental materials at 50,000 cells/cm^2 and viewed by light microscope and SEM at 2 hours, 1, 4, and 8 days. Results showed that carbon had no effect on adherence although fabrics were only nominally rinsed and thus these results need further examination. Cell growth and spreading, however, occurred only on the pyrolytic carbon-coated Dacron® (Ber 92). Sbarbati et al. found that pyrolytic carbon coatings on PTFE and Dacron grafts enhanced cell attachment, cell growth, and reduced PGI_2 and LDH production. Endothelial cells were seeded at 45000 cells/cm^2 and counted using SEM after 2 and 4 days (Sba 91). Granchi et al. compared leukocyte activation by PET and pyrolytic carbon-coated PET. Neither changed the expression of adhesion molecules in lymphocytes which suggests that no specific immune response is stimulated (Gra 97).

Gold and Palladium

Gold has also been shown to be bioacceptable. Its primary use is in dental restorations due to superior performance and longevity. It has not been widely used elsewhere, i.e. in orthopaedic applications, due to high cost, high density, and insufficient strength (Bro 95).

Palladium is a metal which is highly resistant to tarnish and corrosion. Because of these properties, it is typically used in dental inlays, bridgework, and orthodontic appliances (And 94).

Polypyrrole

Polypyrrole has been used in several biomedical applications such as biosensors, regulation of biological functions, and drug delivery devices. Biosensor research has included devices that determine lactate, glucose, dopamine, and penicillin levels (Kra 96, Fur 94, Gao 94, Nis 92). The effect of electronically controlling enzyme activities and electron transfer of cytochrome-c have been studied using polypyrrole (Aiz 94, Zha 90). Drug delivery devices have been studied using polypyrrole in two different ways. One is to use polypyrrole films to trap electrically charged drugs and to then release the drugs by changing the charge character of the polymer (Bid 95). The other approach is to use polypyrrole compounds as drugs themselves by binding them to the minor groove of DNA where oxidative breakdown occurs (Lee 91).

Wong et al. studied electrically conducting polymers, specifically polypyrrole, to control the shape and growth of mammalian cells. They found that with electrical stimulation, a layer of fibronectin adhered to polypyrrole films, and further, that endothelial cells attached to the fibronectin-coated surface. No studies were performed to determine the morphology and proliferation of cells on uncoated polypyrrole (Won 94).

Jakubiec et al. studied the *in vitro* cellular response of endothelial cells to 5 polypyrrole-coated Dacron® samples from Milliken Corporation. Resistivity levels of these samples ranged from 45,000 to 123 ohms/square. The experiments did not involve application of electrical currents and multiple cell types were present. Results were based on a variety of extractable analyses but no cell counts. It was concluded that the fabrics with lower resistivity (more conducting) exhibited less cell migration, proliferation, and viability (Jak 98).

Objectives of This Research

Further understanding of the growth and adhesion characteristics of endothelial cells is important to improved vascular wound healing and developments of better prostheses. By use of electroactive coatings on vascular grafts, endothelial cell growth might be controlled and encouraged noninvasively and without additional medication. Confluent endothelial cell linings on vascular grafts may reduce the thrombogenicity and produce more biomimetic prostheses with improved patency. If successful, fewer reoperations would be needed, saving money in the cost-conscious health care system. Additionally, the quality of life for patients with vascular grafts would improve, allowing more active and extended quality of life.

The specific objectives of this research were therefore to determine the effect of electrical fields on the growth and adhesion characteristics of endothelial cells *in vitro* as a first step toward the stated goal. The effect of electric field parameters on endothelial cell adhesion and proliferation was studied on various electroactive substrates, including indium tin oxide, carbon, gold-palladium, and polypyrrole, especially to compare voltage (0, 0.5, and 1 volt) and time (12, 24, and 36 hours) effects. Characterization of growth and adhesion was determined microscopically using cell counts and using a 6-keto-prostaglandin-$F_{1\alpha}$ release assay for measuring cell viability.

CHAPTER 3
MATERIALS

Endothelial cells

Porcine endothelial cells harvested from the pulmonary vein were used in this research. All endothelial cells used were fifth generation. After harvesting, they were split three times and frozen in liquid nitrogen. Cells were thawed as needed, allowed to come to confluence, and split once more.

Indium Tin Oxide Glass

Indium tin oxide glass (ITO-Glass) (Delta Technologies, LTD) is a soda lime glass coated with indium tin oxide by electron beam deposition. In this process, the glass is first passivated with silicon dioxide. The indium tin oxide is then deposited as a result of a controlled oxygen bleed into the vacuum system as the metal oxide is evaporated onto the glass substrate. The end result is a glass slide with a conductive, transparent coating (Del 97).

The resistance of the coatings being used is 100 Ω (Del 97). This glass was used as a representative material because it is transparent and can be used with an inverted microscope. Additionally, endothelial cells grow well on this substrate thereby making it easy to test and compare cell growth with and without electrical stimulation.

Poly(ethylene terephthalate)

Mylar® is the Dupont® tradename for extruded poly(ethylene terephthalate) [PET] sheet. Dupont® product number 700D1 was used in this research. The structure of PET is shown in Figure 3. It is a semi-crystalline polymer with a glass transition temperature of 70°C and a melting temperature of 270°C. PET is synthesized through a condensation reaction between ethylene glycol and the dimethyl ester of terephthalic acid. Mylar® sheet is typically extrusion cast with barrel zones set to approximately 250 - 320°C. During processing it is biaxially oriented and coated on one or two sides with silica in order to control slip in further processing.

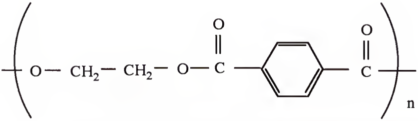

Figure 3.1: Structure of Poly(ethylene terephthalate)

Dacron® is the Dupont® tradename for woven PET fabric. Melt-spun fibers are collected on spools and then woven into flat sheets, tubes or various other shapes. Vascular grafts are commonly made of Dacron® tubes with various crimping patterns employed.

Carbon and gold-palladium were coated onto Meadox Dacron® vascular grafts in an effort to make a conducting fabric surface to be compared to polypyrrole-coated Dacron®. Because the coatings only covered the surface and not the complete individual fibers, the fabrics were not conductive and therefore were not used in this research.

Indium Tin Oxide-coated Poly(ethylene terephthalate)

Indium tin oxide-coated poly(ethylene terephthalate) (ITO-Mylar) (Delta Technologies, LTD.) is a Mylar® sheet coated with indium tin oxide by the same electron beam deposition process as previously described for ITO-Glass. The resistance of the coatings used is 100 Ω (Del 97). This material is transparent like the ITO-Glass and therefore can also be used with an inverted microscope.

Carbon-coated Mylar®

The carbon-coated Mylar® (C-Mylar) samples used in these studies were coated using the Ion Equipment Corporation Carbon Coater at the Major Analytical Instrument Center (MAIC) at the University of Florida. This coater uses thermal evaporation of carbon to coat surfaces. The process is performed at 10^{-5} to 10^{-6} Torr, and evaporation is caused by an arc between two carbon rods. Samples were coated twice to achieve desired coating properties.

Unlike the previous samples described (ITO-Glass, ITO-Mylar, AuPd-Mylar), the resistivity of the carbon coatings was approximately the same as that of the growth medium. Therefore it was important to distinguish between the cell-growth effects of conduction through the growth medium alone and conduction through the substrate in addition to the growth medium. To demonstrate this principle, carbon-coated Mylar samples were compared where the current flowed only through the growth medium and where the current flowed both through the substrate and the growth medium. Additional C-Mylar samples were made using the procedure previously described. The coatings were then intentionally scratched in parallel lines at specified distances, as shown in Figure 2, thereby increasing the resistivity to infinity. This allowed for electrical conduction through the culture medium only versus both through the carbon surface and the culture medium. The coating did however, still gave a common surface to be compared with the intact carbon-coated surface. These samples are referred to as SC-Mylar.

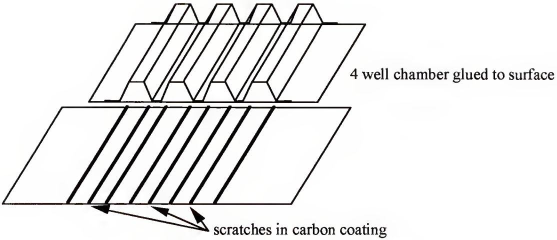

Figure 3.2: Diagram of SC-Mylar Coatings

Gold-Palladium-coated Mylar®

The gold-palladium-coated Mylar® (AuPd-Mylar) samples used in these studies were coated using the Technics Sputter Coater also at MAIC. In this process, a gold-palladium target is exposed to an argon plasma in a low vacuum. The gold-palladium atoms are energized through the transfer of increasing kinetic energy from the argon molecules striking the gold and palladium atoms and causing those atoms to sputter to the surface being coated. Samples were coated for 12 minutes to achieve desired coating properties.

Polypyrrole-coated Dacron®

The polypyrrole-coated Dacron® (PPy-Dacron) used in these studies was graciously donated by Milliken Corporation in Spartanburg, SC. The specific fabric used was Contex® C-378 textured twill weave polyester with a resistance of 60Ω/square. The polypyrrole is coated on to each individual fiber using dilute aqueous solutions at room temperature (Kuh 93).

The structure of polypyrrole is shown in Figure 2. Electropolymerization of pyrrole yields a conductive polymer with good mechanical properties. The positive charges resulting from the polymerization are balanced by anions to make the material electrically neutral overall. When the polymer is reduced it turns from black to transparent green and becomes an insulator.

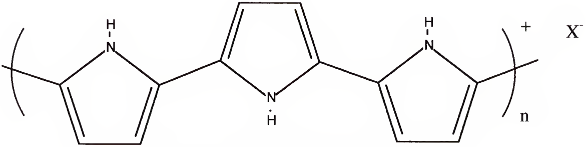

Figure 3.3: Structure of Polypyrrole

Polypyrrole has a conductivity of up to 100 Ω^{-1} cm^{-1} when it is in the oxidized state and is considered to be a semiconductor since its conductivity increases with increasing temperature. Electrochemical removal of electrons generates a delocalized radical cation which is found in the band gap of the polymer (3.0 eV). Therefore electron migration is within access of valence band electrons (All 90, Sch 95, Rey 88).

Cell Growth Medium

Cell culture medium was made by adding 100 mL Fetal Bovine Serum (FBS), 10 mL Penicillin (10,000 units)-Streptomycin (10 mg) (Pen-Strep) solution, and 10 mL 200 mM L-glutamine to 500 mL Medium 199. All solutions were purchased from Sigma Chemical Company.

Trump's Fixative Solution

Trump's solution, used for fixing cells, was prepared by adding 2.85 g NaOH and 12.5 g NaH_2PO_4 to 400 mL ultrapure water and stirring until solids were dissolved. To this solution 100 mL 37% w/w formaldehyde, 40 mL 50% w/w glutaraldehyde, and 460 mL ultrapure water were added. The solution was then stirred for 30 minutes, and the pH was adjusted to 7.4 at room temperature. Finally, the solution was filtered through a 0.45 µm Vacucap 90 filter (Gelman Sciences) and refrigerated. The salts and aldehydes used to prepare this solution were all purchased from Fisher Scientific.

CHAPTER 4
METHODS

Porcine Endothelial Cell Harvesting

Porcine endothelial cells were harvested from the pulmonary vein. Arteries were obtained from a slaughterhouse in Lake City, FL with the assistance of Nina Klingman in Dr. James Seeger's research group. Veins were transported in a refrigerated antibiotic/growth medium solution.

The following instruments were steam autoclaved in preparation for harvesting: two 250 mL beakers, one 100 mL beaker, one 20 mL beaker, dissecting scissors, two clamps, forceps, gauze and a petri dish.

Ten milliliters of a 0.1% collagenase solution was prepared in Hank's Buffered Saline Solution (HBSS, Sigma H-2513). This solution was filtered with a 0.45 μm filter before use.

A fibronectin solution was prepared by bringing the fibronectin to room temperature (1 mg/1 mL) and injecting 1 mL of sterile water. This combination equilibrated for 30 minutes without agitation. Then 19 mL of serum-free Medium 199 was added. Approximately 7 mL of this final solution was added to a 25 cm^2 culture flask and allowed to sit for at least 30 minutes.

While the fibronectin solution was sitting in the culture flask, the aorta and the pulmonary vein were separated. Remnants of the lung and other extraneous material were removed. The aorta can be distinguished from the pulmonary vein because it is larger and harder than the pulmonary vein. Additionally, any remnants of lung are attached to the pulmonary vein.

The pulmonary vein was rinsed with HBSS using a 20 cc syringe. One clamp was attached to seal one end of the vein. The filtered collagenase solution was poured into the open end of the vein which was then clamped. The sealed vessel was then placed into approximately 50 mL HBSS, covered lightly and placed into a 37°C water bath for 20 minutes.

The growth medium used during the harvesting procedure was prepared in a 50 mL conical tube and adding 38.2 mL Medium 199, 10 mL FBS, 0.5 mL Pen-Strep solution, 1.0 mL HEPES (17.87 g in 100 mL ultrapure water, pH 7.0), 0.025 mL gentamycin, 0.025 mL Amakin® (amikacin), and 0.1 mL fungizone. The solution was mixed lightly by inverting the conical tube several times.

After the 20 minutes had elapsed, the collagenase solution and 10 mL of growth medium was added to a 50 mL conical tube. The pulmonary vein was massaged and rinsed with HBSS into the conical tube until 50 mL was obtained. The cell suspension was centrifuged for 20 minutes at approximately 1800 rpm.

After centrifugation, the supernatant was discarded as well as the excess fibronectin in the culture flask. Approximately 3 mL of growth medium was added to the cell pellet which was broken up by pipetting. The cell suspension was added to the culture flask, and an additional 3 mL of growth medium was used to rinse the conical tube and then also added to the culture flask. The flask was then incubated for one hour at 5% CO_2 and 95% relative humidity after which the growth medium was discarded and replaced with fresh medium. The growth medium was changed after 24 hours and every two days thereafter.

Porcine Endothelial Growth Technique

The incubator used in these experiments was a NuAire CO_2 water-jacketed incubator (Model #NU-2500, NuAire, Inc., Plymouth, MN), and conditions were consistently 5% CO_2 and 95% relative humidity. Cells were fed every other day with the growth medium described in Chapter 3.

Porcine Endothelial Cell Splitting

After hood and hand sterilization with an aqueous 70% ethanol solution, a cell culture flask was removed from the incubator and the growth medium in the flask was discarded. Cells were rinsed three times with Hank's Balanced Salt Solution (HBSS: Sigma H-2513) which was discarded after each rinse. Cells were observed through an inverted microscope after the addition of 3 mL of trypsin-EDTA solution (Sigma T-3924). After two to three minutes, the cells generally began to show a rounded morphology. Cells were removed from the bottom of the flask by striking the flask sharply against a hard surface. To stop the trypsinization process, approximately 20 mL of growth medium (described in Chapter 3) were added to the cell culture flask. Cells grown in a 25 cm^2 culture flask were then poured into a 75 cm^2 culture flask. Cells grown in a 75 cm^2 flask were split evenly between four separate 75 cm^2 culture flasks. Growth medium was added to a total volume of approximately 30 mL. Finally, flasks were sterilized by wiping with an aqueous 70% ethanol solution and returned to the incubator.

Porcine Endothelial Cell Freezing

Cells were washed and trypsinized as previously described. After quenching the trypsinization with growth medium, the cell suspension was added to a sterile 50 mL centrifuge tube and centrifuged for 20 minutes at approximately 1800 rpm. The supernatant was then discarded, and the remaining cell pellet was resuspended in 2/3 the desired volume of growth medium. The remaining 1/3 growth medium supplemented with 10% dimethyl sulfoxide (DMSO) (Origen®, Fisher Scientific) was added to yield a 5% DMSO complete medium. DMSO is added to the growth medium in order to reduce ice crystal expansion which ruptures cell membranes and causes cell death.

The cells were allowed to equilibrate in the DMSO complete medium for at least 15 minutes but no longer than 60 minutes. Aliquots were then placed into 1.0 mL Nalgene cryogenic vials (Fisher Scientific), and the vials were placed in a Nalgene cryobox (Fisher Scientific). The cryobox was placed in a styrofoam cooler which in turn was placed in a -20°C freezer for 24 hours. This procedure was followed to provide a more controlled cooling process and therefore increase cell survival. Small quantities of liquid nitrogen were added to the cooler after the 24 hour freezing period in order to reduce the temperature of the cryobox and cells relatively slowly. When the cryobox was sufficiently cold, it was placed in the Locator, Jr. Cryobiological Storage Vessel with Liquid Nitrogen Level Monitor (Fisher Scientific). Locations and contents of vials and cryoboxes were carefully labeled for safety and ease of retrieval.

Porcine Endothelial Cell Thawing

A cryobox was removed from the Locator, Jr. Cryobiological Storage Vessel using appropriate safety precautions. A vial was removed from the cryobox and placed in a sterile hood. The cryobox was then returned to the Locator, Jr. The vial was placed in a 37°C water bath in order to thaw the cell suspension as quickly as possible. The cell suspension was then placed directly into a 75 cm^2 cell culture flask and growth medium was added to achieve a final volume of approximately 30 mL. Flasks were sterilized with a 70% ethanol in water solution and placed in the incubator. Cells generally became confluent within 7 to 10 days at which time they were split and allowed to become confluent again before use in experimentation.

Porcine Endothelial Cell Fixing and Staining

To fix cells for further evaluation, growth medium was removed from the cell/experimental surface. Trump's solution (described in Chapter 4) was added using a 60 cc syringe with a 0.2 μm syringe filter and allowed to sit for at least 5 minutes. The

Trump's solution was then discarded and replaced with approximately 1 mL/cm^2 phosphate buffered saline (PBS). The PBS also sat for at least 5 minutes and then was discarded. The same amount of deionized water was added, allowed to sit for at least five minutes, and then discarded. Approximately 0.05 mL (2 - 3 drops) of 1% aqueous Gentian violet stain were added to the cell/experimental surfaces, and tap water was added to allow for complete surface staining. The staining solution remained on the surface for at least 5 minutes, and then was gently flushed using tap water from a squirt bottle until the water ran clear. The clear water was discarded and the cell/experimental substrates were allowed to dry thoroughly before counting.

Porcine Endothelial Cell Dehydration

Cells were fixed and rinsed with PBS and deionized water as previously described. Substrates were then adhered to scanning electron microscopy (SEM) stubs using double-sided tape. Stubs with samples were placed in a small beaker and were dehydrated using a serial dilution. The concentrations of ethanol/water solutions used were as follows: 30%, 50%, 70%, 90% and 100%. Each solution remained in the beaker for at least 5 minutes before being discarded, and the next solution was added. After the 100% ethanol drying, samples were removed and placed in a desiccator.

Cell Concentration Experiment

A study was conducted to investigate the effect of cell concentration on growth rate. Three concentrations were tested: 50,000, 100,000 and 150,000 cells/mL. One milliliter of cell solution was placed in each well of a 24-well polystyrene culture plate. Cells were stored in the incubator at 37°C, 95% relative humidity (RH), and 5% CO_2 and fed at 8, 24, 32, 48 and 52 hours. Cells in three wells were fixed every 4 hours to track the growth rate as shown in Figure 4.1. The duration of the test for the two higher concentrations was 32 hours and 56 hours for 50,000 cells/mL.

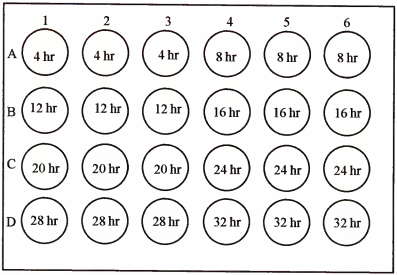

	1	2	3	4	5	6
A	4 hr	4 hr	4 hr	8 hr	8 hr	8 hr
B	12 hr	12 hr	12 hr	16 hr	16 hr	16 hr
C	20 hr	20 hr	20 hr	24 hr	24 hr	24 hr
D	28 hr	28 hr	28 hr	32 hr	32 hr	32 hr

Figure 4.1 Configuration of Cell Concentration Experiment Culture Plate

Effect of Trump's Fixative on Morphology

An experiment was performed to better understand the effect of Trump's solution on the morphology and viability of cells because results of the cell concentration experiment showed cells in the ball and stick and the rounded morphologies. The cell concentration used for this experiment was 50,000 cell/mL and 1 mL cell solution was used for each well tested. Cell plates were stored in the incubator at 37°C, 95% relative humidity (RH), and 5% CO_2. Cells were fixed every 4 hours, and the duration of the experiment was twelve hours. The following configurations shown in Fig. 4.2 - Fig. 4.5 were tested. The shaded circles represent the wells in the culture plates with cells in them. These different configurations were tested to determine distance versus the effect of Trump's vapors on cell morphology.

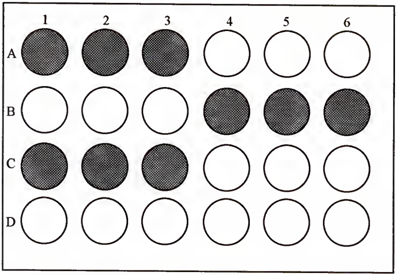

Figure 4.2 Alternating Row Configuration of Trump's Experiment

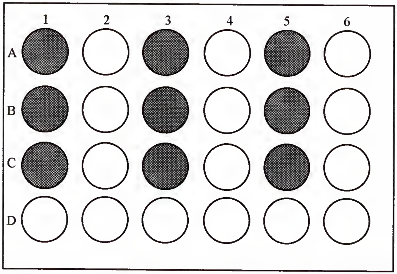

Figure 4.3 Alternating Column Configuration of Trump's Experiment

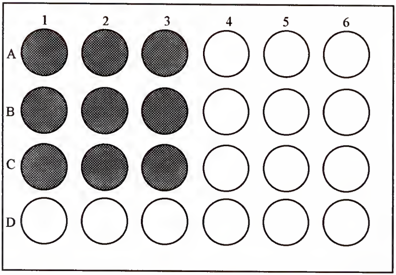

Figure 4.4 Adjacent Column Configuration of Trump's Experiment

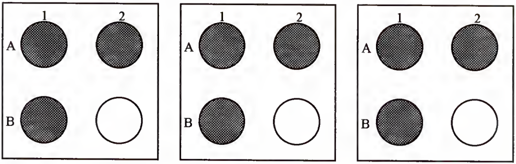

Figure 4.5 4-well Plate Configuration of Trump's Experiment

Feeding Rate Experiment

A feeding rate experiment was performed to determine the feeding frequency at which the cells grew best, defined by the growth rate and the probability for contamination. Cell concentrations of 50,000 and 100,000 cells/mL were used. One milliliter of cell solution was used in each well of 4-well polystyrene culture plates which were then stored in the incubator at 37°C, 95% relative humidity (RH), and 5% CO_2. The feeding rate was varied such that cells were fed every 6, 12 or 24 hours. One culture plate was fixed every 6 hours, and the duration of the experiment was 48 hours.

Cytotoxicity Experiments

Cytotoxicity tests were performed on all the substrates used in this research to determine whether the materials were favorable for cell growth. One milliliter of a high cell concentration solution ($\sim 10^6$ cells/mL) was placed in each well of a culture plate with the given substrate. The substrate and the cells were incubated for 24 hours at 37°C, 95% relative humidity (RH), and 5% CO_2. After 24 hours, the samples were viewed to see if the cells had lived or died on each substrate. Substrates tested were C-Mylar, AuPd-Mylar, Glass, Mylar, ITO-glass, ITO-Mylar, PPy-Dacron, Dacron, C-Dacron, and AuPd-Dacron.

Chamber Slide Modification

Chamber slides (Fisher) were modified in order to obtain discrete areas on conductive substrates for cell growth rate observation. The polystyrene chamber was removed from the glass slide in the received condition. Silicone glue was applied to the bottom of the polystyrene chambers and then was attached to the conductive substrates. These substrates were cut into 1" by 3" films for the proper fitting of the chambers. After allowing the silicone glue to crosslink for 24 hours, chambers were placed in sterilization packets, and heat sealed. The packets were ethylene oxide (ETO) sterilized for 1 hour and allowed to aerate for at least 10 hours. Most chambers were aerated for much longer.

Pilot Experiment for Voltage Effects

The analysis of the literature presented previously indicated that a voltage drop of equal to or less than one volt was the most effective stimulation rate for improved cell growth and adhesion. A pilot study was conducted using ITO Glass as a conductive test substrate to verify this result. Single well chamber slides were modified as previously described and 5 mL of cell solution was added to each chamber. Two concentrations were used in these studies, 50,000 and 100,000 cells/mL. The voltages tested were 0, 0.5, 1, 2, and 5 volts. Cells were incubated at each stimulation rate for 24 hours at 37°C, 95% relative humidity (RH), and 5% CO_2.

Electrostimulated Cell Growth Experiments

The primary objective of the research presented in this dissertation was to determine the effect of electrical stimulation on growth rates. These specific experiments were designed to determine the effect of electrical stimulation on endothelial cell growth rate (using cell counts) and 6-k-$PGF_{1\alpha}$ production. Two cell concentrations were used; 50,000 and 100,000 cells/mL. One milliliter of cell solution was placed in each well of modified 4-well chamber slides (Fisher Scientific) so that four separate growth measurements could be made for each condition. The growth medium was removed every 12 hours, saved for 6-Keto-prostaglandin-$F_{1\alpha}$ analysis, and replaced with fresh growth medium. The duration of the experiments was 36 hours, and the electrical stimulation levels used were 0, 0.5, and 1 volt (DC). During the experimentation cells and substrates were incubated at 37°C, 95% relative humidity (RH), and 5% CO_2. Substrates used in these experiments were ITO-glass, ITO-Mylar®, AuPd-Mylar®, C-Mylar®, Mylar®, glass, polypyrrole-coated Dacron®, and C-Mylar® with the coating scratched so that conduction was through the growth medium instead of the substrate.

A large growth plate was constructed so that multiple conditions could be evaluated simultaneously. Copper tape was wrapped around the edge of five glass plates. The 4-well chamber slides were attached to the copper tape on the glass plates with more copper tape. The glass plates were attached to copper strips using clothespins. The copper strips were attached to a Plexiglas (PMMA) plate with brass screws and nuts. A schematic of the growth plate is shown in Fig. 4.6, and an actual photograph is shown in Fig. 4.7.

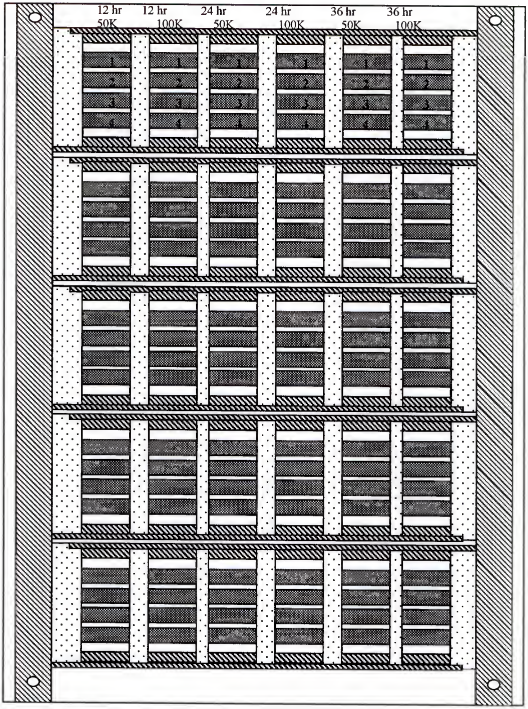

□ - plexiglass plate (20"x 12"x 1/4")
▧ - copper strips (20"x 3/4"x1/64")
▨ - copper tape (1/4")
⬚ - glass plate
▩ - cell solution in 4-well
chamber slides
○ - brass screw and nut

Figure 4.6 Growth plate schematic

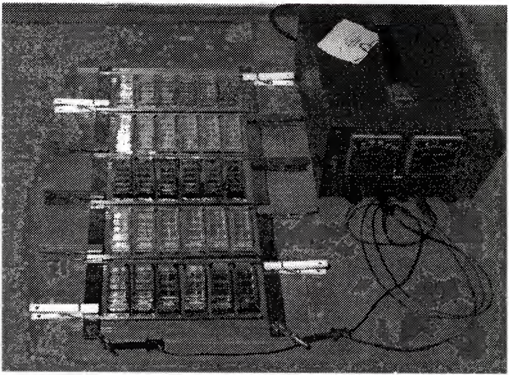

Figure 4.7 Photograph of Growth Plate

Adhesion Experiments

A secondary objective of this research was to understand the adhesion characteristics of endothelial cells with varying levels of electrical stimulation. Two cell concentrations were used for these studies, 50,000 and 100,000 cells/mL. The substrates tested were ITO-glass, ITO-Mylar®, AuPd-Mylar®, C-Mylar®, Mylar®, and glass. Six samples of each material were incubated with the cells at a given electrical stimulation level at 37°C, 95% RH, and 5% CO_2 for 12 hours. Stimulation levels were 0, 0.5, and 1 volt. Figure 4.8 shows a picture of the incubation/stimulation chamber used in these studies. This chamber was a 15 cm diameter Pyrex® petri dish with cover (Fisher Scientific). To stimulate cells on the test substrates, a structure made from copper strips and wire was constructed. Copper tape (Structure Probe Industries) connected the test substrates to the copper framework. The framework was connected to the power supply via copper tape. All portions of copper that came in contact with the growth medium were insulated with silicone glue.

The adhesion flow chamber was constructed to determine the adhesion characteristics of endothelial cells to various substrates with different levels of electrical stimulation. A picture of the system is shown in Figure 4.9. Pulsed pressurization and one-way check valves provide continuous fluid flow through the system and simulate physiological conditions experienced by vascular grafts. This set-up also minimized the necessary amount of culture medium and lengthened the duration of the studies.

The principal of operation of the adhesion flow chamber was as follows. Argon pressurizes and compresses the air space in the collection reservoir and forces the liquid through the initial one-way check valve. The liquid continues through a double four-port manifold, into the four outer channels of the chamber block, back through a reversed double four-port manifold and into the excess reservoir. When the pressure on

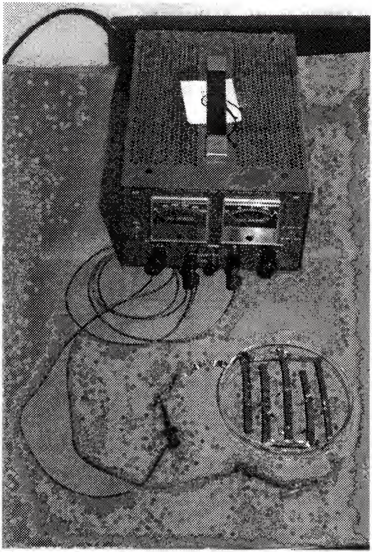

Figure 4.8 Incubation/Stimulation Chamber

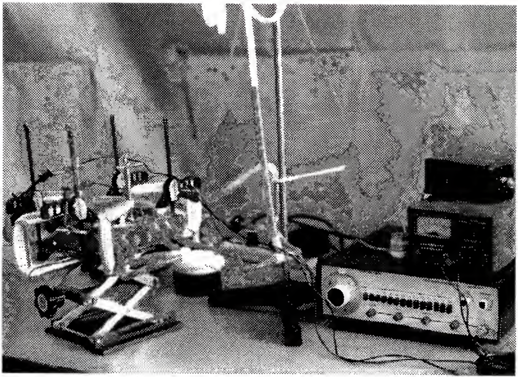

Figure 4.9 Adhesion Flow Chamber

the system is released using a pinch valve, the airspace expands forcing the culture medium in the excess reservoir to flow through the second one-way check valve and return to the collection reservoir.

The adhesion flow chamber was assembled using the following method. A 250 mL polypropylene jar with a screw-top lid (Fisher Scientific) was used as the collection reservoir. Four holes were punched in the lid to accommodate two 1/4" x 3/4" and two 1/8" x 5/8" nylon bulkhead connectors (Cole Parmer). A silicone gasket (Shin-Etsu) was inserted between the lid and the bulkhead connectors to ensure that there was no air leakage. NPT male pipe adapters (1/4" x 1/4" and 1/8" x 1/8" - Cole Parmer) were screwed into the bulkhead connectors so that four were extending out of the collection reservoir lid, and one was extending into the collection reservoir. To one 1/8"x1/8" pipe adapter, silicone tubing (1/8" I.D., 3/16" O.D.) was attached to a 2-way, normally open, 12 VDC direct lift solenoid valve (Cole-Parmer) via 1/4-28 barb fittings UNF(M) (Cole-Parmer). The solenoid was driven by a waveform generator (Wavetek) using a sine wave with 60 beats per minute. Silicone tubing (1/8" I.D., 3/16" O.D.) attached the other 1/8"x1/8" pipe adapter to a tank of argon which pressurized the system with 1 psi of gas.

Silicone tubing (1/4" I.D., 3/8" O.D. - Cole Parmer) was attached to both 1/4" x 1/4" pipe adapters extending out of the collection reservoir lid. To both of these 6" pieces of tubing were attached the one-way check valves (nylon body, silicone diaphragm - Cole-Parmer). Four inch pieces of silicone tubing were connected to the opposite sides of the check valves, and a nylon 5/16" T-connector(Cole-Parmer), with silicone tubing attached, was inserted to accommodate the pressure transducer.

On the inlet side of the chamber block, silicone tubing connected the T-connector to double nylon 4-port manifolds with a capped port (Value Plastics). The remaining four ports held open flow integral male barbed pipe adapters (Value Plastics) with silicone tubing leading to the chamber block itself. The chamber block (8.5" x 6" x 1.5",6-1/4" diameter channels) was made using a mold and Shin-Etsu two-part silicone. The four pieces of silicone tubing were placed in the outer four channels leaving the two inner channels plugged with corks for zero-flow controls. The exit side of the chamber block was a mirror image of the inlet side with the exception of the addition of a T connector for the excess reservoir in between the double 4-port manifold and the T-connector for the pressure transducer.

A 7.5" x 5" x 1/4" Plexiglas® plate was used as a transparent cover for the chamber block. It was held in place with four Quick-Grip® (American Tool) miniature clamps and four deep, 2 1/2" C-clamps.

Copper tape was placed on the surface of the chamber block in order to stimulate the endothelial cells on the test substrates during the adhesion flow testing. The copper tape was attached to the test substrates with copper tape and to the power supply via alligator clips and test leads.

The number of different materials in used in the adhesion flow chamber was minimized to reduce the system material effects on the test substrates and cells. The primary material used was silicone with small amounts of nylon, poly(methyl methacrylate), and polypropylene.

Culture medium 199 without any additives was used as the flow medium. The medium was saved and frozen for subsequent prostacyclin-level analysis. The average flow of culture medium through the adhesion flow chamber was 46 ± 13 cc/min, which is somewhat lower than physiological conditions. Shear rates were not calculated for this system since it was in turbulent, pulsatile flow, not steady-state. A typical flow waveform is shown in Figure 4.10 and indicates the regularity of the pulsatile flow of the adhesion flow chamber.

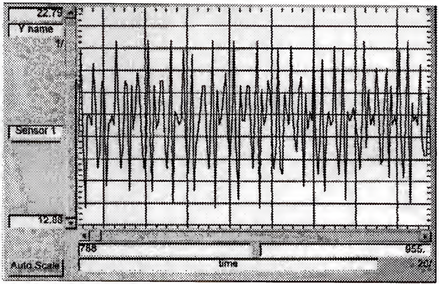

Figure 4.10 Typical Flow Waveform of the Adhesion Flow Chamber

Samples were tested in the adhesion flow chamber for four hours. This was determined by an experiment in which the test substrates were placed in the adhesion flow system for 1, 2, 3, and 4 hours. This experiment was performed on ITO Mylar with no electrical stimulation. After each time period, the cells remaining on the test substrates were viewed and compared with controls. The data indicated that at 4 hours a difference in cell counts could be seen between the control and the flow samples, yet there were still enough cells on the flow samples to obtain meaningful data.

Cell Motility Experiments

Several cell motility experiments were performed with endothelial cells on ITO glass using the system developed by Dr. Richard B. Dickinson. This system is comprised of an inverted microscope with a motorized stage, a digital camera and an image analysis program on a desktop computer. It takes a picture of defined fields within wells of a cell culture plate at specific time intervals. The images are processed via tracking and multiple calculations to show how far individual cells moved per unit of time. Experiments proceeded well with ITO glass when the substrates were glued with silicone to the cell culture plates. Due to variations (small bubbles) in the Mylar® films, the computer was unable to distinguish between the cells and the irregularities in the films. Therefore, no useful data could be obtained on ITO Mylar, Mylar, C-Mylar or AuPd-Mylar. PPy-Dacron samples could not be used with this instrumentation either due to its opacity. Some experiments using FITC-labeled lectins were attempted in order to view the endothelial cells on the aforementioned substrates. The particular experiments run were not successful and therefore the cell motility experiments were terminated.

Characterization techniques

Optical microscopy

In order to count the number of cells over time, cells were fixed and stained at various time intervals. Using a Photozoom inverted microscope (Bausch and Lomb), a Plan 10 objective, 10X eyepieces, and a 23 mm recticle (Edmund Scientific), cells were counted, and the numbers recorded. Since the recticle encloses an area of 0.25 mm^2 as determined by calibration with a Brightline Hemacytometer (Fisher Scientific), cell counts were multiplied by 4 to obtain the number of cells/mm^2.

Scanning electron microscopy

Scanning electron microscopy (SEM) was performed on a 6400 JEOL Scanning Electron Microscope at the MAIC facilities at the University of Florida. The accelerating voltage used was 5 keV, and the probe current was set at 12. Prior to viewing, cells were fixed on substrates, and samples were then dehydrated in serial solutions of alcohol as previously described. SEM samples were gold-palladium sputter coated for 3 minutes.

6-Keto-prostaglandin-$F_{1\alpha}$ Assay

Growth medium was collected at all tested time intervals to analyze the 6-keto-prostaglandin-$F_{1\alpha}$ (6-k-$PGF_{1\alpha}$) levels as a function of electrical stimulation and substrate. After the growth medium was removed from the substrates, it was frozen in 5 mL polystyrene test tubes. Assays were purchased from Neogen Corporation in Lexington, KY.

Before the assay could be performed, extraction of the samples was necessary to remove the remaining fetal bovine serum which is a competing factor for binding sites with the 6-k-$PGF_{1\alpha}$. The growth medium samples were thawed at room temperature. Each sample was vortexed for 15 seconds after adding 0.2 mL of methanol. To precondition the C18 Snap-Cap® columns (Phenomenex), each column was washed with 2 mL of methanol followed by 2 mL of deionized water. The sample was then filtered through the Snap-Cap cartridge followed by 2 mL of 15% methanol in deionized water and 2 mL of petroleum ether. The 6-k-$PGF_{1\alpha}$ was eluted with 2 mL of methyl formate which was subsequently evaporated with a stream of argon. Just before the assay was performed, the 6-k-$PGF_{1\alpha}$ residue was resuspended in 1 mL of extraction buffer found in the assay kit.

Stock solutions were made following instructions in the assay kit and resulted in the following concentrations: 0, 0.005, 0.01, 0.02, 0.04, 0.1, 0.2, and 0.4 ng/mL. The standards and resuspended test samples were added in duplicate in 50 μL volumes to the appropriate wells in the assay plate, and 50 μL of diluted enzyme conjugate were also added. The assay plate was gently agitated and incubated at room temperature for 1 hour. The contents of the plate were discarded after one hour, and each well was washed three times with 300 μL of diluted washing buffer. The plate was incubated at room temperature for 30 minutes after the addition of 150 μL of substrate to each well and gentle agitation. The plate was then read at 650 nm and 490 nm in a microplate reader. Average concentration values were calculated from the optical density measurements of the samples as compared with the standard concentration curve for each plate. The range of R^2 values of the concentration curves of five test plates was 0.905 to 0.976.

Resistivity

The resistivity of the electroactive coatings was determined using a Radio Shack multimeter (Model # 22-174, sensitivity: 0.01Ω to 19.9MΩ). Electrodes were placed at each end of a 1" by 3/8" sample, and the resistance was read from the display of the multimeter. Several readings were taken for each sample. The resistivity was calculated by multiplying by the electrode length (width of the sample) and dividing by the length of the sample. The units for resistivity are reported as ohms/square (Ω/□).

Contact Angle

The contact angle of all substrates was determined using the captive bubble method with a goniometer. Angles on each side of five 2μL air bubbles were measured for a total of ten data points for each sample. These values were averaged and reported in degrees.

CHAPTER 5
RESULTS AND DISCUSSION

Cell Concentration Experiment

The purpose of this study was to determine the appropriate cell concentrations to be used in future studies. Endothelial cells have a minimum concentration at which they will grow. It was also important to be able to track the growth rate of the cells in the experiments. Therefore a range of concentrations was tested, 50,000 cells/mL, 100,000 cells/mL, and 150,000 cells/mL. After approximately 36 hours, the 100,000 cells/mL and the 150,000 cells/mL concentrations were confluent; the 50,000 cells/mL concentration was not. Small distinctions in growth rate and morphology became difficult to distinguish with the 150,000 cells/mL concentration whereas with the lower concentrations these distinctions were readily apparent. Concentrations of 50,000 and 100,000 cells/mL were chosen for future studies because both allowed for the ability to distinguish small differences in cell numbers and morphology and provided an opportunity to understand the effect of concentration with electrical fields.

The cell counts as a function of time for various cell concentrations are shown in Figure 5.1.

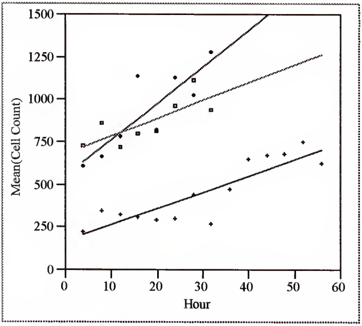

Linear fit for 50,000 cells/mL: y = 168.54 + 9.64x RSquare = 0.767
Linear fit for 100,000 cells/mL: y = 550.90 + 21.36x RSquare = 0.735
Linear fit for 150,000 cells/mL: y = 679.99 + 10.51x RSquare = 0.598

Figure 5.1 Cell Counts as a Function of Time at Various Cell Concentrations: 50,000 cells/mL (+), 100,000 cells/mL (◆), and 150,000 cells/mL (▣). (n = 9)

Effect of Trump's Fixative

The purpose of this study was to determine the effect of Trump's vapors on adjoining test wells in various configurations in 4- and 24-well test plates as described in Chapter 4. The results are shown in Figures 5.2-5.5.

This experiment showed that in order to accurately determine the morphology and proliferation rate of endothelial cells, the test wells need to be separated from each other during the experiment. The wells must be separated even further than alternating rows or columns in a 24-well plate, i.e. in separate plates, so that the Trump's vapors do not come in contact with live cells in the continuing study. Four-well culture plates are adequate for this purpose and were used in the feeding rate experiment and the concept for the stimulated growth experiments.

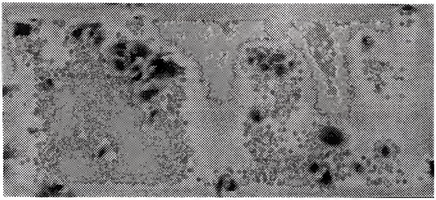

4 hour

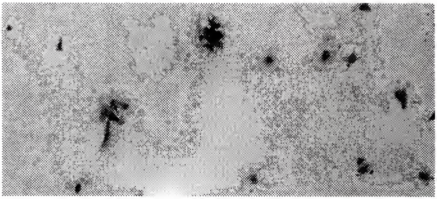

8 hour

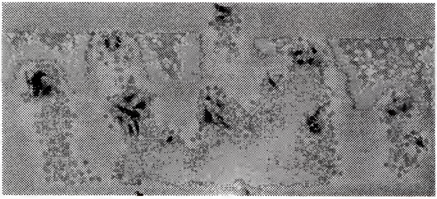

12 hour

Figure 5.2 Alternating Row Configuration of Trump's Experiment

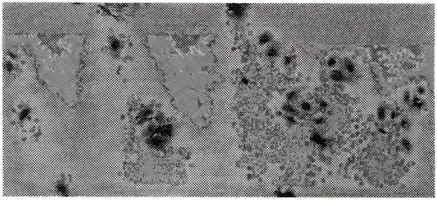

4 hour

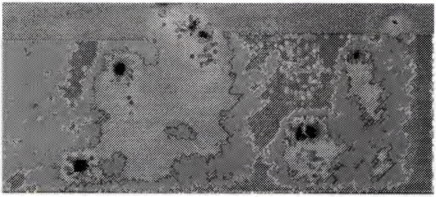

8 hour

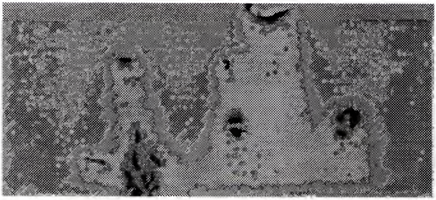

12 hour

Figure 5.3 Alternating Column Configuration of Trump's Experiment

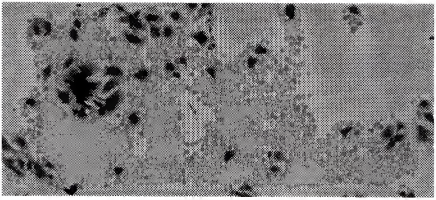

4 hour

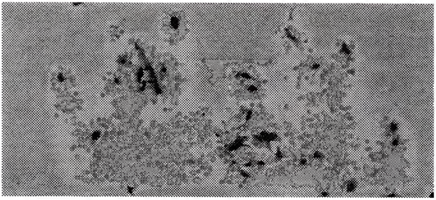

8 hour

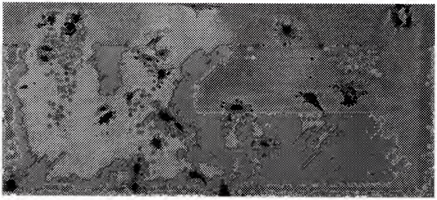

12 hour

Figure 5.4 Adjacent Column Configuration of Trump's Experiment

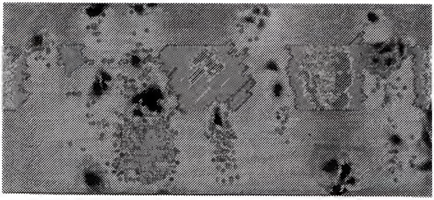

4 hour

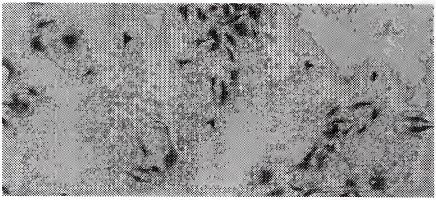

8 hour

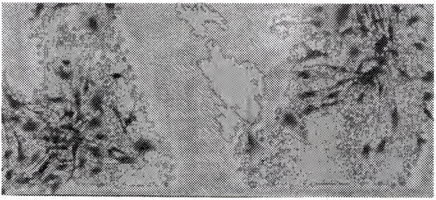

12 hour

Figure 5.5 4-well plate Configuration of Trump's Experiment

Feeding Rate Experiment

The purpose of the feeding rate experiment was to determine how often the growth medium should be changed during the stimulated growth studies. The three feeding rates tested were one feeding per 6, 12, and 24 hours. Photographs of the cells at 18 and 48 hours are shown in Figures 5.6-5.9. Two main conclusions were made from this study. Most importantly, the study showed that the 12-hour feeding rate was best for cell growth. The 6-hour rate had a higher potential of contamination with no observable benefit in cell growth rate or health. The cells fed at the 24-hour rate were more rounded indicating that they were not receiving an adequate amount of nourishment. Secondly, this study confirmed the results of the cell concentration study, that 50,000 and 100,000 cells/mL and a 36 hour time limit were appropriate for the stimulated growth studies.

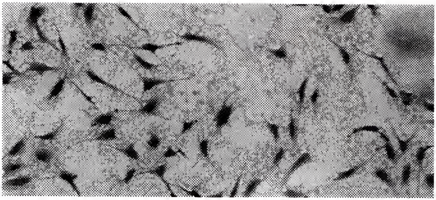

6 hour feeding rate

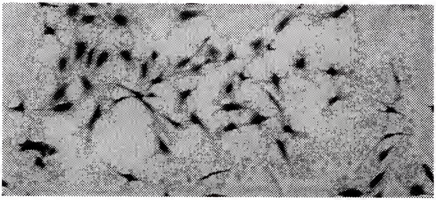

12 hour feeding rate

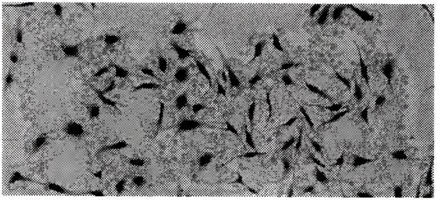

24 hour feeding rate

Figure 5.6 Feeding Rate Study: 50,000 cells/mL at 18 hours

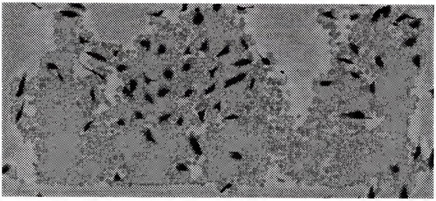

6 hour feeding rate

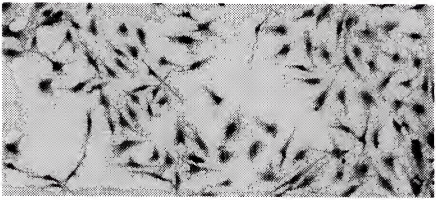

12 hour feeding rate

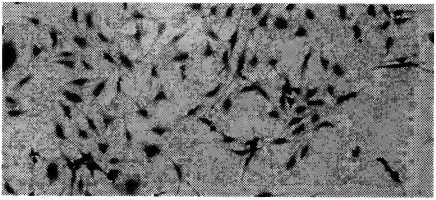

24 hour feeding rate

Figure 5.7 Feeding Rate Study: 100,000 cells/mL at 18 hours

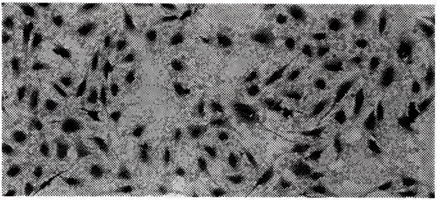

6 hour feeding rate

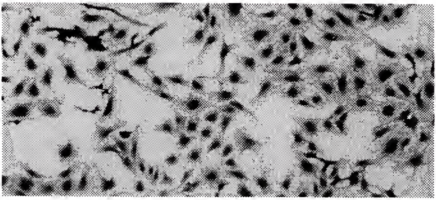

12 hour feeding rate

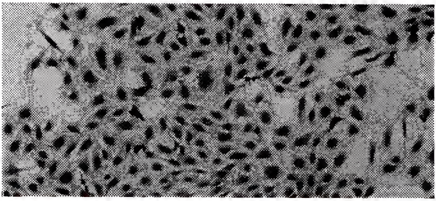

24 hour feeding rate

Figure 5.8 Feeding Rate Study: 50,000 cells/mL at 48 hours

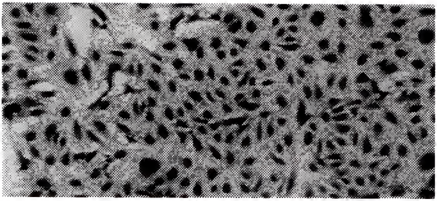

6 hour feeding rate

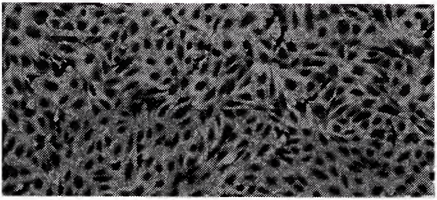

12 hour feeding rate

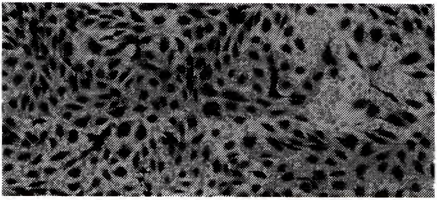

24 hour feeding rate

Figure 5.9 Feeding Rate Study: 100,000 cells/mL at 48 hours

Substrate Characterization

The measured resistivities of the substrates used in this research are given in Table 5.1. Manufacturer specifications listed the ITO-Glass and ITO-Mylar resistivities as 100Ω and the PPy Dacron resistivity as 60Ω. Resistance heating was assumed to be negligible due to the low resistivities of the substrates, the low voltages being tested and the large heat sink of the growth medium and the incubator itself.

Table 5.1 Resistivities of Test Substrates

Substrate	Resistivity (Ω)
Glass	∞
Mylar	∞
ITO-Glass	177 ± 45
ITO-Mylar	99 ± 12
C-Mylar	99 ± 20 kΩ
AuPd-Mylar	121 ± 28
PPy-Dacron	60

The contact angles of the substrates (captive bubble method) used in this research are given in Table 5.2.

Table 5.2 Contact Angles of Test Substrates

Substrate	Contact Angle (°)
Glass	51 ± 7
Mylar	73 ± 3
ITO-Glass	50 ± 4
ITO-Mylar	86 ± 3
C-Mylar	51 ± 4
AuPd-Mylar	79 ± 5

Scanning electron micrographs (SEMs) of all the test substrates are shown in Figures 5.10-5.16.

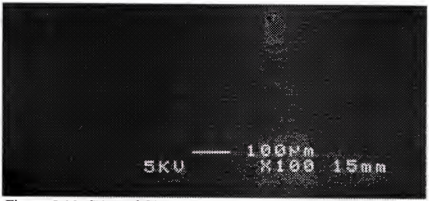

Figure 5.10 SEM of Glass

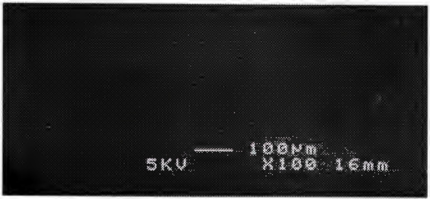

Figure 5.11 SEM of Mylar

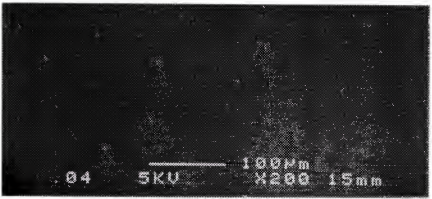

Figure 5.12 SEM of ITO-Glass

Figure 5.13 SEM of ITO-Mylar

Figure 5.14 SEM of C-Mylar

Figure 5.15 SEM of AuPd-Mylar

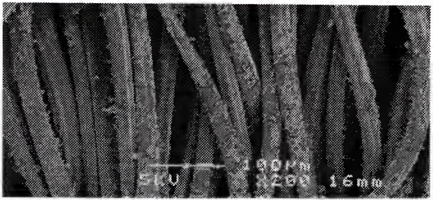

Figure 5.16 SEM of PPy-Dacron

Cytotoxicity Experiments

Cytotoxicity experiments were performed on all substrates before stimulated growth and adhesion experiments ensued. As shown in Figures 5.17-5.23, all substrates except the PPy-Dacron fabric showed favorable growth characteristics. No cells were seen on the PPy-Dacron fabric, and it was not apparent whether this was due to cytotoxicity or to processing techniques. Therefore, it was used in the stimulated growth experiments to determine if a change in prostacyclin levels would give an indication of cell viability.

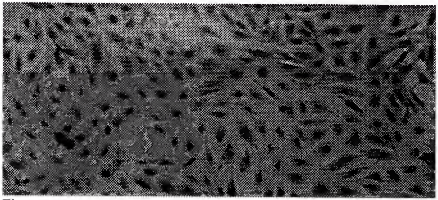

Figure 5.17 Cytotoxicity Test with Glass

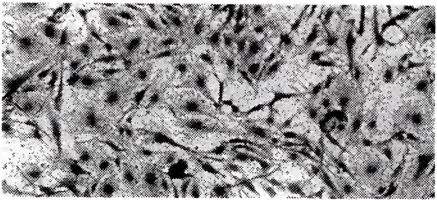

Figure 5.18 Cytotoxicity Test with Mylar

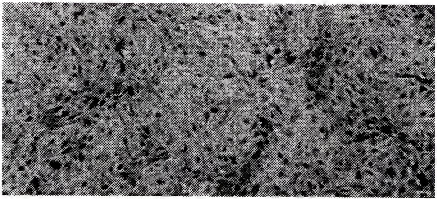

Figure 5.19 Cytotoxicity Test with ITO-Glass

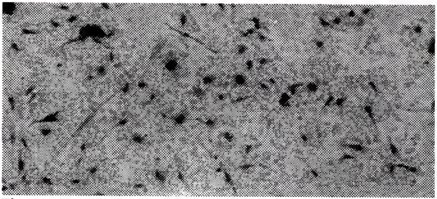

Figure 5.20 Cytotoxicity Test with ITO-Mylar

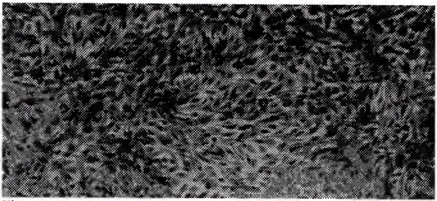

Figure 5.21 Cytotoxicity Test with C-Mylar

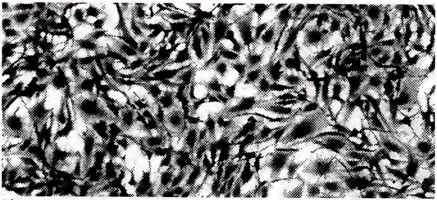

Figure 5.22 Cytotoxicity Test with AuPd-Mylar

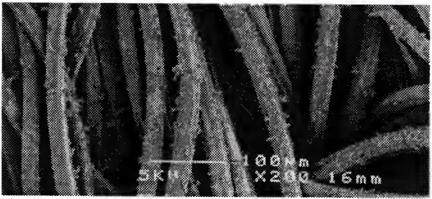

Figure 5.23 Cytotoxicity Test with PPy-Dacron

Pilot Experiment for Voltage Effects

The appropriate voltage levels were determine using experiments previously described. Figures 5.24-5.28 show the morphology of endothelial cells at the various voltages after 24 hours. At 0, 0.5, and 1 volt, the cells are well spread, indicating that they are growing normally. At 2 volts, the cells are somewhat spread but also begin to move to the ball and stick morphology which indicates that the cells are no longer in a growth-friendly environment. At 5 volts, the endothelial cells are very rounded, indicating poor growth conditions. This study indicated that the trends in the literature were correct, and that the appropriate voltage range for the stimulated growth and adhesion studies was 0 to 1 volt.

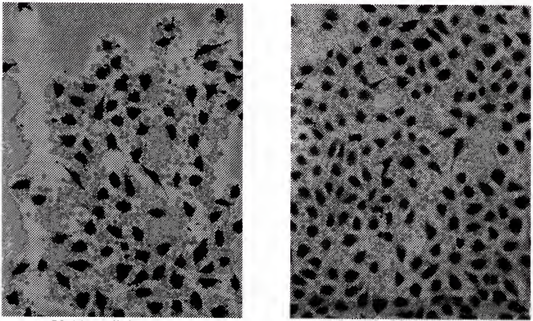

50,000 cells/mL 100,000 cells/mL

Figure 5.24 Endothelial Cells at 0 volts, 24 hours

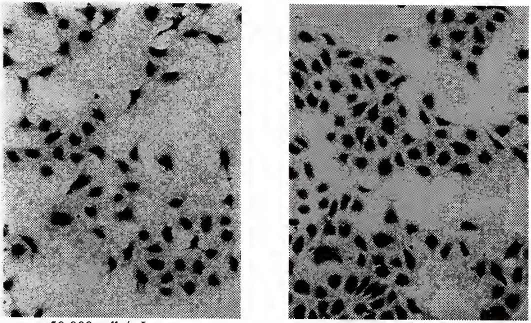

50,000 cells/mL 100,000 cells/mL

Figure 5.25 Endothelial Cells at 0.5 volts, 24 hours

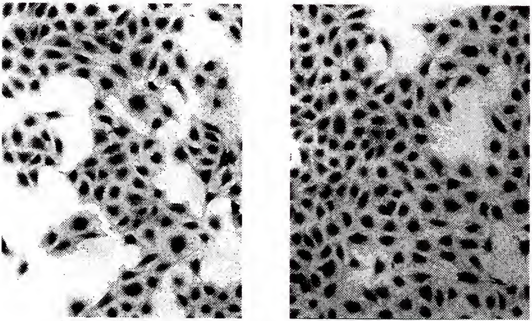

50,000 cells/mL 100,000 cells/mL

Figure 5.26 Endothelial Cells at 1 volt, 24 hours

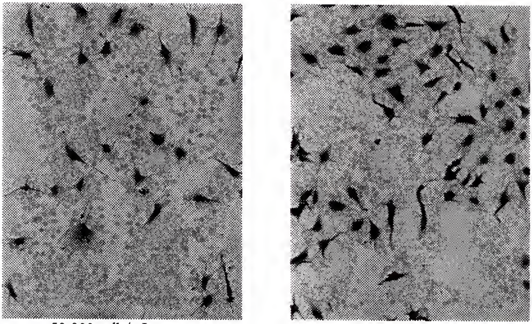

50,000 cells/mL
100,000 cells/mL

Figure 5.27 Endothelial Cells at 2 volts, 24 hours

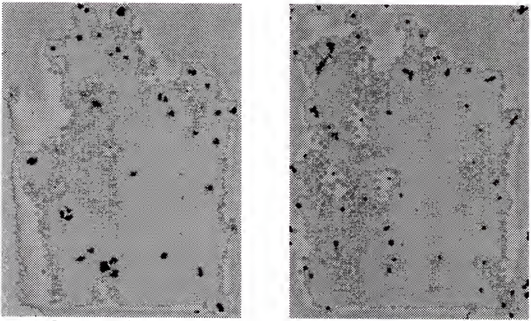

50,000 cells/mL
100,000 cells/mL

Figure 5.28 Endothelial Cells at 5 volts, 24 hours

Electrostimulated Cell Growth Experiments at 0 to 1 Volt

The growth characteristics of endothelial cells over time were determined for substrates at 0, 0.5, and 1 volt. The results of these studies are shown in Figures 5.29-5.40. Table 5.3 provides a summary of the relative favorability of voltages for each material and concentration combination. The data show that for ITO-Mylar and ITO-Glass, the voltage promoting the best growth was 0.5 volt, followed by the no-voltage control as second best. For C-Mylar, SC-Mylar, and AuPd-Mylar, 1 volt gave the highest cell counts, with the second best stimulation rate being 0.5 volt.

Table 5.3 Relative Favorability of Voltages in Growth Experiments

Material	Concentration (cells/mL)	Most Favorable Voltage for Cell Proliferation (v)	Least Favorable Voltage for Cell Proliferation (v)	Resistivity (Ω)
ITO-Glass	50,000	0.5	1 <> 0	177
	100,000	0.5	1	
ITO-Mylar	50,000	0.5	1	99
	100,000	0.5	1	
AuPd-Mylar	50,000	1	0	121
	100,000	1	0	
C-Mylar	50,000	1	0	98.7
	100,000	1	0	
SC-Mylar	50,000	1	0	∞
	100,000	1	0 <> 0.5	

The difference in voltage rankings may be explained by the quality of the substrate coatings. The ITO-Glass and ITO-Mylar were commercially manufactured, whereas C and AuPd coatings were applied to Mylar strips in a laboratory environment. As is shown in Figures 5.41-5.44, there is little correlation between growth rates and conductivity or hydrophilicity of the substrates. The dotted lines represent the 95% confidence limit, the interval most likely to contain the true population mean.

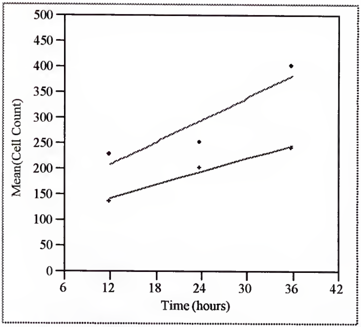

Linear Fit for 50,000 cells/mL:	y = 89.83 + 4.38x	RSquare = 0.98
Linear Fit for 100,000 cells/mL:	y = 122 + 7.25x	RSquare = 0.85

Figure 5.29 Proliferation of Endothelial Cells on Glass at 50,000 cells/mL (+) and at 100,000 cells/mL (◆). Mean cell count units are cells/mm^2 (n = 8).

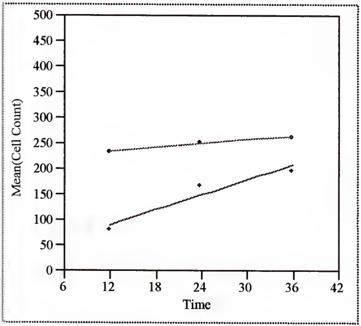

Linear Fit for 50,000 cells/mL:	y = 33.33 + 4.88x	RSquare = 0.92
Linear Fit for 100,000 cells/mL:	y = 222 + 1.21x	RSquare = 0.99

Figure 5.30 Proliferation of Endothelial Cells on Mylar at 50,000 cells/mL (+) and at 100,000 cells/mL (◆). Mean cell count units are cells/mm^2 (n = 8).

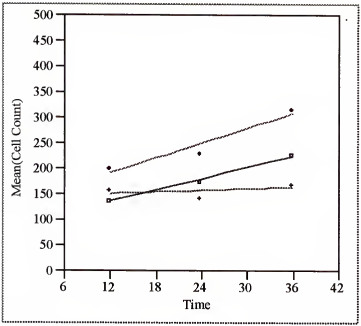

Linear fit for 0 volts: y = 146 + 0.52x RSquare = 0.20
Linear fit for 0.5 volts: y = 134.67 + 4.83x RSquare = 0.93
Linear fit for 1 volt: y = 93.5 + 3.67x RSquare = 0.99

Figure 5.31 Proliferation of Endothelial Cells on ITO-Glass (50,000 cells/mL) at 0 volts (+), 0.5 volt (◆), and 1 volt (◘). Mean cell count units are cells/mm^2 (n = 8).

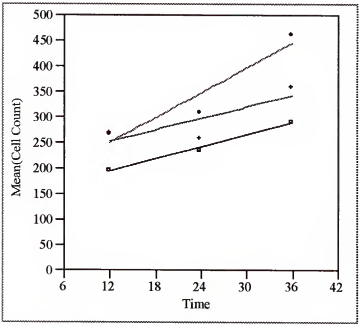

Linear fit for 0 volts: y = 208.67 + 3.75x RSquare = 0.67
Linear fit for 0.5 volts: y = 153 + 8.17x RSquare = 0.90
Linear fit for 1 volt: y = 149.17 + 3.92x RSquare = 0.99

Figure 5.32 Proliferation of Endothelial Cells on ITO-Glass (100,000 cells/mL) at 0 volts (+), 0.5 volt (◆), and 1 volt (◘). Mean cell count units are cells/mm^2 (n = 8).

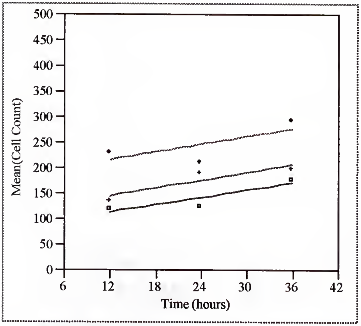

Linear fit for 0 volts:	y = 115.83 + 2.56x	RSquare = 0.83
Linear fit for 0.5 volts:	y = 187.17 + 2.54x	RSquare = 0.54
Linear fit for 1 volt:	y = 86.17 + 2.40x	RSquare = 0.81

Figure 5.33 Proliferation of Endothelial Cells on ITO-Mylar (50,000 cells/mL) at 0 volts (+), 0.5 volt (◆), and 1 volt (▣). Mean cell count units are cells/mm^2 (n = 8).

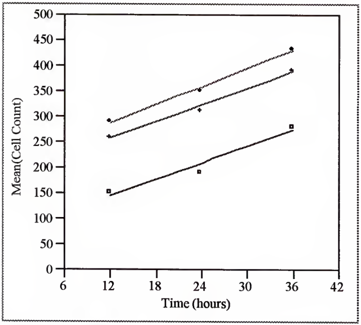

Linear fit for 0 volts:	y = 192.33 + 5.48x	RSquare = 0.98
Linear fit for 0.5 volts:	y = 218.33 + 5.97x	RSquare = 0.99
Linear fit for 1 volt:	y = 82.5 + 5.33x	RSquare = 0.95

Figure 5.34 Proliferation of Endothelial Cells on ITO-Mylar (100,000 cells/mL) at 0 volts (+), 0.5 volt (◆), and 1 volt (▣). Mean cell count units are cells/mm^2 (n = 8).

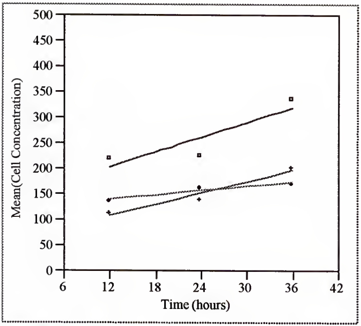

Linear fit for 0 volts: y = 63.67 + 3.73x RSquare = 0.94
Linear fit for 0.5 volts: y = 23.5 + 1.44x RSquare = 0.93
Linear fit for 1 volt: y = 147.5 + 4.79x RSquare = 0.78

Figure 5.35 Proliferation of Endothelial Cells on C-Mylar (50,000 cells/mL) at 0 volts (+), 0.5 volt (◆), and 1 volt (◘). Mean cell count units are cells/mm^2 (n = 8).

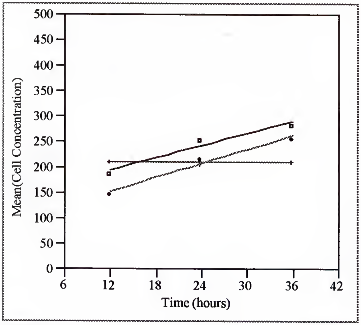

Linear fit for 0 volts: y = 210.67 + 0.063x RSquare = 0.04
Linear fit for 0.5 volts: y = 100 + 4.54x RSquare = 0.98
Linear fit for 1 volt: y = 148.83 + 3.96x RSquare = 0.95

Figure 5.36 Proliferation of Endothelial Cells on C-Mylar (100,000 cells/mL) at 0 volts (+), 0.5 volt (◆), and 1 volt (◘). Mean cell count units are cells/mm^2 (n = 8).

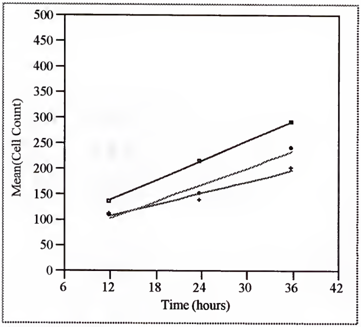

Linear fit for 0 volts: $y = 63.67 + 3.73x$ RSquare = 0.94
Linear fit for 0.5 volts: $y = 38.33 + 5.46x$ RSquare = 0.96
Linear fit for 1 volt: $y = 62.67 + 6.44x$ RSquare = 1.00

Figure 5.37 Proliferation of Endothelial Cells on SC-Mylar (50,000 cells/mL) at 0 volts (+), 0.5 volt (◆), and 1 volt (◘). Mean cell count units are cells/mm^2 (n = 8).

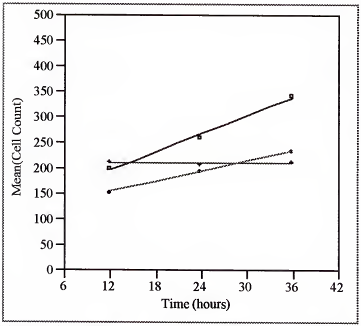

Linear fit for 0 volts: $y = 210.67 + 0.06x$ RSquare = 0.04
Linear fit for 0.5 volts: $y = 114.83 + 3.38x$ RSquare = 1.00
Linear fit for 1 volt: $y = 127.5 + 5.88x$ RSquare = 0.99

Figure 5.38 Proliferation of Endothelial Cells on SC-Mylar (100,000 cells/mL) at 0 volts (+), 0.5 volt (◆), and 1 volt (◘). Mean cell count units are cells/mm^2 (n = 8).

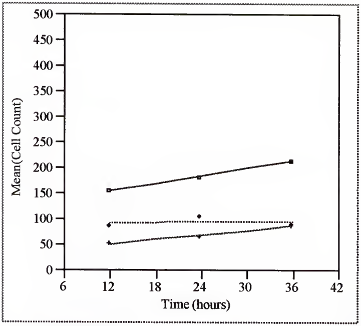

Linear fit for 0 volts: y = 35.17 + 1.44x RSquare = 0.99
Linear fit for 0.5 volts: y = 92 + 0.15x RSquare = 0.03
Linear fit for 1 volt: y = 126.67 + 2.46x RSquare = 1.00

Figure 5.39 Proliferation of Endothelial Cells on AuPd-Mylar (50,000 cells/mL) at 0 volts (+), 0.5 volt (◆), and 1 volt (■). Mean cell count units are cells/mm^2 (n = 8).

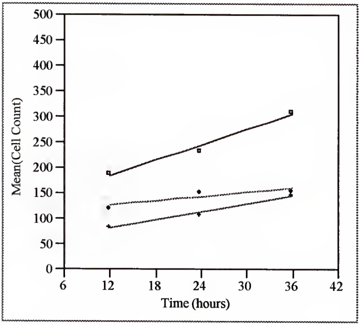

Linear fit for 0 volts: y = 50 + 2.65x RSquare = 0.98
Linear fit for 0.5 volts: y = 110.17 + 1.44x RSquare = 0.80
Linear fit for 1 volt: y = 126.33 + 5x RSquare = 0.98

Figure 5.40 Proliferation of Endothelial Cells on AuPd-Mylar (100,000 cells/mL) at 0 volts (+), 0.5 volt (◆), and 1 volt (■). Mean cell count units are cells/mm^2 (n = 8).

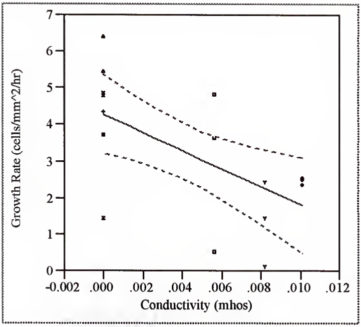

y = 4.31 – 247.86x RSquare = 0.37

Figure 5.41 Growth Rate versus Conductivity for 50,000 cells/mL Growth Samples.

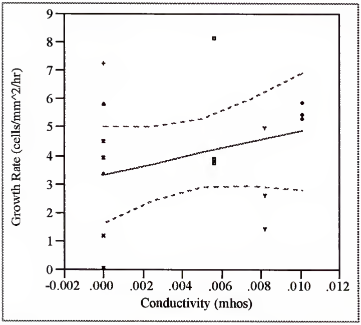

y = 3.36 + 150.76x RSquare = 0.08

Figure 5.42 Growth Rate versus Conductivity for 100,000 cells/mL Growth Samples.

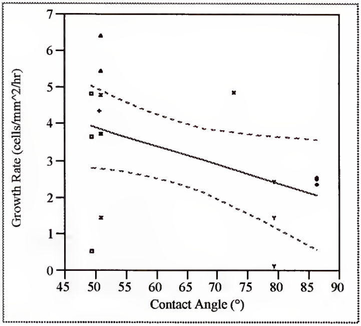

y = 6.46 – 0.05x RSquare = 0.21

Figure 5.43 Growth Rate versus Contact Angle for 50,000 cells/mL Growth Samples.

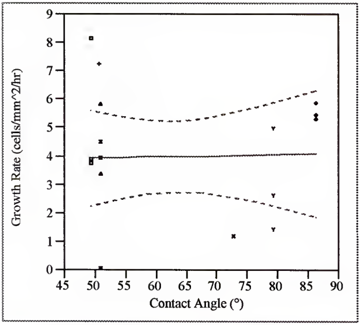

y = 3.73 + 0.004x RSquare = 0.0009

Figure 5.44 Growth Rate versus Contact Angle for 100,000 cells/mL Growth Samples.

AuPd-Mylar had statistically (n=8) lower cell counts than any other material except for Mylar, which had a broad distribution, even though AuPd-Mylar showed no sign of cytotoxicity. Cell counts of all other materials were not statistically significantly different from each other. The statistical analysis determined by JMP (SASS Institute) are shown in Figure 5.45 Diamond height represents the 95% confidence interval around the mean indicated by the central horizontal lines in each diamond. Comparison circles to the right indicate AuPd-Mylar cell counts (bold black circle) are significantly lower than all other materials (bold gray circles, italicized text) except for Mylar (thin black circle). The data are further defined in Table 5.4-5.7. These table display the average cell count, the standard deviation thereof, and comparisons of significance between materials and voltages.

There is no statistically significant difference between the C-Mylar and the SC-Mylar cell counts. This shows that it does not matter whether the electrical stimulation is through the substrate on which the cells are growing or through the growth medium.

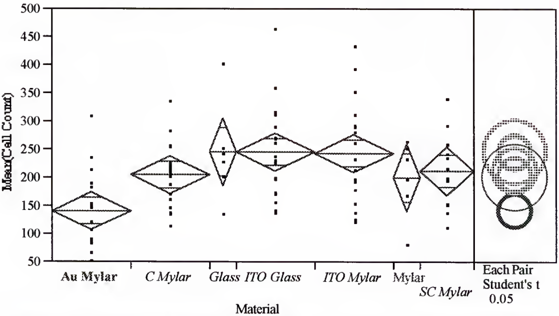

Figure 5.45 Statistical Significance Rankings of Cell Counts from Substrates used in Growth Experiments.

Table 5.4 Statistical Significance of Cell Counts when Comparing Substrates with Cell Concentrations of 50,000 cells/mL in Growth Experiments

				Significant vs.:						
Substrate	n	Ave. # Cells/ mm^2	St. Dev.	ITO-Glass	ITO-Mylar	C-Mylar	SC-Mylar	AuPd-Mylar	Glass	Mylar
ITO-Glass	72	197	80	-				yes		
ITO-Mylar	72	190	75		-			yes		
C-Mylar	72	191	82			-		yes		
SC-Mylar	72	193	77				-	yes		
AuPd-Mylar	72	117	63	yes	yes	yes	yes	-		
Glass	24	195	78						-	
Mylar	24	150	79							-

Table 5.5 Statistical Significance of Cell Counts when Comparing Substrates with Cell Concentrations of 100,000 cells/mL in Growth Experiments

				Significant vs.:						
Substrate	n	Ave. # Cells/ mm^2	St. Dev.	ITO-Glass	ITO-Mylar	C-Mylar	SC-Mylar	AuPd-Mylar	Glass	Mylar
ITO-Glass	72	297	95	-		yes		yes		
ITO-Mylar	72	298	120		-	yes		yes		
C-Mylar	72	222	78	yes	yes	-				
SC-Mylar	72	232	78				-			
AuPd-Mylar	72	168	95	yes	yes			-	yes	
Glass	24	296	121					yes	-	
Mylar	24	251	72							-

Table 5.6 Statistical Significance of Cell Counts when Comparing Voltages with Cell Concentrations of 50,000 cells/mL in Growth Experiments

Substrate	n	Voltage (V)	Ave. # Cells/mm^2	St. Dev.	Significant vs.: 0 volt	0.5 volt	1 volt
ITO-Glass	24	0	158	73	-	yes	
	24	0.5	251	73	yes	-	
	24	1	182	65			-
ITO-Mylar	24	0	177	69	-		
	24	0.5	248	67		-	yes
	24	1	144	46		yes	-
C-Mylar	24	0	153	71	-		yes
	24	0.5	158	41		-	yes
	24	1	262	77	yes	yes	-
SC-Mylar	24	0	153	71	-		
	24	0.5	169	69		-	
	24	1	217	79			-
AuPd-Mylar	24	0	70	31	-		yes
	24	0.5	96	34		-	yes
	24	1	186	48	yes	yes	-

Table 5.7 Statistical Significance of Cell Counts when Comparing Voltages with Cell Concentrations of 100,000 cells/mL in Growth Experiments

Substrate	n	Voltage (V)	Ave. # Cells/mm^2	St. Dev.	Significant vs.: 0 volt	0.5 volt	1 volt
ITO-Glass	24	0	299	84	-		
	24	0.5	349	104		-	
	24	1	243	67			-
ITO-Mylar	24	0	324	131	-		
	24	0.5	360	93		-	yes
	24	1	210	77		yes	-
C-Mylar	24	0	212	81	-		
	24	0.5	209	82		-	
	24	1	244	68			-
SC-Mylar	24	0	212	81	-		
	24	0.5	196	62		-	
	24	1	268	77			-
AuPd-Mylar	24	0	114	46	-		yes
	24	0.5	145	55		-	yes
	24	1	246	112	yes	yes	-

The current through individual samples is shown in Table 5.8. As is indicated, there is no correlation between the individual sample currents and the growth characteristics of the endothelial cells on different substrates. This is also shown in Figures 5.46 and 5.47.

Table 5.8 Currents Through Individual Growth Samples

Material	Individual Sample Current at 0.5 volt (μA)	Individual Sample Current at 1 volt (μA)
ITO-Glass	26.1	52.2
ITO-Mylar	46.7	93.2
AuPd-Mylar	38.3	76.5
C-Mylar	0.047	0.094
SC-Mylar/Growth Medium	0.047	0.094
PPy Dacron	77.2	154

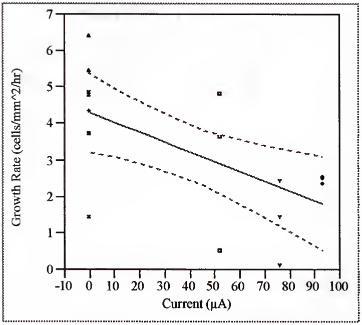

y = 4.31 – 0.03x RSquare = 0.37

Figure 5.46 Growth Rate versus Individual Sample Current for 50,000 cells/mL Growth Samples.

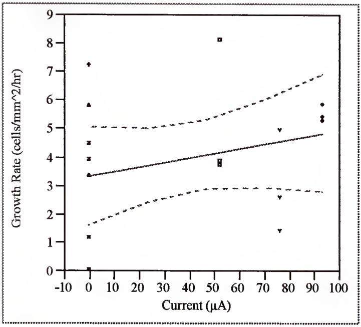

y = 3.36 + 0.02x RSquare = 0.08

Figure 5.47 Growth Rate versus Individual Sample Current for 100,000 cells/mL Growth Samples.

The release of 6-keto-prostaglandin-F$_{1\alpha}$ (6-k-PGF$_{1\alpha}$) was measured for growth samples to determine if the release of prostacyclin by the endothelial changed over time at different voltages. The results of this study are shown in Figures 5.48 - 5.61. The data is generally linear in nature, but has some variability associated with it. This is most likely due to small sample volumes and the limited number of samples tested. Thymadine uptake may have been a more indicative of the cell growth stimulus and cycle.

Mylar and PPy Dacron had lowest overall release of 6-k-PGF$_{1\alpha}$ over time, and cells on both materials showed statistically significant lower quantities than those on C-Mylar. Conversely, cells on C-Mylar had the highest overall release of 6-k-PGF$_{1\alpha}$ over time and showed statistically significant higher quantities than those on Mylar, PD, and ITO-Mylar. This statistical analysis determined by JMP is illustrated in Figure 5.62. Diamond height represents the 95% confidence interval around the mean indicated by the central horizontal lines in each diamond. Comparison circles to the right denote PPy

Dacron with a bold black circle, C-Mylar with a bold gray circles, and all other materials with a thin black circle. Tables 5.9 and 5.10 define the data further and denote that at the 100,000 cells/mL concentration, C-Mylar had statistically higher release rates than ITO-Mylar, AuPd-Mylar, Mylar and PPy-Dacron. There was a significant difference between release of 6-k-PGF$_{1\alpha}$ between the voltages tested overall, but generally not for individual substrates as shown in Tables 5.11 and 5.12. A table showing the voltages with the highest and lowest 6-k-PGF$_{1\alpha}$ release is given in Table 5.13.

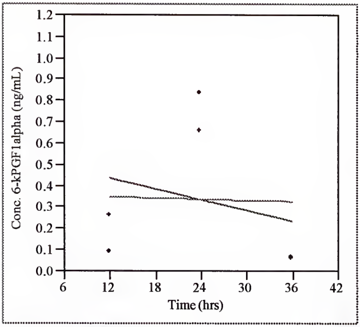

Linear Fit for 50,000 cells/mL: y = 0.54 – 0.01x RSquare = 0.11
Linear Fit for 100,000 cells/mL: y = 0.36 – 0.001x RSquare = 0.0007

Figure 5.48 Release of 6-k-PGF$_{1\alpha}$ from Endothelial Cells on Glass at 50,000 cells/mL (+) and at 100,000 cells/mL (◆).

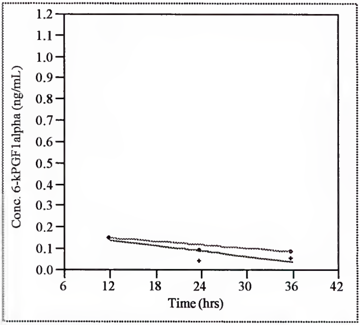

Linear Fit for 50,000 cells/mL: y = 0.19 – 0.004x RSquare = 0.66
Linear Fit for 100,000 cells/mL: y = 0.19 – 0.003x RSquare = 0.79

Figure 5.49 Release of 6-k-PGF$_{1\alpha}$ from Endothelial Cells on Mylar at 50,000 cells/mL (+) and at 100,000 cells/mL (◆).

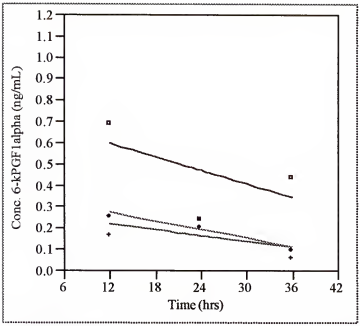

Linear fit for 0 volts: $y = 0.28 - 0.004x$ RSquare = 0.32
Linear fit for 0.5 volts: $y = 0.358 - 0.007x$ RSquare = 0.96
Linear fit for 1 volt: $y = 0.727 - 0.01x$ RSquare = 0.31

Figure 5.50 Release of 6-k-PGF$_{1\alpha}$ from Endothelial Cells on ITO-Glass (50,000 cells/mL) at 0 volts (+), 0.5 volt (◆), and 1 volt (■).

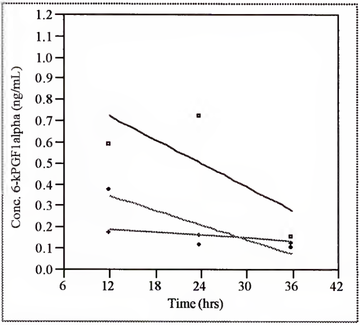

Linear fit for 0 volts: $y = 0.22 - 0.002x$ RSquare = 0.94
Linear fit for 0.5 volts: $y = 0.49 - 0.01x$ RSquare = 0.79
Linear fit for 1 volt: $y = 0.95 - 0.02x$ RSquare = 0.54

Figure 5.51 Release of 6-k-PGF$_{1\alpha}$ from Endothelial Cells on ITO-Glass (100,000 cells/mL) at 0 volts (+), 0.5 volt (◆), and 1 volt (■).

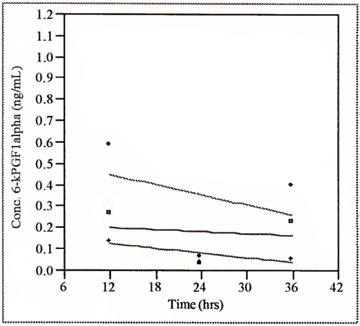

Linear fit for 0 volts: $y = 0.17 - 0.004x$ RSquare = 0.66
Linear fit for 0.5 volts: $y = 0.55 - 0.008x$ RSquare = 0.13
Linear fit for 1 volt: $y = 0.22 - 0.002x$ RSquare = 0.02

Figure 5.52 Release of 6-k-PGF$_{1\alpha}$ from Endothelial Cells on ITO-Mylar (50,000 cells/mL) at 0 volts (+), 0.5 volt (◆), and 1 volt (■).

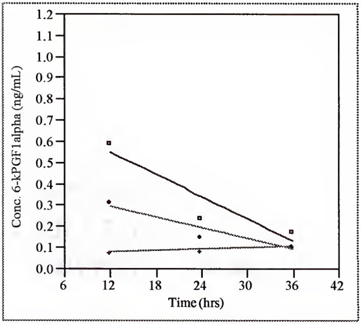

Linear fit for 0 volts: $y = 0.07 + 0.001x$ RSquare = 0.87
Linear fit for 0.5 volts: $y = 0.41 - 0.009x$ RSquare = 0.90
Linear fit for 1 volt: $y = 0.77 - 0.02x$ RSquare = 0.87

Figure 5.53 Release of 6-k-PGF$_{1\alpha}$ from Endothelial Cells on ITO-Mylar (100,000 cells/mL) at 0 volts (+), 0.5 volt (◆), and 1 volt (■).

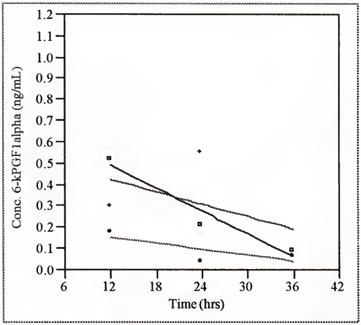

Linear fit for 0 volts: y = 0.54 – 0.01x RSquare = 0.23
Linear fit for 0.5 volts: y = 0.21 – 0.005x RSquare = 0.58
Linear fit for 1 volt: y = 0.71 – 0.02x RSquare = 0.94

Figure 5.54 Release of 6-k-PGF$_{1\alpha}$ from Endothelial Cells on C-Mylar (50,000 cells/mL) at 0 volts (+), 0.5 volt (◆), and 1 volt (■).

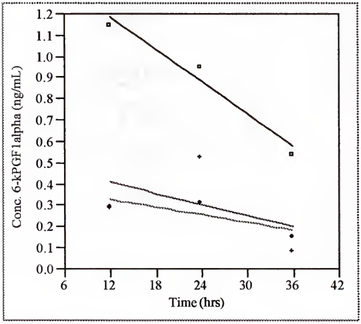

Linear fit for 0 volts: y = 0.51 – 0.009x RSquare = 0.21
Linear fit for 0.5 volts: y = 0.40 – 0.006x RSquare = 0.67
Linear fit for 1 volt: y = 1.49 – 0.03x RSquare = 0.96

Figure 5.55 Release of 6-k-PGF$_{1\alpha}$ from Endothelial Cells on C-Mylar (100,000 cells/mL) at 0 volts (+), 0.5 volt (◆), and 1 volt (■).

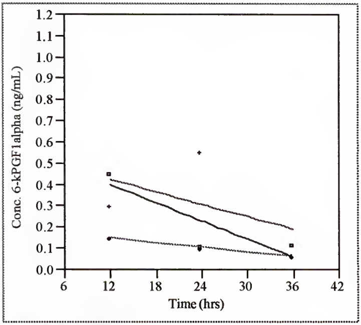

Linear fit for 0 volts: $y = 0.54 - 0.01x$ RSquare = 0.23
Linear fit for 0.5 volts: $y = 0.2 - 0.004x$ RSquare = 0.99
Linear fit for 1 volt: $y = 0.57 - 0.01x$ RSquare = 0.75

Figure 5.56 Release of 6-k-PGF$_{1\alpha}$ from Endothelial Cells on SC-Mylar (50,000 cells/mL) at 0 volts (+), 0.5 volt (◆), and 1 volt (▣).

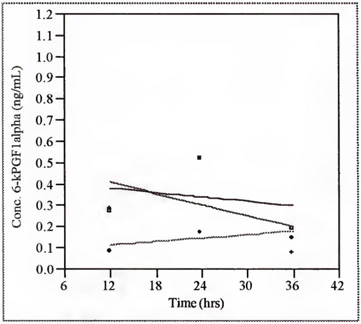

Linear fit for 0 volts: $y = 0.51 - 0.009x$ RSquare = 0.21
Linear fit for 0.5 volts: $y = 0.09 + 0.003x$ RSquare = 0.48
Linear fit for 1 volt: $y = 0.42 - 0.003x$ RSquare = 0.05

Figure 5.57 Release of 6-k-PGF$_{1\alpha}$ from Endothelial Cells on SC-Mylar (100,000 cells/mL) at 0 volts (+), 0.5 volt (◆), and 1 volt (▣).

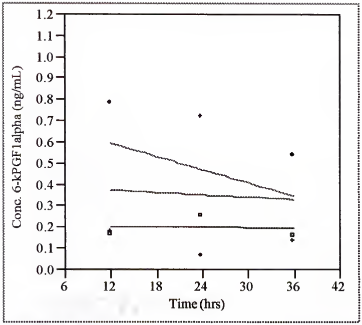

Linear fit for 0 volts: $y = 0.40 - 0.002x$ RSquare = 0.004
Linear fit for 0.5 volts: $y = 0.72 - 0.01x$ RSquare = 0.111
Linear fit for 1 volt: $y = 0.21 - 0.0003x$ RSquare = 0.004

Figure 5.58 Release of 6-k-PGF$_{1\alpha}$ from Endothelial Cells on AuPd-Mylar (50,000 cells/mL) at 0 volts (+), 0.5 volt (◆), and 1 volt (◘).

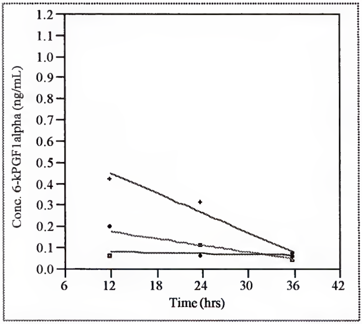

Linear fit for 0 volts: $y = 0.64 - 0.02x$ RSquare = 0.95
Linear fit for 0.5 volts: $y = 0.24 - 0.005x$ RSquare = 0.67
Linear fit for 1 volt: $y = 0.09 - 0.0007x$ RSquare = 0.048

Figure 5.59 Release of 6-k-PGF$_{1\alpha}$ from Endothelial Cells on AuPd-Mylar (100,000 cells/mL) at 0 volts (+), 0.5 volt (◆), and 1 volt (◘).

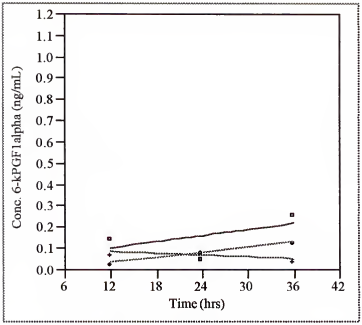

Linear fit for 0 volts:	y = 0.11 – 0.001x	RSquare = 0.58
Linear fit for 0.5 volts:	y = -0.01 + 0.004x	RSquare = 1.00
Linear fit for 1 volt:	y = 0.05 + 0.005x	RSquare = 0.28

Figure 5.60 Release of 6-k-PGF$_{1\alpha}$ from Endothelial Cells on PPy Dacron (50,000 cells/mL) at 0 volts (+), 0.5 volt (◆), and 1 volt (■).

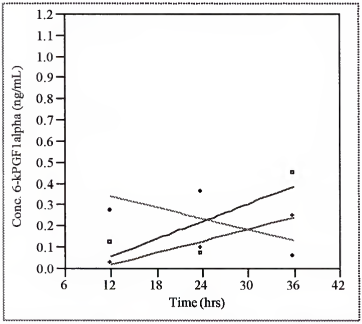

Linear fit for 0 volts:	y = -0.09 + 0.009x	RSquare = 0.95
Linear fit for 0.5 volts:	y = 0.45 – 0.009x	RSquare = 0.47
Linear fit for 1 volt:	y = -0.11 + 0.01x	RSquare = 0.64

Figure 5.61 Release of 6-k-PGF$_{1\alpha}$ from Endothelial Cells on PPy Dacron (100,000 cells/mL) at 0 volts (+), 0.5 volt (◆), and 1 volt (■).

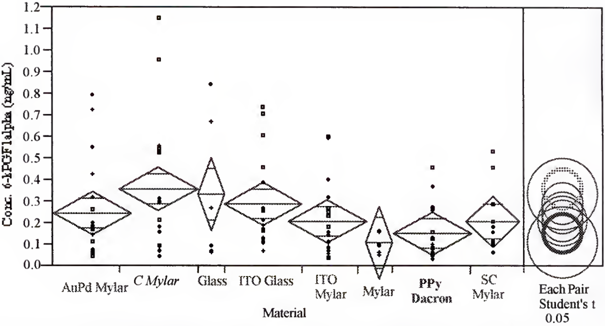

Figure 5.62 Statistical Significance Rankings of 6-k-PGF$_{1\alpha}$ Release from Endothelial Cells on Substrates used in Growth Experiments.

Table 5.9 Statistical Significance of Concentrations of 6-k-PGF$_{1a}$ when Comparing Substrates with Cell Concentrations of 50,000 cells/mL in Growth Experiments

				Significant vs.:							
Substrate	n	Ave. Conc. (ng/mL)	St. Dev.	ITO-Glass	ITO-Mylar	C-Mylar	SC-Mylar	AuPd-Mylar	Glass	Mylar	PPy-Dacro
ITO-Glass	9	0.28	0.19	-							
ITO-Mylar	9	0.21	0.19		-						
C-Mylar	9	0.23	0.20			-					
SC-Mylar	9	0.17	0.14				-				
AuPd-Mylar	9	0.34	0.27					-			yes
Glass	3	0.34	0.31						-		
Mylar	3	0.09	0.06							-	
PPy-Dacron	9	0.11	0.07					yes			-

Table 5.10 Statistical Significance of Concentrations of 6-k-PGF$_{1a}$ when Comparing Substrates with Cell Concentrations of 100,000 cells/mL in Growth Experiments

				Significant vs.:							
Substrate	n	Ave. # Cells/ mm^2	St. Dev.	ITO-Glass	ITO-Mylar	C-Mylar	SC-Mylar	AuPd-Mylar	Glass	Mylar	PPy-Dacron
ITO-Glass	9	0.29	0.23	-							
ITO-Mylar	9	0.21	0.17		-	yes					
C-Mylar	9	0.48	0.36		yes	-		yes		yes	yes
SC-Mylar	9	0.25	0.15				-				
AuPd-Mylar	9	0.15	0.14			yes		-			
Glass	3	0.34	0.44						-		
Mylar	3	0.12	0.04			yes				-	
PPy-Dacron	9	0.20	0.15			yes					-

Table 5.11 Statistical Significance of Concentrations of 6-k-PGF$_{1a}$ when Comparing Voltages with Cell Concentrations of 50,000 cells/mL in Growth Experiments

					Significant vs.:		
Substrate	n	Voltage (V)	Ave. Conc. (ng/mL)	St. Dev.	0 volt	0.5 volt	1 volt
ITO-Glass	3	0	0.17	0.09	-		yes
	3	0.5	0.20	0.08		-	
	3	1	0.48	0.23	yes		-
ITO-Mylar	3	0	0.08	0.05	-		
	3	0.5	0.36	0.27		-	
	3	1	0.18	0.1			-
C-Mylar	3	0	0.31	0.24	-		
	3	0.5	0.10	0.07		-	
	3	1	0.28	0.22			-
SC-Mylar	3	0	0.31	0.24	-		
	3	0.5	0.11	0.05		-	
	3	1	0.23	0.20			-
AuPd-Mylar	3	0	0.35	0.33	-		
	3	0.5	0.47	0.37		-	
	3	1	0.20	0.05			-
PPy-Dacron	3	0	0.07	0.02	-		
	3	0.5	0.08	0.05		-	
	3	1	0.16	0.11			-

Table 5.12 Statistical Significance of Concentrations of 6-k-PGF$_{1a}$ when Comparing Voltages with Cell Concentrations of 100,000 cells/mL in Growth Experiments

Substrate	n	Voltage (V)	Ave. Conc. (ng/mL)	St. Dev.	Significant vs.: 0 volt	0.5 volt	1 volt
ITO-Glass	3	0	0.17	0.03	-		
	3	0.5	0.21	0.16		-	
	3	1	0.50	0.30			-
ITO-Mylar	3	0	0.10	0.01	-		
	3	0.5	0.20	0.11		-	
	3	1	0.35	0.23			-
C-Mylar	3	0	0.31	0.22	-		yes
	3	0.5	0.26	0.09		-	yes
	3	1	0.88	0.31	yes	yes	-
SC-Mylar	3	0	0.31	0.22	-		
	3	0.5	0.15	0.05		-	
	3	1	0.34	0.17			-
AuPd-Mylar	3	0	0.27	0.19	-		
	3	0.5	0.12	0.08		-	
	3	1	0.08	0.04			-
PPy-Dacron	3	0	0.13	0.11	-		
	3	0.5	0.24	0.15		-	
	3	1	0.22	0.21			-

Table 5.13 Relative Favorability of Voltages for Release of 6-k-PGF$_{1\alpha}$ in Growth Experiments

Material	Concentration (cells/mL)	Voltage with Highest 6-k-PGF$_{1\alpha}$ Release Rate (v)	Voltage with Lowest 6-k-PGF$_{1\alpha}$ Release Rate (v)
ITO-Glass	50,000	1	0
	100,000	1	0
ITO-Mylar	50,000	0.5	0
	100,000	1	0
AuPd-Mylar	50,000	0.5	1
	100,000	0	1
C-Mylar	50,000	1 < > 0	0.5
	100,000	1	0.5
SC-Mylar	50,000	0	0.5
	100,000	1	0.5
PPy Dacron	50,000	1	0
	100,000	0.5 < > 1	0 < > 0.5

The control samples (0V) have very low release rates which is typical of that reported in literature (Mye 96, Cha 96, Bri 98). The release rates for the majority of the electrically stimulated samples (0.5 and 1 volt) were negative, indicating that the release of 6-k-PGF$_{1\alpha}$ decreased over time on these samples.

Release rates of 6-k-PGF$_{1\alpha}$ versus conductivity, contact angle, and individual sample current are shown in Figures 5.63-5.68. These figures show the trend of increasing release rates with increasing conductivity and individual sample current. However, these trends are not statistically significant. There is no correlation between contact angle and release rate of 6-k-PGF$_{1\alpha}$.

Summary of Electrostimulated Cell Growth Experiments

Overall, the results of the growth experiments indicate that low voltage direct current is beneficial to cell growth compared to no voltage. However, no correlation was found between conductivity, hydrophobicity, or current through individual samples and growth rates. Production of 6-k-PGF$_{1\alpha}$ decreased over time with electrical stimulation, although release rates tend to increase with increasing voltage.

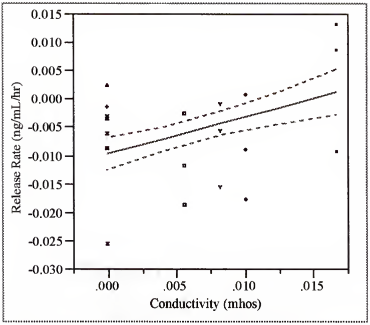

y = -0.01 + 0.65x

RSquare = 0.48

Figure 5.63 Release Rate of 6-k-PGF$_{1\alpha}$ versus Conductivity for 50,000 cells/mL Growth Samples.

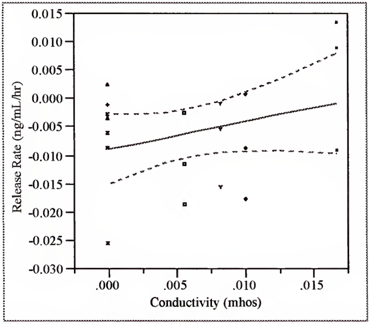

y = -0.01 + 0.49x

Rsquare = 0.10

Figure 5.64 Release Rate of 6-k-PGF$_{1\alpha}$ versus Conductivity for 100,000 cells/mL Growth Samples.

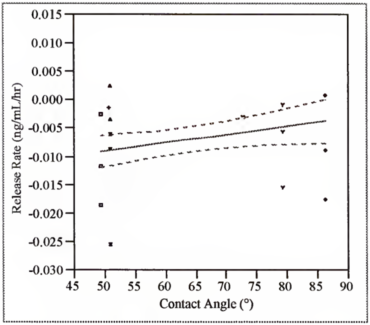

y = -0.02 + 0.0002x RSquare = 0.24

Figure 5.65 Release Rate of 6-k-PGF$_{1\alpha}$ versus Contact Angle for 50,000 cells/mL Growth Samples.

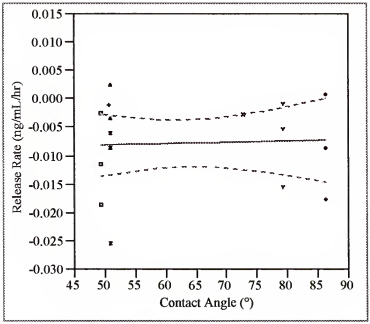

y = -0.009 + 0.00003x RSquare = 0.003

Figure 5.66 Release Rate of 6-k-PGF$_{1\alpha}$ versus Contact Angle for 100,000 cells/mL Growth Samples.

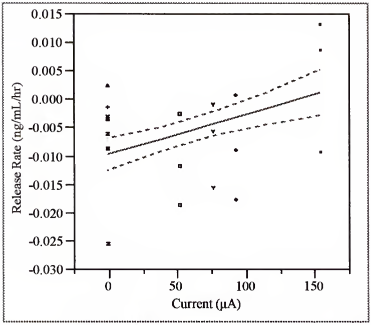

y = -0.01 + 0.00007x RSquare = 0.48

Figure 5.67 Release Rate of 6-k-PGF$_{1\alpha}$ versus Individual Sample Current for 50,000 cells/mL Growth Samples.

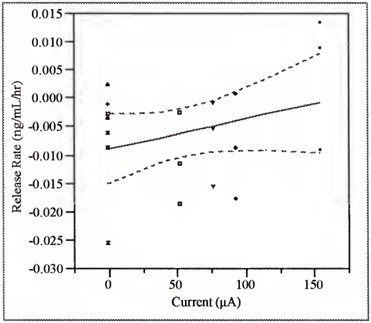

y = -0.01 + 0.00005x RSquare = 0.10

Figure 5.68 Release Rate of 6-k-PGF$_{1\alpha}$ versus Individual Sample Current for 100,000 cells/mL Growth Samples.

Cell Adhesion Experiments

The adhesion characteristics of endothelial cells over time were determined for substrates at 0, 0.5, and 1 volt using the adhesion flow chamber previously described. The results of these studies are shown in Figures 5.69-5.78.

Cells on all substrates showed a spread morphology at 0 volts, and most substrates had cells with rounded morphologies at 0.5 and 1 volt. None of the endothelial cells were noted to have elongated in the direction of flow during the course of the experiment.

Comparable cell adhesion behavior was observed across all three voltages on the following samples: 50,000 cells/mL and 100,000 cells/mL ITO-Mylar, 50,000 cells/mL C-Mylar, and 100,000 cells/mL ITO-Glass. All other material/concentration combinations varied widely over the three voltages. These samples showed high cell adhesion numbers at 0 volt and low at 0.5 volt.

AuPd-Mylar, C-Mylar, ITO-Glass, and ITO-Mylar had very similar adhesion characteristics, with ITO-Mylar showing the poorest cell adhesion. Mylar had statistically significantly higher cell adhesion than all other substrates. Glass also had statistically significantly higher cell adhesion than all other substrates except for ITO-Glass. A graph showing the statistical analysis determined by JMP (SASS Institute) is shown in Figure 5.79. Diamond height represents the 95% confidence interval around the mean indicated by the central horizontal lines in each diamond. Comparison circles to the right indicate AuPd-Mylar and C-Mylar cell counts with bold black circles, Mylar and Glass with a bold gray circle, and ITO-Mylar and ITO-Glass with thin black circles. Localized galvanic corrosion of the AuPd-Mylar coatings was observed on adhesion samples and is most likely the reason for its poor performance in those experiments. The data are further defined in Tables 5.14-5.17 by comparing statistical significance between materials and voltages.

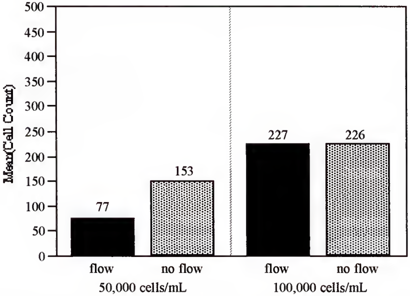

Figure 5.69 Adhesion of Endothelial Cells on Glass at 50,000 cells/mL and at 100,000 cells/mL. Mean cell count units are cells/mm^2. (flow: n = 8, no flow: n=4)

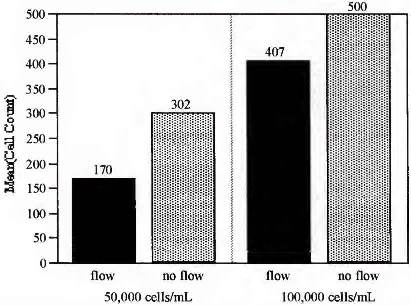

Figure 5.70 Adhesion of Endothelial Cells on Mylar at 50,000 cells/mL and at 100,000 cells/mL. Mean cell count units are cells/mm^2. (flow: n = 8, no flow: n=4)

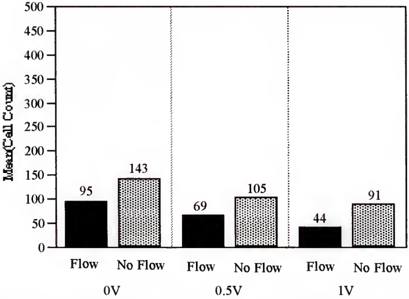

Figure 5.71 Adhesion of Endothelial Cells on ITO-Glass (50,000 cells/mL) at 0 volts, 0.5 volt, and 1 volt. Mean cell count units are cells/mm^2. (flow: n = 8, no flow: n=4)

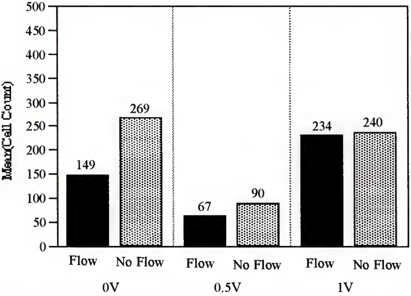

Figure 5.72 Adhesion of Endothelial Cells on ITO-Glass (100,000 cells/mL) at 0 volts, 0.5 volt, and 1 volt. Mean cell count units are cells/mm^2. (flow: n = 8, no flow: n=4)

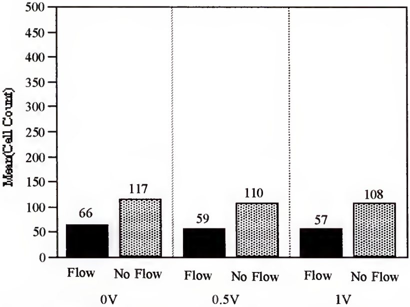

Figure 5.73 Adhesion of Endothelial Cells on ITO-Mylar (50,000 cells/mL) at 0 volts, 0.5 volt, and 1 volt. Mean cell count units are cells/mm^2. (flow: n = 8, no flow: n=4)

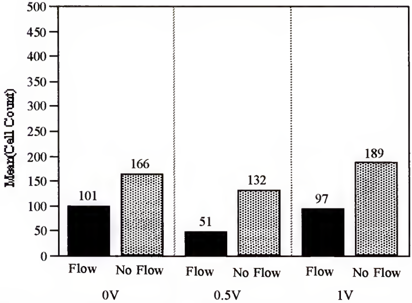

Figure 5.74 Adhesion of Endothelial Cells on ITO-Mylar (100,000 cells/mL) at 0 volts, 0.5 volt, and 1 volt. Mean cell count units are cells/mm^2. (flow: n = 8, no flow: n=4)

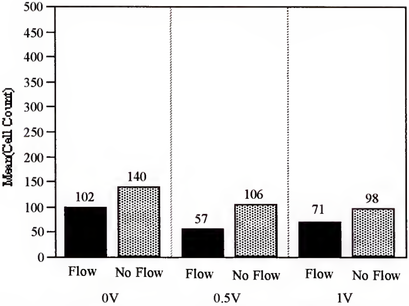

Figure 5.75 Adhesion of Endothelial Cells on C-Mylar (50,000 cells/mL) at 0 volts, 0.5 volt, and 1 volt. Mean cell count units are cells/mm^2. (flow: n = 8, no flow: n=4)

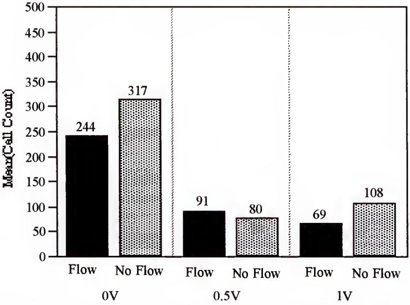

Figure 5.76 Adhesion of Endothelial Cells on C-Mylar (100,000 cells/mL) at 0 volts, 0.5 volt, and 1 volt. Mean cell count units are cells/mm^2. (flow: n = 8, no flow: n=4)

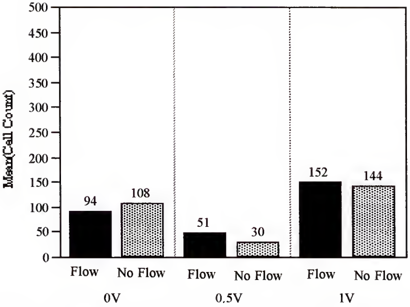

Figure 5.77 Adhesion of Endothelial Cells on AuPd-Mylar (50,000 cells/mL) at 0 volts, 0.5 volt, and 1 volt. Mean cell count units are cells/mm^2. (flow: n = 8, no flow: n=4)

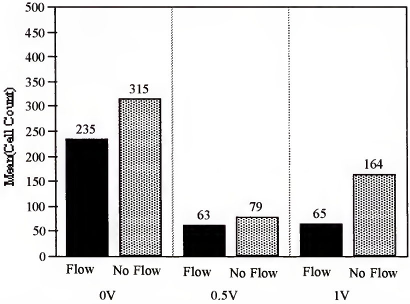

Figure 5.78 Adhesion of Endothelial Cells on AuPd-Mylar (100,000 cells/mL) at 0 volts, 0.5 volt, and 1 volt. Mean cell count units are cells/mm^2. (flow: n = 8, no flow: n=4)

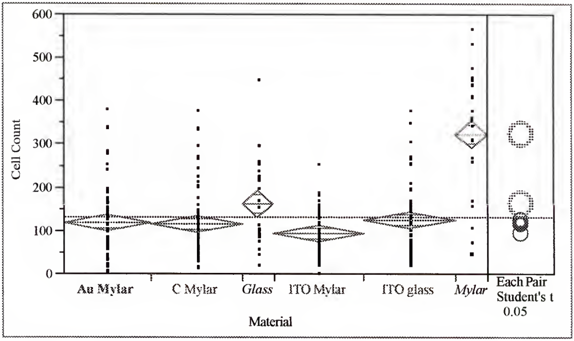

Figure 5.79 Statistical Significance Rankings of Cell Counts from Substrates used in Adhesion Experiments.

Table 5.14 Statistical Significance of Cell Counts when Comparing Substrates with Cell Concentrations of 50,000 cells/mL in Adhesion Experiments

				Significant vs.:					
Substrate	n	Ave. # Cells/ mm^2	St. Dev.	ITO-Glass	ITO-Mylar	C-Mylar	AuPd-Mylar	Glass	Mylar
ITO-Glass	36	91	33	-					yes
ITO-Mylar	34	86	28		-				yes
C-Mylar	36	96	29			-			yes
AuPd-Mylar	32	96	49				-		yes
Glass	12	115	54					-	yes
Mylar	12	236	93	yes	yes	yes	yes	yes	-

Table 5.15 Statistical Significance of Cell Counts when Comparing Substrates with Cell Concentrations of 100,000 cells/mL in Adhesion Experiments

Significant vs.:

Substrate	n	Ave. # Cells/ mm^2	St. Dev.	ITO-Glass	ITO-Mylar	C-Mylar	SC-Mylar	AuPd-Mylar	Glass	Mylar
ITO-Glass	36	175	85	-						yes
ITO-Mylar	36	123	50		-					yes
C-Mylar	36	152	103			-				yes
AuPd-Mylar	36	153	105					-		yes
Glass	12	226	0.7						-	yes
Mylar	12	453	66	yes	yes	yes	yes	yes	yes	-

Table 5.16 Statistical Significance of Cell Counts when Comparing Voltages with Cell Concentrations of 50,000 cells/mL in Adhesion Experiments

Significant vs.:

Substrate	n	Voltage (V)	Ave. # Cells/mm^2	St. Dev.	0 volt	0.5 volt	1 volt
ITO-Glass	12	0	111	37	-	yes	yes
	12	0.5	91	31	yes	-	
	12	1	60	37	yes		-
ITO-Mylar	12	0	83	40	-		
	12	0.5	76	48		-	
	12	1	74	36			-
C-Mylar	12	0	115	28	-	yes	yes
	12	0.5	73	38	yes	-	
	12	1	80	31	yes		-
AuPd-Mylar	12	0	99	24	-	yes	yes
	12	0.5	44	39	yes	-	yes
	12	1	149	46	yes	yes	-

Table 5.17 Statistical Significance of Cell Counts when Comparing Voltages with Cell Concentrations of 100,000 cells/mL in Adhesion Experiments

Substrate	n	Voltage (V)	Ave. # Cells/mm^2	St. Dev.	Significant vs.: 0 volt	0.5 volt	1 volt
ITO-Glass	12	0	189	86	-	yes	
	12	0.5	74	31	yes	-	yes
	12	1	236	68		yes	-
ITO-Mylar	12	0	123	50	-	yes	
	12	0.5	78	42	yes	-	yes
	10	1	134	60		yes	-
C-Mylar	12	0	268	59	-	yes	yes
	12	0.5	88	33	yes	-	
	12	1	82	43	yes		-
AuPd-Mylar	12	0	262	71	-	yes	yes
	12	0.5	68	39	yes	-	
	8	1	90	56	yes		-

When simply observing the data relative to the voltage drop, it does not seem to correlate to the growth data previously presented. However, Table 5.18 shows the currents through the individual samples which are much higher (mA) than those observed in the growth experiments (µA). This would indicate that current may be a more important factor to consider for electrical stimulation studies than voltage drop, contrary to what the literature indicates.

Table 5.18 Currents Through Individual Adhesion Samples

Material	Individual Sample Current at 0.5 volt (mA)	Individual Sample Current at 1 volt (mA)	Resistivity (Ω)
ITO-Glass	1.06	2.11	177
ITO-Mylar	1.89	3.77	99
AuPd-Mylar	1.55	3.11	121
C-Mylar	0.0019	0.0038	99

Relatively no correlation was observed between cell adhesion and either conductivity or hydrophilicity of the substrates as indicated in Figures 5.80 - 5.83.

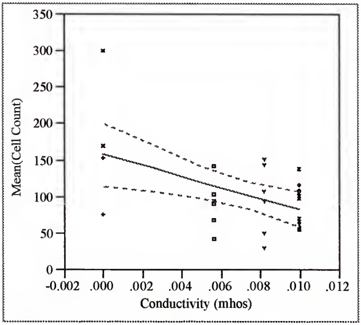

y = 158.991 – 7540.83x RSquare = 0.24

Figure 5.80 Cell adhesion versus Conductivity for 50,000 cells/mL adhesion samples. Mean cell count units are cells/mm^2.

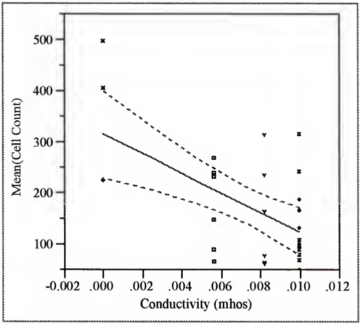

y = 316.502 – 19105.6x RSquare = 0.34

Figure 5.81 Cell adhesion versus Conductivity for 100,000 cells/mL adhesion samples. Mean cell count units are cells/mm^2.

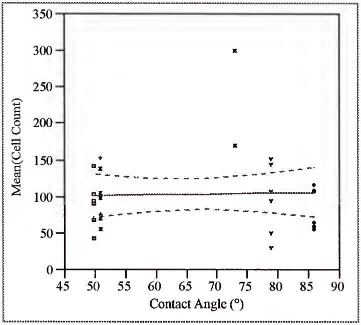

y = 96.687 + 0.11403x RSquare = 0.001

Figure 5.82 Cell adhesion versus Contact Angle for 50,000 cells/mL adhesion samples. Mean cell count units are cells/mm^2.

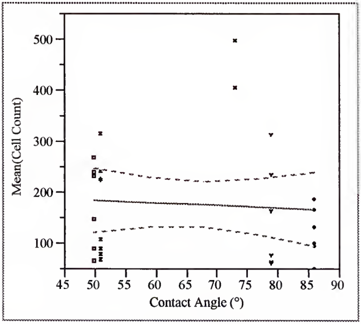

y = 211.246 – 0.5098x RSquare = 0.005

Figure 5.83 Cell adhesion versus Contact Angle for 100,000 cells/mL adhesion samples. Mean cell count units are cells/mm^2.

The release of 6-k-$PGF_{1\alpha}$ from endothelial cells used in the cell adhesion experiments was also measured The results from these studies is shown in Figures 5.84 - 5.89. Note that the concentrations of 6-k-$PGF_{1\alpha}$ are an order of magnitude less than in the growth experiments. This is due to the small sample area and therefore small number of cells available to secrete 6-k-$PGF_{1\alpha}$. Additionally, a much greater volume of cell culture medium was used compared to the growth experiments. The exception to this observation is the concentration of 6-k-$PGF_{1\alpha}$ from cells on ITO-Glass at 0 volts. The higher concentration does not correspond with a higher number of cells on ITO-Glass at 0 volts. This anomaly is most likely due to sampling error. Statistical comparisons of 6-k-$PGF_{1\alpha}$ release rate from cells adhered to the substrates tested are shown in Tables 5.19 and 5.20.

Summary of Cell Adhesion Experiments

The results of the cell adhesion experiments were inconclusive. The cell counts indicate that no voltage results in better endothelial cell adhesion than with any electrical field. However, current through individual samples was not taken into consideration in this study and most likely made a significant difference in the results. Local galvanic corrosion of AuPd coatings on Mylar was observed. Data on the production of 6-k-$PGF_{1\alpha}$ was also inconclusive.

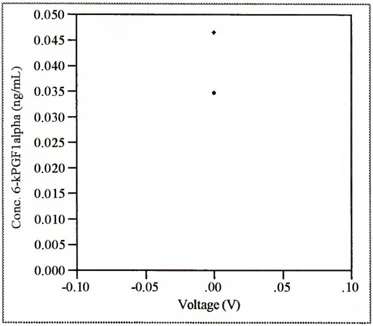

Figure 5.84 Release of 6-k-PGF$_{1\alpha}$ from Endothelial Cells on Glass at 50,000 cells/mL (+) and at 100,000 cells/mL (◆).

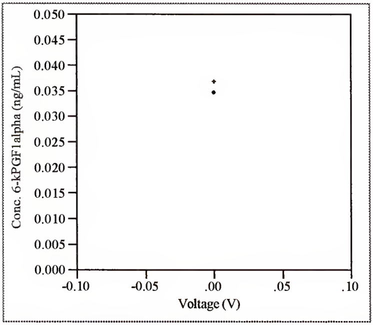

Figure 5.85 Release of 6-k-PGF$_{1\alpha}$ from Endothelial Cells on Mylar at 50,000 cells/mL (+) and at 100,000 cells/mL (◆).

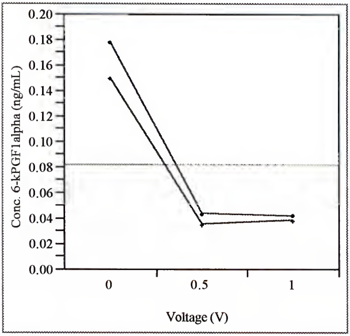

Figure 5.86 Release of 6-k-PGF$_{1\alpha}$ from Endothelial Cells on ITO-Glass at 50,000 cells/mL (+) and at 100,000 cells/mL (◆).

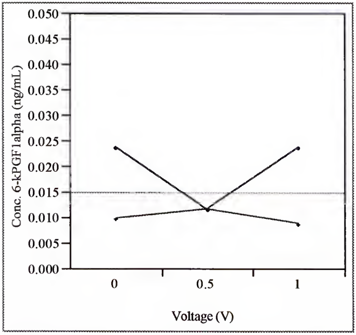

Figure 5.87 Release of 6-k-PGF$_{1\alpha}$ from Endothelial Cells on ITO-Mylar at 50,000 cells/mL (+) and at 100,000 cells/mL (◆).

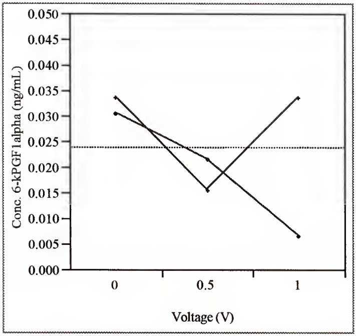

Figure 5.88 Release of 6-k-PGF$_{1\alpha}$ from Endothelial Cells on C-Mylar at 50,000 cells/mL (+) and at 100,000 cells/mL (◆).

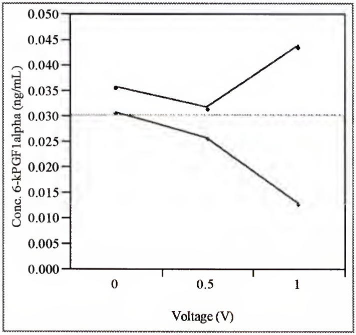

Figure 5.89 Release of 6-k-PGF$_{1\alpha}$ from Endothelial Cells on AuPd-Mylar at 50,000 cells/mL (+) and at 100,000 cells/mL (◆).

Table 5.19 Statistical Significance of Concentrations of 6-k-PGF$_{1a}$ when Comparing Substrates with Cell Concentrations of 50,000 cells/mL in Adhesion Experiments

Substrate	n	Ave. Conc. (ng/mL)	St. Dev.	Significant vs.: ITO-Glass	ITO-Mylar	C-Mylar	AuPd-Mylar	Glass	Mylar
ITO-Glass	3	0.08	0.07	-	yes				
ITO-Mylar	3	0.01	0.002	yes	-				
C-Mylar	3	0.03	0.01			-			
AuPd-Mylar	3	0.02	0.009				-		
Glass	1	0.05	-					-	
Mylar	1	0.04	-						-

Table 5.20 Statistical Significance of Concentrations of 6-k-PGF$_{1a}$ when Comparing Substrates with Cell Concentrations of 100,000 cells/mL in Adhesion Experiments

Substrate	n	Ave. Conc. (ng/mL)	St. Dev.	Significant vs.: ITO-Glass	ITO-Mylar	C-Mylar	AuPd-Mylar	Glass	Mylar
ITO-Glass	3	0.09	0.08	-					
ITO-Mylar	3	0.02	0.007		-				
C-Mylar	3	0.02	0.01			-			
AuPd-Mylar	3	0.04	0.006				-		
Glass	1	0.04	-					-	
Mylar	1	0.04	-						-

CHAPTER 6
SUMMARY AND CONCLUSIONS

Several conclusions can be drawn from this research. The most significant is that low voltage direct current electrical fields moderately increase the growth rate of endothelial cells on conducting biomaterials substrates. However, endothelial cell adhesion to substrates appears to be decreased.

A review of the literature indicates that low voltage, constant, direct current are the most effective conditions for increased cell proliferation, adhesion, and motility. However, this conclusion for endothelial cells is suspect based on the results of this research. Proliferation of endothelial cells was increased with electric fields, but cell adhesion was reduced. Voltage drops were the same across corresponding samples in both experiments, but currents in individual samples increased by 3 orders of magnitude, from μA in growth experiments to mA in adhesion experiments. This indicates that there may be a threshold current below which endothelial cells will grow and spread very well and above which they will round and die.

Growth studies produced several conclusions. There was no correlation between growth rates and conductivity, hydrophobicity, or current through the individual samples. The lack of correlation between hydrophobicity and growth rate is most likely due to the number of proteins on the surface of the substrates. There were no proteins on the surface of the substrates while measuring the contact angle and an abundance present in the actual growth studies due to the serum in the growth medium. There was no difference in growth characteristics between cells grown on C-Mylar and those grown on SC-Mylar, indicating that the cells grow equally well when stimulated through the substrate surface or through electric fields in the culture medium. Production of 6-k-

$PGF_{1\alpha}$ was shown to decrease over time with electrical stimulation, and 6-k-$PGF_{1\alpha}$ release rates tended to increase with increasing voltage.

In growth and adhesion studies, low cell counts were noted for the AuPd-Mylar samples compared to all other substrates. This may be due to the coatings being of poorer laboratory quality instead of manufactured quality. Additionally, localized galvanic corrosion was evident macroscopically in the adhesion samples. This corrosion could also have occurred in the growth sample coating although it was not microscopically evident.

Adhesion studies showed opposite trends from the growth studies. Endothelial cells on samples with no voltage adhered better than those with voltage. Data for production of 6-k-$PGF_{1\alpha}$ were inconclusive. Improvements need to be made to the adhesion flow chamber used in these studies. The flow rates need to be higher to more closely simulate physiological conditions experienced by vascular grafts. The incubation stimulation chamber needs to be redesigned to reduce the amount of current flowing through individual samples. The method of stimulating the samples in the flow chamber needs to be improved for easier access and for practicality. With these improvements, the effect of electrical fields on endothelial cell adhesion could be reexamined.

Based on this research, further studies using low-voltage direct current appear warranted for developing technologies aimed at enhancing endothelialization of vascular grafts and for promoting soft tissue would healing.

CHAPTER 7
SUGGESTED FUTURE WORK

The research presented here suggests that low voltage electrical stimulation can increase endothelial cell growth. While this is an important finding, it also leads to many further questions that need to be answered. These questions can be divided into two major categories, biological developments and material developments.

Biological Developments

Biological research can focus on a number of different areas. 1.) What is the species dependency on endothelial cell growth and adhesion with electrical stimulation (i.e. will human endothelial cells react differently than the porcine endothelial cells presented in this research)? 2.) Smooth muscle cells play an important role in vascular wound healing and in intimal thickening. What effect does electrical stimulation have on their growth rates and adhesion characteristics? 3.) Methods need to be developed to track endothelial cell motility on opaque substrates with and without electrical stimulation. 4.) Assays of other growth factors should be measured to better understand the characteristics of various cell types. 5.) Platelet and complement activation may be affected by electrostimulation and thus could be investigated. 6.) Further development of the adhesion flow experiment and studies on the effect of electrical fields on endothelial cell adhesion should be reexamined. Additionally, the interaction between flow rate and electric fields should be studied.

The ultimate goal of the biological studies is to develop *in vivo* designs for useful electrical stimulation technology confirmed by animal and human testing.

Materials Developments

Test methods are needed to measure cell growth rates, adhesion characteristics, and motility rates on opaque materials. Suppliers capable of coating Dacron® vascular graft materials with ITO- or carbon-coatings could be identified, and further testing on these Dacron® substrates could be performed. Research might also be expanded to include e-PTFE substrates with electroactive coatings.

REFERENCES

Aar 93 R.K. Aaron and D.M. Ciombor, Therapeutic effects of electromagnetic fields in the stimulation of connective tissue repair, *Journal of Cellular Biochemistry* **52**, pp. 42-46, 1993.

Abb 80 W. Abbott, R. Walden, G. L'Italien and J. Mergerman, Matched elastic properties and successful arterial grafting, *Archives of Surgery* **115**, pp. 1166-1169, 1980.

Age 82 A. Ager, J.L. Gordon, S. Moncada, J.D. Pearson, J.A. Salmon and M.A. Trevethick, Effects of isolation and culture on prostaglandin synthesis by porcine aortic endothelial and smooth muscle cells, *Journal of Cellular Physiology* **110**, pp. 9-16, 1982.

Ågr 94 M.S. Ågren, M.A. Engel and P.M. Mertz, Collagenase during burn wound healing: influence of a hydrogel dressing and pulsed electrical stimulation, *Plastic and Reconstructive Surgery* **94 (3)**, pp. 518-524, 1994.

Aiz 94 M. Aizawa, T. Haruyama, G.F. Khan, E. Kobatake and Y. Ikariyama, Electronically modulated biological functions of molecular interfaced enzymes and living cells, *Biosensors-Bioelectronics* **9(9-10)**, pp. 601-610, 1994.

Alb 91 S.F. Albert and E. Wong, Electrical stimulation of bone repair, *Clinics in Podiatric Medicine and Surgery* **8(4)**, pp. 923-935, 1991.

All 90 H.R. Allcock and F.W. Lampe, *Contemporary Polymer Chemistry: Second Edition*, Prentice Hall, Englewood Cliffs, NJ, ©1990.

Ame 97 D. Amery, Surface modification of polymer and metallic vascular prostheses and endoluminal stents, ©1997.

And 94 L.E. Anderson, ed. *Mosby's Medical Dictionary Fourth Edition*, Mosby, St. Louis, MO, ©1994.

Bad 93 M.A. Badea, R. Vasilco, D. Sandru, L. Paslaru, V. Jieanu and S. Comorosan, The effect of pulsed electromagnetic field (Diapulse) on cellular systems, *Romanian Journal Physiology* **30(1-2)**, pp. 65-71, 1993.

Bar 45 T.C. Barnes, Healing rate of human skin determined by measurement of the electrical potential of experimental abrasions: a study of treatment with petrolatum and with petrolatum containing yeast and liver extracts, *American Journal of Surgery* **69(1)**, pp. 82-88, 1945.

Ben 94 A. Benbrahim, G.J. L'Italien, B.B. Milinazzo, D.F. Warnock, S. Dhara, J.P. Gertler, R.W. Orkin and W.M. Abbott, A compliant tubular device to study the influences of wall strain and fluid shear stress on cells of the vascular wall, *Journal of Vascular Surgery* **20(2)**, pp. 184-194, 1994.

Ber 92 F. Bernex, J.P. Mazzucotelli, J.L. Roudiere, N. Benhaiem-Sigaux, J. Leandri and D. Loisance, In vitro endothelialization of carbon-coated Dacron vascular grafts, *International Journal of Artificial Organs* **15**, pp. 172-180, 1992.

Bid 95 G. Bidan, C. Lopez, F. Mendes-Viegas, E. Vieil and A. Gadelle, Incorporation of sulphonated cyclodextrins into polypyrrole: as approach for the electro-controlled delivering of neutral drugs, *Biosensors - Bioelectronics* **10(1-2)**, pp. 219-229, 1995.

Bla 92 L. Blatterfein and S.H. Payne, Bioelectric stimulation and residual ridge resorption, *Journal of Prosthetic Dentistry* **67**, pp. 67-71, 1992.

Bor 93 R.B. Borgens, J.P. Toombs, A.R. Blight, M.E. McGinnis, M.S. Bauer, W.R. Widmer and J.R. Cook, Jr., Effects of applied electric fields on clinical cases of complete paraplegia in dogs, *Restorative Neurology and Neuroscience* **5**, pp. 305-322, 1993.

Bot 89 R. Botting and J.R. Vane, The receipt and dispatch of chemical messengers by endothelial cells, *Prostaglandins in Clinical Research: Cardiovascular System*, pp.1-11, Alan R. Liss, Inc., New York, NY, ©1989.

Bri 96 S. Britland and C. McCaig, Embryonic *Xenopus* neurites integrate and respond to simlutaneous electrical and adhesive guidance cues, *Experimental Cell Research* **225**, pp. 31-38, 1996.

Bri 98 A. Brinkman, W. Seeling, C.F. Wolf, E. Kneitinger, N. Vogt, G. Steinbach, K.-H. Orend, P. Radermacher and M. Georgieff, Ibuprofen does not impair renal function in patients undergoing infrarenal aortic surgery with epidural anaesthesia, *Intensive Care Medicine* **24**, pp. 322-328, 1998.

Bro 94 M.J. Brown and L.M. Loew, Electric field-directed fibroblast locomotion involves cell surface molecular reorganization and is calcium independent, *The Journal of Cell Biology* **127(1)**, pp. 117-128, 1994.

Bro 95a J.D. Bronzino, ed., *The Biomedical Engineering Handbook*, CRC Press and IEEE Press, Boca Raton, FL, ©1995.

Bro 95b M. Brown, P.P. Gogia, D.R. Sinacore and D.N. Menton, High-voltage galvanic stimulation on wound healing in guinea pigs: longer-term effects, *Archives of Physical Medical Rehabilitation* **76**, pp. 1134-1137, 1995.

Bus 92 F. Bussolino, M.F. Di-Renzo, M. Ziche, E. Bocchietto, M. Olivero, L. Naldini, G. Gaudino, L. Tamagnone, A. Coffer and P.M. Comoglio, Hepatocyte growth factor is a potent angiogenic factor which stimulates endothelial cell motility and growth, *The Journal of Cell Biology* **119(3)**, pp. 629-641, 1992.

Byl 94 N.N. Byl, A.L. McKenzie, J.M. West, J.D. Whitney, T.K. Hunt, H. Williams Hopf and H. Scheuenstuhl, Pulsed microamperage stimulation: a controlled study of healing of surgically induced wounds in Yucatan pigs, *Physical Therapy* **74(3)**, pp. 201-218, 1994.

Can 31 J. Cantacuzene and E. Soru, The mechanism of adhesions of the omentum to damaged tissues of the peritoneal cavity electrostatic interactions, *Archives of Romanian Pathology: Microbiology* 173(4), 1931.

Cas 95 E. Castillo, H. Sumano, T.I. Fortoul and A. Zepeda, The influence of pulsed electromagnetic stimulation on the wound healing of burned rat skin, *Archives of Medical Research* **26(2)**, pp. 185-189, 1995.

Ceb 91 A. Ceballos, O. Pereda, R. Ortega and R. Balmaseda, Electrically-induced osteogenesis in external fixation treatment, *Acta Orthopaedica Belgica* **57(2)**, pp. 102-108, 1991.

Cha 90 D.A. Chakkalakal, L. Lippiello, R.L. Shindell and J.F. Connolly, Electrophysiology of direct current stimulation of fracture healing in canine radius, *IEEE Transactions on Biomedical Engineering* **37(11)**, pp. 1048-1058, 1990.

Cha 91 W.H. Chang, I.M. Hwang and H.C. Liu, Enhancement of fracture healing by specific capacitively-coupled electric field stimulation, *Frontiers in Medical Biology Engineering* **3(1)**, pp. 57-64, 1991.

Cha 96 E. Chabielska, V. Kolpakov, M.C. D'Adamo, A. De Curtis, W. Buczko, L. Iacoviello and M.B. Donati, Morphological and hemostatic changes in rats with abdominal arterial prosthesis, *Thrombosis Research* **82(1)**, pp. 69-77, 1996.

Chi 92 M. Chiang, K.R. Robinson and J.W. Vanable, Jr., Electrical fields in the vicinity of epithelial wounds in the isolated bovine eye, *Experimental Eye Reserch* **54**, pp. 999-1003, 1992.

Chu 90 C. Chu, A.T. McManus, A.D. Mason, Jr., C.V. Okerberg and B.A. Pruitt, Jr., Multiple graft harvestings from deep partial-thickness scald wounds healed under the influence of weak direct current, *The Journal of Trauma* **30(3)**, pp. 1044-1050, 1990.

Chu 91 C.-S. Chu, A.T. McManus, C.V. Okerberg, A.D. Mason, Jr. and B.A. Pruitt, Jr., Weak direct current acccelerates split-thickness graft healing on tangentially excised second-degree burns, *Journal of Burn Care Rehabilitation* **12**, pp. 285-293, 1991.

Chu 95 C.-S. Chu, A.T. McManus, N.P. Matylevich, A.D. Mason, Jr. and B.A. Pruitt, Jr., Enhanced survival of autoepidermal-allodermal composite grafts in allosensitized animals by use of silver-nylon dresssigs and direct current, *The Journal of Trauma: Injury, Infection and Critical Care* **39(2)**, pp. 273-278, 1995.

Chu 96 C. Chu, N.P. Matylevich, A.T. McManus, A.D. Mason, Jr. and B.A. Pruitt, Jr., Direct current reduces wound edema after full-thickness burn injury in rats, *The Journal of Trauma: Injury, Infection and Critical Care*, **40(5)**, pp. 738-472, 1996.

Dav 84 P.F. Davies, HLBI Workshop, November 1984.

Dav 93 S.C. Davis and L.G. Ovington, Electrical stimulation and ultrasound in wound healing. *Wound Healing* **11(4)**, pp. 775-781, 1993.

Dav 95 P.F. Davies, Flow-mediated endothelial mechanotransduction, *Physiological Reviews* **75(3)**, pp. 519-560, 1995.

Del 97 Delta Technologies, Ltd., Product literature, March 1997.

Din 93 H. Dindar, N. Renda, M. Barlas, A. Akinay, E. Yazgan, T. Tincer, M. Cakmak, R. Konkan, I.H. Gokcora and S. Yucesan, The effect of electromagnetic field stimulation on corticosteroids-inhibited intestinal wound healing, *Tokai Journal of Experimental Clinical Medicine* **18(1-2)**, pp. 49-55, 1993.

Eri 84 C.A. Erickson and R. Nuccitelli, Embryonic fibroblast motility and orientation can be influenced by physiological electric fields, *The Journal of Cell Biology* **98**, pp. 296-307, 1984.

Fee 85	J.A. Feeder and L.C. Kloth, Acceleration of wound healing with high voltage pulsating direct current, *Physical Therapy* **65(5)**, p. 741, 1985.
Fee 91	J.A. Feedar, L.C. Kloth and G.D. Gentzkow, Chronic dermal ulcer healing enhanced with monophasic pulsed electrical stimulation, *Physical Therapy* **71(9)**, pp. 639-649, 1991.
Fit 92	R.J. Fitzsimmons, D.D. Strong, S. Mohan and D.J. Baylink, Low-amplitude, low-frequency electric field stimulated bone cell proliferation may in part be mediated by increased IGF-II release, *Journal of Cellular Physiology* **150**, pp. 84-89, 1992.
Fit 93	G. K. Fitzgerald and D. Newsome, Treatment of a large infected thoracic spine wound using high voltage pulsed monophasic current, *Physical Therapy* **73(6)**, pp. 355-360, 1993.
Fle 96	K.J. Fleischer, P.J. Goldschmidt-Clermont, J.D. Fonger, G.M. Hutchins, R.H. Hruban and W.A. Baumgartner, One-month histologic response of transmyocardial laser channels with molecular intervention, *Annals of Thoracic Surgery* **62(4)**, pp. 1051-1058, 1996.
Fra 90	A. Franke, R. Reding and D. Tessmann, Electrostimulation of healing abdominal incisional hernias by low frequency, bipolar, symmetrical rectangular pulses, *Acta Chir Scandanavia* **156**, pp. 701-705, 1990.
Fuj 92	M. Fujita, S. Hukuda and Y. Doida, The effect of constant direct electrical current on intrinsic healing in the flexor tendon *in vitro*. *Journal of Hand Surgery* **17B(1)**, pp. 94-98, 1992.
Fur 94	J.W. Furbee, Jr., T. Kuwana and R.S. Kelly, Fractured carbon fiber-based biosensor for glucose, *Analytical Chemistry* **66(9)**, pp. 1575-1577, 1994.
Gao 94	Z. Gao, B. Chen and M. Zi, Voltammetric determination of dopamine in the presence of ascorbic acid at over-oxidized polypyrrole-indigo carmine film-coated electrodes, *Analyst* **119(3)**, pp. 459-464, 1994.
Gau 76	W.R. Gault and P.F. Gatens, Jr., Use of low intensity direct current in management of ischemic skin ulcers, *Physical Therapy* **56(3)**, pp. 265-269, 1976.
Gea 93	R.L. Geary, T.R. Kohler, S. Vergel, T.R. Kirkman and A.W. Clowes, Time course of flow-induced smooth muscle cell proliferation and initmal thickening in endothelialized baboon vascular grafts, *Circulation Research* **74(1)**, pp.14-23, 1993.

Gen 91 G.D. Gentzkow and K.H. Miller, Electrical stimulation for dermal wound healing, *Clinics in Podiatric Medicine and Surgery* **8(4)**, pp. 827-841, 1991.

Gen 93 G.D. Gentzkow, Electrical stimulation to heal dermal wounds, *Journal of Dermatological Surgery and Oncology* **19**, pp. 753-758, 1993.

Gho 93 P.M. Ghosh, C.R. Keese and I. Giaever, Monitoring electropermeabilization in the plasma membrane of adherent mammalian cells, *Biophysics Journal* **64**, pp. 1602-1609, 1993.

Gil 96 C. Gillis, L. Bengtsson, B. Wiman and A. Hægerstrand, Secretion of prostacyclin, tissue plaminogen activator and its inhibitor by cultured adult human endothelial cells grown on different matrices, *European Journal of Endovascular Surgery* **11**, pp. 127-133, 1996.

Gog 92 P.P. Gogia, R.R. Marquez and G.M. Minerbo, Effects of high voltage galvanic stimulation on wound healing, *Ostomy/Wound Management* **38(1)**, pp. 29-35, 1992.

Gol 90 M.A. Golden, S.R. Hanson, T.R. Kirkman, P.A. Schneider and A.W. Clowes, Healing of polytetrafluoroethylene arterial grafts is influenced by graft porosity, *Journal of Vascular Surgery* **11(6)**, pp. 838-845, 1990.

Gol 96 E.P. Goldberg, Advances in biomedical polymers: problems and opportunities for ophthalmic, cardiovascular and mammary implants and tissue-protective surgical devices, *Medical Plastics Technology News,* **Oct.-Dec**, p. 7, 1996.

Gra 97 D. Granchi, E. Cenni, E. Verri, G. Ciapetti, S. Gamberini, A. Gori and A. Pizzoferrato, Flow-cytometric analysis of leukocyte activation induced by polyethylene-terephthalate with and without pyrolytic carbon coating, *Journal of Biomedical Materials Research* **39**, pp. 549-553, 1998.

Gre 92 C.G. Greenough, The effects of pulsed electromagnetic fields on blood vessel growth in the rabbit ear chamber, *Journal of Orthopaedics Research* **10**, pp. 256-262, 1992.

Gri 91 J.W. Griffin, R.E. Tooms, R.A. Mendius, J.K. Clifft, R. Vander Zwagg and F. El-Zeky, Efficacy of high voltage pulsed current for healing of pressure ulcers in patients with spinal cord injury, *Physical Therapy* **71(6)**, pp. 433-444, 1991.

Gup 90 T.D. Gupta, V.K. Jain and P.N. Tandon, Electrical fields in direct current stimulation system for bone healing, *Medical and Biological Engineering and Computing* **28**, pp. 260-263, 1990.

Gup 91 T.D. Gupta, V.K. Jain and P.N. Tandon, Comparative study of bone growth by pulsed electromagnetic fields. *Medical and Biological Engineering and Computing* **29**, pp. 113-120, 1991.

Guz 94 N. Guzelsu, A.J. Salkind, X. Shen, U. Patel, S. Thaler and R.A. Berg, Effect of Electromagnetic stimulation with different waveforms on cultured chick tendon fibroblasts, *Bioelectromagnetics* **15**, pp. 115-131, 1994.

Hal 93 R. Hallworth, B.N. Evans and P. Dallos, The locomotion and mechanism of electromotility in guinea pig outer hair cells, *Journal of Neurophysiology* **30(2)**, pp. 549-558, 1993.

Ier 90 M. Ieran, S. Zaffuto, M. Bagnacani, M. Annovi, A. Moratti and R. Cadossi, Effect of low frequency pulsing electromagnetic fields on skin ulcers of venous origin in humans: a double-blind study, *Journal of Orthopaedic Research* **8(2)**, pp. 276-282, 1990.

Igl 96 D. Iglesia, E. Cragoe, Jr. and J.W. Vanable, Jr., Electric field strength and epithelialization in the newt, *The Journal of Experimental Zoology* **274**, pp. 56-62, 1996.

Ish 94 K. Ishihara, H. Inoue, K. Kurita and N. Nakabayashi, Selective adhesion of platelets on a polyion complex composed of phospholipid polymers containing sulfonate groups and quarternary ammonium groups, *Journal of Biomedical Materials Research* **28**, pp. 1347-1355, 1994.

Ito 91 M. Itoh, J.S. Montemayor, Jr., E. Matsumoto, A. Eason, M.H.M. Lee and F.S. Folk, Accelerated wound healing of pressure ulcers by pulsed high peak power electromagnetic energy (Diapulse), *Decubitus* **4(1)**, pp. 24-34, 1991.

Ito 95 K. Itoh, B. Stevens, M. Schachner and R.D. Fields, Regulated expression of the neural cell adhesion molecule L1 by specific patterns of neural impulses, *Science* **270**, pp. 1369-1372, 1995.

Jak 98 B. Jakubiec, Y. Marois, Z. Zheng, R. Roy, M.-F. Sigot-Luizard, F.J. Dugré, M.W. King, L. Dao, G. Laroche and R. Guidoin, *In vitro* cellular response to polypyrrole-coated woven polyester fabrics: potential benefits of electrical conductivity, *Journal of Biomedical Materials Research* **41**, pp. 519-526, 1998.

Jam 90 N.L. James, K. Schindhelm, P. Slowiaczek, B.K. Milthorpe, N.P. Dudman, G. Johnson and J.G. Steele, Endothelial cell seeding of small diameter vascular grafts, *Artificial Organs* **14(5)**, pp. 355-360, 1990.

Joh 80 A.R. Johnson, Human pulmonary endothelial cells in culture, *Journal of Clinical Investigation* **65**, pp. 841-850, 1980.

Kah 90 N. Kahanovitz and S.P. Arnoczky, The efficacy of direct current electrical stimulation to enhance canine spinal fusion, *Clinical Orthopaedics and Related Research* **251**, pp. 295-299, 1990.

Kah 94 N. Kahanovitz, S.P. Arnoczky, J. Nemzek and A. Shores, The effect of electromagnetic pulsing on posterior lumbar spinal fusions in dogs, *Spine* **19(6)**, pp. 705-709, 1994.

Kam 93 H.E. Kambic, E. Reyes, T. Manning, K.C. Water and S.I. Reger, Influence of AC and DC electrical stimulation on wound healing in pigs: a biomechanical analysis, *Journal of Investigative Surgery* **6**, pp. 535-543, 1993.

Kat 95 S. Kato, C.T. Ivester, G. Cooper IV, M.R. Zile and P.J. McDermott, Growth effects of electrically stimulated contraction on adult feline cardiocytes in primary culture, *American Journal of Physiology* **268(37)**, pp. H2495 - H2504, 1995.

Kim 90 K. Kim, Biochemical study of human peridontal ligament: preparation of cell attachment materials induced by pulsed electromagnetic fields, *Bulletin of Kanagawa Dental College* **18(2)** pp. 89-98, 1990.

Kin 89 C.B. Kincaid and K.H. Lavoie, Inhibition of bacterial growth in vitro following stimulation with high voltage, monophasic, pulsed current, *Physical Therapy* **69(8)**, pp. 651/29-655/33, 1989.

Klo 88 L.C. Kloth and J.A. Feedar, Acceleration of wound healilng with high voltage, monophasic, pulsed current, *Physical Therapy* **68(4)**, pp. 503-508, 1988.

Koj 91 J. Kojima, H. Shinohara, Y. Ikariyama, M. Aizawa, K. Nagaike and S. Morioka, Electrically controlled proliferation of human carcinoma cells cultured on the surface of an electrode, *Journal of Biotechnology* **18**, pp. 129-140, 1991.

Kot 96 K. Kottke-Marchant, A.A. Veenstra and R.E. Marchant, Human endothelial cell growth and coagulant function varies with respect to interfacial properties of polymeric substrates, *Journal of Biomedical Materials Research* **30**, pp.209-220, 1996.

Kra 96 T. Krawczynski-vel-Krawczyk, M. Trojanowicz, M. Lewenstam and A. Moszczynska, Lactate solid-state biosensor with multilayer of electrodeposited polymers for flow-injection clinical analysis, *Biosensors - Bioelectronics* **11(11)**, pp. 1155-1165, 1996.

Kuh 93 H.H. Kuhn, Characterization and application of polypyrrole-coated textiles, *Intrinsically Conducting Polymers: An Emerging Technology*, pp. 25-34, Kluwer Academic Publishers, Netherlands, ©1993.

Lam 97 M. Lampin, R. Warocquier-Clerout, C. Legris, M. Degrange and M.F. Sigot-Luizard, Correlation between substratum roughness and wettability, cell adhesion, and cell migration, *Journal of Biomedical Materials Research* **36**, pp. 99-108, 1997.

Lee 91 H.H. Lee, M. Boyd, G.L. Gravatt and W.A. Denny, Pyrazole anaolgues of the bispyrrolecarboxamide anti-tumor antibiotics: synthesis, DNA binding and anti-tumor properties, *Anticancer Drug Design* **6(5)**, pp. 501-517, 1991.

Lee 93 R.C. Lee, D.J. Canaday and H. Doong, A review of the biophysical basis for the clinical application of electric fields in soft-tissue repair, *Journal of Burn Care Rehabilitation* **14**, pp. 319-335, 1993.

Lee 94 J.H. Lee, H.W. Jung, I.-K. Kang and H.B. Lee, Cell behaviuor on polymer surfaces with different functional groups, *Biomaterials* **15(9)**, pp.705-711, 1994.

Lef 94 D.J. Leffmann, D.A. Arnall, P.R. Holmgren and M.W. Cornwall, Effect of microamperage stimulation on the rate of wound healing in rats: a histological study, *Physical Therapy* **74(3)**, pp. 195-200, 1994.

Lib 93 R.P. Liburdy, T.R. Sloma, R. Sokolic and P. Yaswen, ELF magnetic fields, breast cancer, an dmelatonin: 60 Hz fields block melatonin's oncostatic action on ER+ breast cancer cell proliferation, *Journal of Pineal Research* **14**, pp. 89-97, 1993.

Lin 92 Y. Lin, R. Nishimura, K. Nozaki, N. Sasaki, T. Kadosawa, N. Goto, M. Date and A. Takeuchi, Effects of pulsing electromagnetic fields on the ligament healing in rabbits, *Journal of Veterinary Medical Science* **54(5)**, pp. 1017-1022, 1992.

Lip 90 L. Lippiello, D. Chakkalakal and J.F. Connolly, Pulsing direct current-induced repair of articular cartilage in rabbit osteochondral defects, *Journal of Orthopaedic Research* **8**, pp. 266-275, 1990.

Lit 94 D.S. Litke and L.E. Dahners, Effects of different levels of direct current on early ligament healing in a rat model. *Journal of Orthopedic Research* **12(5)**, pp. 683-688, 1994.

Liv 91 G.K. Livingston, K.L. Witt, O.P. Gandhi, I. Chatterjee and J.L. Roti Roti, Reproductive integrity of mammalian cells exposed to power frequency electromagnetic fields, *Environmental and Molecular Mutagenesis* **17**, pp. 49-58, 1991.

Lun 92 T.C.M. Lundeberg, S.V. Eriksson and M. Malm, Electrical nerve stimulation improves healing of diabetic ulcers, *Annals of Plastic Surgery* **29(4)**, pp. 328-331, 1992.

Lyt 91 M. Lyte, J.E. Gannon and G.D. O'Clock, Jr., Effects of *in vitro* electrical stimulation on enhancement and suppression of malignant lymphoma cell proliferation, *Journal of the National Cancer Institute* **83**, pp. 116-119, 1991.

Mak 93 S.A. Makohliso, R.F. Valentini and P. Aebischer, Magnitude and polarity of a fluoroethylene propylene electret substrate charge influences neurite outgrowth *in vitro*, *Journal of Biomedical Materials Research* **27**, pp. 1075-1085, 1993.

Mam 93 G.I. Mammi, R. Rocchi, R. Cadossi, L. Massari and G.C. Traina, The electrical stimulation of tibial osteotomies, *Clinical Orthopedics and Related Research* **288**, pp. 246-253, 1993.

Mar 91 L.B. Margolis and S.V. Popov, Induction of cell processes by local force, *Journal of Cell Science* **98**, pp. 369-373, 1991.

Mar 94 D.J. Margolis and J.H. Cohen, Management of chronic venous leg ulcers: a literature-guided approach, *Clinics in Dermatology* **12**, pp. 19-26, 1994.

Mat 97 E.J.R. Mattsson, T.R. Kohler, S.M. Vergel and A.W. Clowes, Increased blood flow induces regression of intimal hyperplasia, *Arteriosclerosis, Thrombosis, and Vascular Biology* **17(10)**, pp.2245-2249, 1997.

Men 93 K. Mentak, Tissue-protective hydrophilic polymer solutions and surface modifications, ©1993.

Moh 94 H. Mohamed-Ali, H. Kolkenbrock, N. Ulbrich, H. Sorenson, K.D. Kramer and H.J. Merker, Influence of electromagnetic fields on the enzyme activity of rheumatoid synovial fluid cells *in vitro*, *European Journal of Clinical Chemistry and Clinical Biochemistry* **32(4)**, pp. 319-326, 1994.

Mon 82 S. Moncada, Biological importance of prostacyclin, *British Journal of Pharmacology* **76**, pp. 3-31, 1982.

Moo 90 V. Mooney, A randomized double-blind prospective study of the efficacy of pulsed electromagnetic fields for interbody lumbar fusions, *Spine* **15(7)**, pp. 708-712, 1990.

Muh 91 A.U.M. Muhsin, K.M.N. Islam, A.M.N. Ahmed, M.S. Islam, K.S. Rabbani, S.M. Rahman, S. Ahmed and M. Hossain, Effect of pulsed electromagnetic field on healing of experimental nonunion in rat tibiae, *Bangladesh Medical Research Council Bulletin* **17(1)**, pp. 1-10, 1991.

Mui 91 R.J. Muirhead, D. Place, W.A. Buswell and J. Heselting, Pulse electromagnetic energy and pre-tibial lacerations: a randomized clinical trial, *Archives of Emergency Medicine* **8**, pp. 152-160, 1991.

Mye 96 D.E. Myers, W.-N. Huang and R.G. Larkins, Lipoprotein-induced prostacyclin production in endothelial cells and effects of lipoprotein modification, *American Journal of Physiology* **271**: *Cell Physiology* **40**, pp. C1504-C1511, 1996.

Nae 91 J.R. Naegele, J. Lipari, D. Chakkalakal, B. Strates and M. Mcguire, Electric field stimulation of human osteosarcoma-derived cells: a dose reponse study, *Cancer Biochemistry and Biophysiology* **12**, pp. 95-101, 1991.

Neo 98 Neogen Corporation, 6-keto-prostaglandin F_{1a} ELISA kit instruction manual, ©1998.

Ngu 93 N.M. Nguyen, J.E. Lehr and K.J. Pienta, Pentosan inhibits angiogenesis *in vitro* and suppresses prostate tumor growth *in vivo*, *Anticancer Research* **13(6A)**, pp. 2143-2147, 1993.

Nic 94 G.L. Nicolson, D.G. Menter, J. Herrmann, P. Cavanaugh, L. Jia, J. Hamada, Z. Yun, M. Nakajima and D. Marchetti, Tumor metastasis to brain: role of endothelial cells, neurotrophins, and paracrine growth factors, *Critical Reviews of Oncogenesis* **5(5)**, pp. 451-471, 1994.

Nic 95 G.L. Nicolson and D.G. Menter, Trophic factors and central nervous system metastasis, *Cancer Metastasis Review* **14(4)**, pp. 303-321, 1995.

Nis 92 M. Nishizawa, T. Matsue and I. Uchida, Penicillan sensor based on a microarray electrode coated with pH-responsive polypyrrole, *Analytical Chemistry* **64(21)**, pp. 2642-2644, 1992.

Nor 93 T. Norimura, H. Imada, N. Kunugita, N. Yoshida and M. Nikaido, Effects of strong magnetic fields on cell growth and radiation response of human T-lymphocytes in culture, *J UOEH* **15(2)**, pp. 103-112, 1993.

Nuc 83 R. Nuccitelli and C. A. Erickson, Embryonic cell motility can be guided by physiological electric fields, *Experimental Cell Research* **147**, pp. 195-201, 1983.

Nuc 88 R. Nuccitelli, Physiological electric fields can influence cell motility, growth and polarity, *Advances in Cell Biology* **2**, pp. 213-233, 1988.

Ort 92 L.F. Ortman, D.M. Casey and M. Deers, Bioelectric stimulation and residual ridge resorption, *The Journal of Prosthetic Dentistry* **67**, pp. 67-71, 1992.

Par 93 A.H. Parola, N. Porat and L.A. Kiesow, Chicken embryo fibroblasts exposed to weak, time-varying magnetic fields share cell proliferation, adenosine deaminase activity, and membrane characteristics of transformed cells, *Bioelectromagnetics* **14**, pp. 215-228, 1993.

Pas 90 G. Pasquinelli, A. Freyrie, P. Preda, T. Curti, M. D'Addato and R. Laschi, Healing of prosthetic arterial grafts, *Scanning Microscopy* **4(2)**, pp. 351-362, 1990.

Pas 96 M. Pasic, W. Muller-Glauser, L. von-Segesser, B. Odermatt, M. Lachat and M. Turina, Endothelial cell seeding improves patency of synthetic vascular grafts: manual versus automatized method, *European Journal of Cardiothoracic Surgery* **10(5)**, pp. 372-379, 1996.

Per 87 E. Perez, L.G. Lopez-Brionez, J. Gallar and C. Belmonte, Effects of chronic sympathetic stimulation on corneal wound healing, *Investigative Ophthalmology and Visual Science* **28**, pp. 221-224, 1987.

Pig 97 B. Pignataro, E. Conte, A. Scandurra and G. Marletta, Improved cell adhesion to ion beam-irradiated polymer surfaces, *Biomaterials* **18**, pp. 1461-1470, 1997.

Pop 90 Popma, J.J., and E.J. Topol, Factors influencing restenosis after coronary angioplasty, *The American Journal of Medicine* **88(1)**, pp. 16N-24N, 1990.

Pra 88 K.J. Pratt, B.E. Jarrell, S.K. Williams, R.A. Carabasi, M.A. Rupnick and F.A. Hubbard, Kinetics of endothelial cell-surface attachment forces, *Journal of Vascular Surgery* **7(4)**, pp. 592-599, 1988.

Pre 95	D. Prentice and K. Theriault, *Clinical Corner, Perspectives* **19(3)**, pp. 7-8, 1995.
Qiu 98	Q. Qiu, M. Sayer, M. Kawaja, X. Shen and J.E. Davies, Attachment, morphology, and protein expression of rat marrow stromal cells cultured on charged substrate surfaces, *Journal of Biomedical Materials Research* **42**, pp. 117-127, 1998.
Rap 95a	L.H. Raptis, H.L. Brownell, S.K.-W. Liu, K.L. Firth, L.W. MacKenzie, C.D. Stiels and J.A. Alberta, Applications of electroporation of adherent cells in situ, on a partly conductive slide, *Molecular Biotechnology* **4**, pp.129-138, 1995.
Rap 95b	L.H. Raptis, S.K.-W. Liu, K.L. Firth, C.D. Stiles and J.A. Alberta, Electroporation of peptides into adherent cells in situ, *Biotechniques* **18(1)**, pp. 104-114, 1995.
Rei 91	J.D. Reich, A.L. Cazzaniga, P.M. Mertz, F.A. Kerdel and W.H. Eaglstein, The effect of electrical stimulation on the number of mast cells in healing wounds. *Journal of the American Academy of Dermatology* **25 (1 Pt. 1)**, pp. 40-46, 1991.
Rey 88	J.R. Reynolds, Electrically conductive polymers, *CHEMTECH* **18**, pp. 440-447, 1988.
Rob 85	K.R. Robinson, The responses of cells to electrical fields: a review, *The Journal of Cell Biology* **101**, pp. 2023-2027, 1985.
Ros 90	S.M. Ross, Combined SC and ELF magnetic fields can alter cell proliferation, *Bioelectromagnetics* **11**, pp. 27-36, 1990.
Sak 91	A. Sakai, K. Suzuki, T. Nakamura, T. Norimura and T. Tsuchiya, Effects of pulsing electromagnetic fields on cultured cartilage cells, *International Orthopaedics* **15**, pp. 341-346, 1991.
Sal 95	C.A. Salzberg, S.A. Cooper-Vastola, F. Perez, M.G. Viehbeck and D.W. Byrne, The effects of non-thermal pulsed electromagnetic energy on wound healing of pressure ulcers in spinal cord-injured patients: a randomized, double-blind study, *Ostomy/Wound Management* **41(3)**, pp. 42-51, 1995.
Sar 95	I. Sarelius, Blood flow channels for use with cultured cells, *Cornell Nanofabrication Facility Research Accomplishments 1994-1995*, pp. 165-166, 1995.

Sba 91 R. Sbarbati, D. Giannessi, M.C. Cenni, G. Lazzerini, F. Verni and R. De Caterina, Pyrolytic carbon coating enhances Teflon and Dacron fabric compatibility with endothelial cell growth, *International Journal of Artificial Organs* **14**, pp.491-498, 1991.

Sch 95 J.P. Schaffer, A. Saxena, S.D. Antolovich, T.H. Sanders, Jr. and S.B. Warner, *The Science and Design of Engineering Materials*, Richard D. Irwin, Inc., Chicago, IL, © 1995.

Sch 97 C.E. Schmidt, V.R. Shastri, J.P. Vacnti and R. Langer, Stimulation of neurite outgrowth using an electrically conducting polymer, *Proceedings of the National Academy of Sciences USA* **94**, pp. 8948-8953, 1997.

See 95 J.M. Seeger, M.D. Ingegno, E. Biagtan, N. Klingman, D. Amery, C. Widenhouse and E.P. Goldberg, Hydrophilic surface modification of metallic endoluminal stents, *Journal of Vascular Surgery* **22(3)**, pp. 327-335, 1995.

Sha 90 W.J.W. Sharrard, A double-blind trial of pulsed electromagnetic fields for delayed union of tibial fractures, *The Journal of Bone and Joint Surgery* **72-B**, pp. 347-355, 1990.

Sha 95 D.M. Shafer, K. Rogerson, L. Norton, and J. Bennett, The effect of electrical perturbation on osseointegration of titanium dental implants, *Journal of Oral Maxillofacial Surgery* **53**, pp. 1063-1068, 1995.

She 96 D.M. Sheridan, R.R. Isseroff and R. Nuccitelli, Imposition of a physiologic DC electric field alters the migratory response of human keratinocytes on extracellular matrix molecules, *The Journal of Investigative Dermatology* **106**, pp. 642-646, 1996.

Sho 92 W.O. Short, L. Goodwill, C.W. Taylor, C. Job, M.E. Arthur and A.E. Cress, Alteration of human tumor cell adhesion by high strength static magnetic fields, *Investigative Radiology* **27**, pp. 836-840, 1992.

Smy 95 J.V. Smyth, M. Welch, H.M. Carr, P.D. Dodd, P.R. Eisenberg and M.G. Walker, Fibrinolysis profiles and platelet activation after endothelial cell seeding of prosthetic vascular grafts, *Annals of Vascular Surgery* **9(6)**, pp. 542-546, 1995.

Sne 90 N.V. Sneed and K.M. VanBree, Treating ununited fractures with electricity: nursing implications, *Journal of Gerontological Nursing* **16(8)**, pp. 26-31, 1990.

Soo 90a H.K. Soong, W.C. Parkinson, S. Bafna, G.L. Sulik and S.C.M. Huang, Movements of cultured corneal epithelial cells and stromal fibroblasts in electric fields, *Investigative Ophthalmology and Visual Science* **31(11)**, pp. 2278-2282, 1990.

Soo 90b H.K. Soong, W.C. Parkinson, G.L. Sulik and S. Bafna, Effects of electrical fields on cytoskeleton of corneal stromal fibroblasts, *Current Eye Research* **9(9)**, pp. 893-901, 1990.

Spa 95 I. Spadinger, D. Agnew and B. Palcic, 3T3 cell motility and morphology before, during and after exposure to extremely-low-frequency magnetic fields, *Bioelectromagnetics* **16**, pp. 178-187, 1995.

Sta 91 J.C. Stanley, Biologic and Synthetic Vascular Prostheses, Grune & Stratton, New York, NY, ©1991.

Ste 90 M. Steiner and W.K. Ramp, Electrical stimulation of bone and its implications for endosseous dental implantation, *Journal of Oral Implantology* **16(1)**, pp. 20-27, 1990.

Ste 93 A. Stefanovska, L Vodocnik, H. Benko and R. Turk, Treatment of chronic wounds by means of electric and electromagnetic fields: part 2 value of FES parameters for pressure sore treatment, *Medical and Biological Engineering and Computing* **31**, pp. 213-220, 1993.

Tam 93 Y. Tamada and Y. Ikada, Cell adhesion to plasma-treated polymer surfaces, *Polymer* **34(10)**, pp. 2208-2212, 1993.

Tam 94 Y. Tamada and Y. Ikada, Fibroblast growth on polymer surfaces and biosynthesis of collagen, *Journal of Biomedical Materials Research* **28**, pp.783-789, 1994.

Tar 90 G. Taraboletti, D. Roberts, L.A. Liotta and R. Giavazzi, Platelet thrombospondin modulates endothelial cell adhesion, motility and growth: a potential angiogenesis regulatory factor, *The Journal of Cell Biology* **111(2)**, pp. 765-772, 1990.

Tsu 93 T. Tsuruta, T. Hayashi. K. Kataoka, K. Ishihara and Y. Kimura, *Biomedical Applications of Polymeric Materials* , CRC Press, Boca Raton, LA, © 1993.

Val 92 R.F. Valentini, T.G. Vargo, J.A. Gardella, Jr. and P. Aebischer, Electrically charged polymeric substrates enhance nerve fibre outgrowth *in vitro*, *Biomaterials* **13(3)**, pp. 183-190, 1992.

Val 93 R.F. Valentini, T.G. Vargo, J.A. Gardella and P. Aebischer, Patterned neuronal attachment and outgrowth on surface modified, electrically charged fluoropolymer substrates, *Journal of Biomaterial Science Polymer Education* **5(1-2)**, pp. 13-36, 1993.

Vod 92a L. Vodovnik and R. Karba, Treatment of chronic wounds by means of electric and electromagnetic fields, *Medical and Biological Engineering and Computing* **30**, pp. 257-266, 1992.

Vod 92b L. Vodovnik, D. Miklavcic and G. Sersa, Modified cell proliferation due to electrical currents, *Medical and Biological Engineering and Computing* **30**, pp. CE21-CE28, 1992.

Wel 92 M. Welch, D. Durrans, H.M. Carr, R. Vohra, O.B. Rooney and M.G. Walker, Endothelial cell seeding: a review, *Annals of Vascular Surgery* **6(5)**, pp. 473-484, 1992.

Wid 96 C.W. Widenhouse, Surface modification of vascular prosthesis and intracorneal lens polymers, ©1996.

Won 94 J.Y. Wong, R. Langer and D.E. Ingber, Electrically conducting polymers can noninvasively control the shape and growth of mammalian cells, *Proceedings of the National Academy of Sciences, USA* **91**, pp. 3201-3204, 1994.

Woo 93 J.M. Wood, P.E. Evans, K.U. Schallreuter, W.E. Jacobson, R. Sufit, J. Newman, C. White and M. Jacobson, A multicenter study on the use of pulsed low-intensity direct current for healing chronic stage II and stage III decubitus ulcers, *Archives of Dermatology* **129**, pp. 999-1009, 1993.

Yam 98 A. Yamamoto, S. Mishima, N. Maruyama and M. Sumita, A new technique for direct measurement of the shear force necessary to detach a cell from a material, *Biomaterials* **19**, pp.871-879, 1998.

Yao 90 M. Yaoita, Y. Ikariyama and M. Aizawa, Electrical effects on the proliferation of living HeLa cells cultured on optically transparent electrode surface, *Journal of Biotechnology* **14**, pp. 321-332, 1990.

Yar 94 G.M. Yarkony, Pressure ulcers: a review, *Archives of Physical Medicine and Rehabilitation* **75**, pp. 908-917, 1994.

Zac 87 R.K. Zacharias, T.R. Kirkman and A.W. Clowes, Mechanisms of healing in synthetic grafts, *Journal of Vascular Surgery* **6(5)**, pp. 429-436, 1987.

Zac 88	R.K. Zacharias, T.R. Kirkman, R.D. Kenagy, D. F. Bowen-Pope and A.W. Clowes, Growth factor production by polytetrafluoroethylene vascular grafts, *Journal of Vascular Surgery* **7(4)**, pp. 606-610, 1988.
Zha 90	W.B. Zhanf, S.H. Song and S.J. Dong, Heterogeneous electron transfer of cytochrome c facilitated by polypyrrole and methylene blue polypyrrole film modified electrodes, *Journal of Inorganic Biochemistry* **40(3)**, pp. 189-195, 1990.
Zie 94	T. Ziegler and R. M. Nerem, Tissue engineering a blood vessel: regulation of vascular biology by mechanical stresses, *Journal of Cellular Biochemistry* **56**, pp. 204-209, 1994.
Zil 93	P. Zilla, U. von Oppell and M. Deutsch, The endothelium: a key to the future, *Journal of Cardiovascular Surgery* **8(1)**, pp. 32-60, 1993.

BIOGRAPHICAL SKETCH

Gwen Elaine Clark was born in Titusville, Pennsylvania on May 18, 1969, to Richard and Jane Clark. She moved to Durham, North Carolina, from Titusville when she was 15. She lived there with her mother until graduating from Charles E. Jordan High School in 1987. Gwen attended North Carolina State University, majoring in Materials Science and Engineering with a Polymers Specialty. Her undergraduate education was funded in part by Aubrey Lee Brooks and the Doshi Scholarships.

While attending NCSU, Gwen was active in the Music department, playing tenor saxophone in the marching, pep, and symphonic bands. She was also active in the Raleigh Wesley Foundation, the student chapter of the Society of Plastics Engineers, Habitat for Humanity, and the NCSU Fellows program. Through these organizations she had many opportunities to travel abroad. During her freshman year, she traveled with a work team to Hidalgo, Mexico, to help build a community center for the local church. In the summer of her sophomore year, she lived in London for a month and then traveled independently throughout Europe for three weeks.

Gwen began her technical career as a freshman at NCSU working as a laboratory assistant in the Precision Engineering Center. Her job responsibilities included assembling an ultrahigh vacuum system and assisting with focused ion beam, scanning tunneling microscopy and atomic force microscopy experimentation. In the summer of her junior year, she moved to Cincinnati, Ohio, to intern with the Procter and Gamble Company developing compostable packaging for orange juice.

After graduation from NCSU in 1991, Gwen returned to Procter and Gamble as a full-time research engineer in materials development working on varied projects including compostable diapers, international diaper upgrades, and mechanical fastening.

In 1995, Gwen returned to academia for her Ph.D. in Materials Science and Engineering at the University of Florida in Gainesville under the direction of Dr. E.P. Goldberg. Her research studied the effect of electrical stimulation on the growth and adhesion characteristics of endothelial cells grown on several substrates.

Gwen will be returning to Procter and Gamble to work as a research engineer in materials development in the Health Care Division. Additionally, Gwen is engaged to be married on May 29, 1999 to Mr. Jeffrey L. Pace.

I certify that I have read this study and that in my opinion it conforms to acceptable standards of scholarly presentation and is fully adequate, in scope and quality, as a dissertation for the degree of Doctor of Philosophy.

Eugene P. Goldberg, Chair
Professor of Materials Science and
Engineering

I certify that I have read this study and that in my opinion it conforms to acceptable standards of scholarly presentation and is fully adequate, in scope and quality, as a dissertation for the degree of Doctor of Philosophy.

Christopher D. Batich
Professor of Materials Science and
Engineering

I certify that I have read this study and that in my opinion it conforms to acceptable standards of scholarly presentation and is fully adequate, in scope and quality, as a dissertation for the degree of Doctor of Philosophy.

Anthony B. Brennan

Anthony B. Brennan
Associate Professor of Materials Science
and Engineering

I certify that I have read this study and that in my opinion it conforms to acceptable standards of scholarly presentation and is fully adequate, in scope and quality, as a dissertation for the degree of Doctor of Philosophy.

Richard B. Dickinson
Assistant Professor of Chemical
Engineering

I certify that I have read this study and that in my opinion it conforms to acceptable standards of scholarly presentation and is fully adequate, in scope and quality, as a dissertation for the degree of Doctor of Philosophy.

James M. Seeger
Professor of Cardiovascular Surgery

This dissertation was submitted to the Graduate Faculty of the College of Engineering and to the Graduate School and was accepted as partial fulfillment of the requirements for the degree of Doctor of Philosophy.

May, 1999

Winfred M. Phillips
Dean, College of Engineering

M. J. Ohanian
Dean, Graduate School